Thermal oscillations in liquids of low Prandtl number.

Milsom, J. A.

Award date:
1978

Awarding institution:
University of Bath

THERMAL OSCILLATIONS IN LIQUIDS OF LOW PRANDTL NUMBER

submitted by

J.A. MILSOM

for the degree of Ph.D. of the University of Bath 1978

SIGNED .J.A. Milsom.....

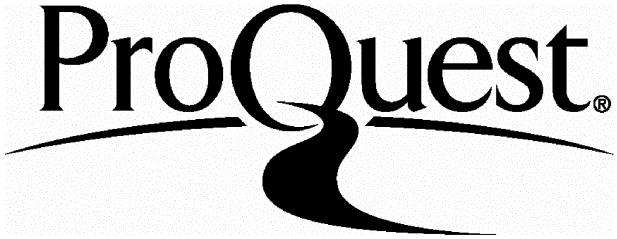

SUMMARY

The main object of this thesis is to attempt to derive an adequate description of the origin and nature of thermal oscillations induced in fluids of low Prandtl number.

Chapter One reviews the hydrodynamic stability of a fluid layer heated from below (results which are equally applicable to a fluid heated from the side) and surveys the current state of theory which is pertinent and linked to the Rayleigh-Bénard convection. The next section examines the current state of crystal growth especially problems focusing attention on the induced thermal oscillations.

Chapter Two commences with an introduction to the basic flow state. If we are going to consider the salient features of thermal oscillations in an annular configuration, a model should be developed and this is the main area of concentration in this chapter. However, certain approximations are introduced to reduce the complexity of the proposed model and still obtain meaningful results.

Turning now to Chapter Three we examine the stability characteristics and transformation of the basic eighth order differential equation describing the fundamental flow pattern into non-dimensional form. The final section of the chapter is concentrated on allowing the converted basic equation of flow be truncated to the small Prandtl number limit.

The final Chapter concentrates on the experimental apparatus: five different annular boats were employed with both mercury and gallium as the working fluid. The final section comprises the experimental results and the comparison between theory and experiment. The main conclusions are as follows:-

The structural state is a pre-requisite for the existence of

large amplitude temperature oscillations, to be initiated and sustained. Furthermore, this links both high and low Prandtl number fluids that together, for specific Rayleigh numbers, exhibit rolls, hexagons et sequ . The square rolls are certainly prominent for liquids whose cell length is greater than its depth. There is a critical temperature which must be exceeded before oscillations can commence. A comparison between the Lorentz model and the wave lengths in the structured state is good. Finally, an estimate of the velocities in a range of fluids is compared. The essential conclusion is that for high Prandtl numbers the magnitude of the velocity, induced in the fluid by Rayleigh-Bénard convection, is not large enough to provide a suitably large vertical shear. Likewise, the stabilizing effect of the vertical temperature gradient becomes too large for oscillations to occur.

CONTENTS

ACKNOWLEDGMENTS'

I am greatly indebted to Dr. B. Pamplin for his patient supervision and guidance, Bob Draper and other members of staff at the School of Physics, Bath University for their practical assistance. My grateful thanks are also extended to Mr. J. Metcalfe and Mr. G. Peck the Principal and Head of the Engineering Department respectively at Chippenham Technical College, for allowing me to carry out this research at the College, also for the help extended by the members of the Engineering Department especially J. Lynch. Finally, to Mrs. S. Rutledge for her ready and willing assistance with the preparation and typing of this thesis.

J.A. MILSOM MSc

PREFACE

At a meeting of the British Association in 1932 Sir Horace Lamb is said to have observed "I am an old man, when I die and go to heaven there are two matters which I hope for enlightenment: one is quantum electrodynamics the other is the turbulent motion of fluids. About the former I am really rather optimistic".

This is a pertinent comment as it is found with an overwhelming majority of flows actually encountered in nature and technology are, in fact, turbulent flows, where laminar flows, which are studied in detail in fluid mechanics, only occur as fairly rare exceptions and any application of hydrodynamics to real fluids is fraught with difficulties.

One of the most fascinating phenomena, not only in physics but also other areas is the spontaneous creation of structured states out of disordered states. In the continuously extended media which, by the change of external parameters, spatial, temporal or even functional structures are created.

There are numerous examples: the laser, the convection instability of fluids, brain models and models of morphogenesis. These examples can provide illustrations of the kind of patterns which may occur in the order state.

Paradoxically, competition is crucial for the laser, for evolution processes of biological molecular and population dynamics, yet co-operation is essential and leads to new structures in the Benard instability.

When fluids are heated from below or the side, for small temperature gradients, the heat is transported by conduction and convection also However, beyond a critical temperature gradient, on the account of buoyancy effects heat is transported mainly by convection initially in

the form of rolls and when the temperature gradient is increased more complicated structures such as hexagons etc. can occur. The warmer parts of the fluid flow upwards, cool down at the upper surface and return to the lower surface. Amazingly, this convection occurs in well regulated spatial patterns.

This thesis is concerned with the following aspects: First the analysis of research work conducted out by other workers both theoretical and practical as the results of fluids driven thermally i.e. the Rayleigh-Benard convection. However, liquids with small Prandtl number, thermal conduction proceeds rapidly and also the internal velocity develops very quickly. These facts, together with the non-linearity of the inertial terms generates an almost intractable differential problem. Nevertheless, the main task is to demonstrate that liquid metals have thermal properties which are similar to liquids of high Prandtl number i.e. Structured states. The existence of thermal oscillations is of great interest and the effect is certainly enhanced in liquid metals and semi-conductors. It has been found by many workers, that unless the oscillations are suitably reduced they result in resistive striations when semi-conductor crystals are grown from melts. A review of the research carried out by workers on temperature oscillations is presented. The intention is to develop a theory and to conduct experiments with liquid metals, and that there will appear, positive correlation, between theory and experiment.

It is hoped that the work carried out will throw considerable light on the essential physics of the problem and afford a method whereby temperature oscillations can be severely reduced in areas of crystal growth

Table of most important symbols

g	-	Acceleration due to gravity
ρ	-	Density of working fluid
α	-	Volume coefficient of expansion
c_p	-	Specific heat capacity
μ	-	Viscosity
ν	-	Kinematic viscosity
χ	-	Thermal diffusity
P	-	Prandtl number
Ra	-	Rayleigh number
Ra_{cr}	-	Critical Rayleigh number
Re	-	Reynolds number
Re_{cr}	-	Critical Reynolds number
G	-	Grashof number
p	-	Pressure
d	-	Depth of working fluid
x	-	Coordinate direction
y	-	Coordinate direction
z	-	Coordinate direction
r	-	Radial direction
ϕ	-	Azimuthal direction
u	-	Velocity in x direction
v	-	Velocity in y direction
w	-	Velocity in z direction
ΔT	-	Temperature difference
T	-	Temperature
θ	-	Temperature perturbation
θ'	-	Temperature perturbation in polar model
U'	-	Basic velocity flow in radial direction

u' - Perturbation velocity in radial direction

v' - Perturbation velocity in azimuthal direction

w' - Perturbation velocity in vertical direction

k - Wave number (k_1, k_2, k_3) respective x, y and z directions

ω - Angular frequency

Φ - Velocity potential

Y_1, Y_2, Y_3 - Linear growth rates

A_1, A_2, A_3 - Amplitudes

c - Constant of integration

δ_1, δ_2 - Numerical coefficients

β_1, β_2 - Numerical co-efficients

T_x - Temperature gradient x direction

T_r - Temperature gradient radial direction

T_z - Non-dimensional vertical temperature gradient

W - Width of boat

f - Frequency of oscillation

U_z - Non-dimensional shear

l - Vertical wave number

n - Horizontal wave number

A, B, C - Numerical constants

E - Non-dimensional ratio

R_o - Outer radius

R_i - Inner radius

q - Velocity vector

h - Aspect ratio

L - Effective boat length

σ_x - Complex frequency

T_L - Temperature at the lower plate

T_V - Temperature at the upper plate

t_c - Characteristic time interval

T - Mean period of oscillation

Y - Reynolds number function

σ' - Variation of viscosity with temperature

ϵ - Expansion parameter

ω' - Vorticity

θ - Temperature function

Constants are defined within the text for convenience of presentation and clarity.

CHAPTER I

Hydrodynamic instability of a fluid layer heated from below

When a vertical downward temperature gradient exists in a fluid, there is an additional destabilization of the flow due to buoyancy, which is similar to the effect of centrifugal forces in curved flow when the rotational velocity of the fluid increases with its distance from the centre of curvature. The converse phenomenon, an upward temperature gradient, has a stabilizing effect on the flow;in the case of curved flow with the velocity it is increasing with distance from the centre of curvature. The problem of the stability of a thin layer of fluid between two infinite planes at different temperatures is analogous to the stability problem of an incompressible fluid between two rotating cylinders.

The solution of the problem of instability will rest within the framework of Boussinesq equations for free convection. The vertical depth of the fluid will be very small when compared to its length i.e. a small aspect ratio. The only external mechanical force to be considered is gravity. It is assumed it is a constant throughout the layer and directed vertically downwards. Variations in density are assumed to be brought about by only moderate heating and are taken into account only in the buoyancy term of the Navier -Stokes equations. Thus density differences are considered to be much smaller than the mean density. Likewise the fluid properties η, k, c_p and α are assumed to be constant

The equations are as follows:

$$u_x + v_y + w_z = 0 \qquad 1.1$$

$$u_t + uu_x + vu_y + wu_z = -\frac{1}{\rho_0} p_x + \nu \nabla^2 u \qquad 1.2$$

$$v_t + uv_x + vv_y + wv_z = -\frac{1}{\rho_0} p_y + \nu \nabla^2 v \qquad 1.3$$

$$w_t + u w_x + v w_y + w w_z = -\frac{1}{\rho_0} P_z + \nu \nabla^2 w - \alpha g T \qquad 1.4$$

$$T_t + u T_x + v T_y + w T_w = \chi^2 \nabla^2 T \qquad 1.5$$

These five equations describe the properties of free convection and are normally called the Boussinesq approximation for fluid mechanics.

Consider a layer of fluid bounded by rigid planes $z = 0$ and $z = d$ which are maintained at respective temperatures T_L and T_V The boundary conditions will be

$$u = 0, \quad T = T_L \qquad z = 0 \qquad 1.6$$

$$u = 0, \quad T = T_V \qquad z = d \qquad 1.7$$

There are also other different physical conditions on the boundary layer. There have been enumerated by (1) Sparrow, Goldstein and Jonsson (1964) and (2) Hurle, Jakeman and Pike (1967).

The steady state stability is independent of the boundary conditions and will also be a state of rest. However, in the analysis the Boussinesq approximation: the density variations with the depth is negligibly small, will be taken for the disturbance equations. The results will, naturally be only valid for relatively thin layers. In the instance of very thin layers the results become invalid due to breakdown in linearity conditions of the temperature profile; this condition is fully tabulated in (3) Sutton (1950) and (4) Segel and Stuart (1962). Into the equations perturbations in velocity, temperature and pressure are introduced and then linearizing the Boussinesq equations in non-dimensional form the following expression for the temperature perturbation is obtained:

$$\Theta(\bar{x},t) = \mathrm{EXP}\left\{\frac{ik_1x}{d} + \frac{ik_2y}{d} - \frac{i\omega\vartheta t}{d^2}\right\}\Theta(\zeta) \qquad 1.8$$

$$\zeta = z/d \qquad 1.9$$

From equation (1.8) it is possible to derive the following eigenvalue problem:

$$\left(\frac{d^2}{d\zeta^2} - k^2\right)\left(\frac{d^2}{d\zeta^2} - k^2 + i\omega\right)\left(\frac{d^2}{d\zeta^2} - k^2 + i\omega P\right)\Theta + k^2 R_a \Theta = 0 \qquad 1.10$$

where $k^2 = k_1^2 + k_2^2$, $P = \frac{\vartheta}{\chi}$, $R_a = \frac{\alpha g \Delta T d^3}{\vartheta \chi}$ 1.11

Using conditions of rigid boundaries and fluid temperature we have the following conditions:

$$\Theta = \frac{d^2\Theta}{d\zeta^2} = \frac{d}{d\zeta}\left\{\frac{d^2}{d\zeta^2} - k^2 + i\omega P_r\right\}\Theta = 0 \qquad 1.12$$

$$\Theta = \frac{d^2\Theta}{d\zeta^2} = \frac{d^4\Theta}{d\zeta^4} = 0 \qquad 1.13$$

More extensive derivations are available in (5) Chandrasekhar (1961), (6) Stuart (1963) and (7) Lin (1955). Similar expressions with boundary conditions such as rigid boundaries of finite conductivity or boundaries with constant heat flux or a linear relationship between the heat flux and the temperature can be found. With every case we obtain an eigenvalue problem, which for a given Prandtl number, has only two parameters: the wave number k and the Rayleigh number Ra. It therefore follows, that for given values of k and Ra there will be a corresponding set of eigenvalues Wj, (k, Ra). The following constraints will be set upon the eigenvalues:

(a) if the lower boundary is at a lower temperature with respect to the upper boundary

(b) when the lower boundary is slightly warmer than the upper, all the eigenvalues Wj, (k, Ra) for all values of k, will have a negative imaginary part; there is associated with a critical temperature difference ΔT a critical value of Racr a value k = kcr will occur for which one of the eigenvalues Wj, (kcr, Racr) has a

zero imaginary part. A rigorous mathematical proof of this feature was first given by [8] Pellew and Southwell (1940).

The loss of stability of the state of rest in a fluid is characterized by obtaining some critical temperature difference say ΔT which leads to steady convection which is periodic with respect to x and y. All the essential features, from a qualitative viewpoint, for the transition from stability into instability in a layer of fluid heated from below were described very clearly by [9] Rayleigh (1916) who analyzed the mathematically simpler problem of convection in a layer of fluid between two free boundaries at constant temperature. In essence this problem reduces to an eigenvalue problem for the differential equation:

$$\left(\frac{d^2}{d\zeta^2} - k^2\right)\left(\frac{d^2}{d\zeta^2} - k^2 + i\omega\right)\left(\frac{d^2}{d\zeta^2} - k^2 + i\omega P\right)\Theta + k^2 R_a \Theta = 0 \qquad 1.14$$

with associated boundary conditions for $\zeta = 0, \quad \zeta = 1$

$$\text{for } \Theta = \frac{d^2\Theta}{d\zeta^2} = \frac{d}{d\zeta}\left(\frac{d^2}{d\zeta^2} - k^2 + i\omega P\ \Theta\right) = 0 \qquad 1.15$$

To estimate the eigenvalue spectrum and the critical Rayleigh number and associated wavelength it is sufficient to consider (1.14) having the value $\omega = 0$, and then (1.14) reduces to:

$$\left(\frac{d^2}{d\zeta^2} - k^2\right)^3 \Theta + k^2 R_a \Theta = 0 \qquad 1.16$$

Kernel solutions of (1.16) which also satisfy (1.15) for $\zeta = 0$ and $\zeta = 1$ are of the form: $\Theta = \sin n\pi\zeta$ where n = 1, 2, ... etc. Therefore for sufficiently large values of Ra we obtain a series of different natural disturbances where $\omega = 0$ and the wave numbers satisfy:

$$\left(\pi^2 n^2 + k^2\right)^3 = k^2 R_a \qquad 1.17$$

The minimum Rayleigh number for every given value of k will correspond to a disturbance for the lowest value of n viz n = 1.

Then the critical Rayleigh number is $Racr = \underset{k}{\text{minimum}} \left(\frac{\pi^2+k^2}{k^2}\right)^3$ 1.18

This will yield $Racr = \frac{27\pi^4}{4}$ where $kcr = \frac{\sqrt{2}\,\pi}{2}$ 1.19

To obtain meaningful results for convection between rigid fluid temperature boundaries, a similar calculation as above, is required; however, numerical methods are introduced. These numerical calculations have been carried out by [10] Low (1929), Pellew and Southwell (1940), Lin (1955), [11] Reid and Harris (1958) and Chandrasekhar (1961). For the rigid boundary conditions $Racr \simeq 1708$ and the critical wavelength, $kcr \simeq 3.12$. The values for k and the first 10 eigenfunctions of the eigenvalue problem is given in the work of [12] Catton (1966). The value of k gives only the periodicity of the flow in the (x,y) plane and not its amplitude and characteristics. It is possible to replace the function $\exp\left\{i\frac{k_1 x + i k_2 y}{d}\right\}$ in equation (1.8) by a more general function of the form $\Phi(x,y)$ which will satisfy the following partial differential equation:

$$\Phi_{xx} + \Phi_{yy} + \Phi_{zz} + \frac{k^2}{d^2}\Phi = 0 \qquad 1.20$$

The new function will predict more accurately, the nature of the pattern with which the cells break into. However, Stuart (1963) showed that the flow will break down into a set of cells termed Benard cells after [13] Benard (1900) who first observed the phenomena, experimentally. The cells adopt the form of hexagonal prisms, where in the centre the fluid flows upwards and on the edges it will move downwards depending on the nature of the initial conditions. [14] Christopherson (1940) determined the exact form of, Φ, and comparisons with velocity fields corresponding to the appropriate eigenfunctions. The basic ideas with observations may be found in Chandrasekhar (1961) and also in [15] Stuart (1964).

An alternative configuration is to have the upper boundary of

the fluid free with a fixed temperature; the only modification is to replace the boundary condition

$$\Theta = \frac{d^2\Theta}{d\zeta^2} = \frac{d}{d\zeta}\left(\frac{d^2}{d\zeta^2} - k + i\omega P\right)\Theta = 0 \qquad 1.21$$

on $\zeta = 1$, by $\Theta = \frac{d^2\Theta}{d\zeta^2} = \frac{d^4\Theta}{d\zeta^4}$ 1.22

This in turn yields a new eigenvalue problem which produces a new value for Θ the loss of stability Racr $\simeq 1100$. The critical Rayleigh value, for convection between rigid boundaries has been confirmed experimentally and the agreement is good. The experimental work has been comprehensively covered in Chandrasekhar (1961) and Sutton (1950). [16] Thompson and Sogin. Critical Rayleigh values for other boundary conditions are quoted in Sparrow, Goldstein and Jonsson (1964) Hurle, Jakeman and Pike (1964) and [17] Nield (1967).

A further increase of the temperature difference, and a corresponding increase in the Rayleigh number above the value of Racr, the steady 'cellular' convection pattern is maintained, but then it becomes unstable and for a Rayleigh number of the order of 5×10^5 disordered turbulent motion arises. The transition from laminar to turbulent flow occurs in a series of discrete jumps. Each region of convections which is more disordered than the preceding one. The characteristics of these regions is discussed more fully in [18] Malkus (1954) and [19] Willis and Deardoff (1967).

Section (ii)

Stability Characteristics of flows

One of the simplest methods of investigating stability of flows associated with disturbances or perturbations of finite amplitude is the 'Energy Method' first introduced by [20] O. Reynolds in (1894). An analogue approach was also employed for thermal convection problems especially by Sorokin [21] (1953, 1954) and [22] Joseph (1965, 1966). Joseph obtained the following result: the convective motion will be universally stable to any disturbance of the velocity

or temperature if $0 < R_a < \frac{\pi^2(\delta - R_c^2)}{2}$

And in the particular case of a stationary horizontal fluid layer, which has $\delta = 3\pi^2$ and $R_c = 0$ we obtain Racrmin > 180 The preceding value was improved by suitable omission of a term in the equation of the balance of intensity and a new value of Racrmin > 360 was obtained. However, the value obtained from linear theory is Racr $=$ 1708, which is not in good agreement.

Employing the methods of variational calculus it is possible to evaluate a minimum eigenvalue of an associated eigenvalue problem for a system of partial differential equations. This eigenvalue problem is in agreement with the eigenvalue problem of linear stability theory corresponding to disturbances governed by the principle of exchange stabilities. This technique was confirmed by Sorokin (1953), who simultaneously gave a proof of the validity of the principle of exchange stabilities in thermal convection problems.

Joseph (1965) also confirmed the work of Sorokin.

In the deduction of the unknown minimum eigenvalue, Racrmin, replaces the parameter Ra of the linear disturbance theory in the boundary value problems. Now the last estimate of Racrmin cannot exceed Racr Hence the energy method, in the case of pure convection, gives a precise value of Racrmin. Furthermore, it confirms that the structure of the Boussinesq approximate theory of convection of a fluid layer heated from below will be stable to arbitrary periodic disturbances of all Rayleigh numbers lower than that predicted by linear disturbance theory.

Other applications of the energy method to thermal convection problems, especially with the nature of flow patterns in the presence of internal heat sources have been considered by [23] Joseph and Smir (1966) [24] Joseph and Carmi (1966) and [25] Joseph, Goldstein and Graham (1968).

Another method of approach to stability theory is to investigate the behaviour of a complete system of non-linear dynamical equations and the Reynolds number will be used. The most general results on the nature of finite disturbances with Re in the region of R_{ecr} which are independent of the form of the hydrodynamical equations which were evaluated by Landau [26] (1944). Consider the situation where $R_e > R_{ecr}$ but with Re - Recr small. When the condition Re=Recr is satisfied there will occur a perturbation of frequency, ω having a zero imaginary part. However, with Re - Recr having a small positive value there will exist an infinitesimal perturbation with velocity field of the form

$$u(\underline{x},t) = A(t)f(\underline{x}) \qquad 1.23$$

where the following conditions are imposed upon

$A(t) = e^{-i\omega t} = e^{\gamma t - i\omega_1 t}$, γ = imaginary $\omega > 0$

and as $\gamma \to 0$, $R_e \to R_{ecr}$ implying that $\gamma << |\omega_1|$

with a very small difference between Re - Recr. Then $f(\underline{x})$ is an eigenfunction of the corresponding eigenvalue problem. Then A(t) will satisfy the differential equation:

$$\frac{d|A|^2}{dt} = 2\gamma|A|^2 \qquad 1.24$$

However, (1.24) is only valid within the framework of linear disturbance theory. Hence, as A(t) increases there will come a juncture when the theory is no longer valid and a theory which encompasses non-linear terms will be necessary. The right hand side of (1.24) may be looked upon as the first term in a power series expansion of $\frac{d|A|^2}{dt}$ It is possible to take account of the non-linear terms by application of other conditions, and the following differential equation arises:

$$\frac{d|A|^2}{dt} = 2\gamma|A|^2 - \delta|A|^4 \qquad 1.25$$

The additional coefficient δ can have a positive or negative sign and may be zero only in exceptional circumstances. The general solution of (1.25) will be:

$$|A(t)|^2 = \frac{Ce^{2\gamma t}}{1+\frac{\delta}{2\gamma}Ce^{2\gamma t}} \qquad 1.26$$

It should be noted the third order terms in A and A^* will contain a periodic factor and they will disappear during the averaging. For the fourth order terms, after averaging, there will only remain a term proportional to $|A|^4$ Returning to solution (1.26). The constant is only a constant of integration. Consider the conditions when: $\delta > 0$, $|A(0)|^2$ the amplitude will initially increase exponentially as with the linear theory, however the rate of increase will slow and as, t, approaches large values and the amplitude will approach a finite value of $A(\infty) = \left(\frac{2\gamma}{\delta}\right)^{1/2}$ which is independent of A(0). Now Y is a function of the Reynolds number and Y = 0 occurs when Re = Recr. However, Y may also be expanded as a power series of the form Re - Recr but having the constraint $\delta \neq 0$ for Re = Recr it then follows that $\gamma \sim (R_e - R_{ecr})$ and consequently the following condition now holds that $A(\infty) = |A|_{MAX} \sim (\mathrm{Re} - \mathrm{Recr})^{\frac{1}{2}}$ for small Re - Recr.

We will not consider the case where $\delta < 0$ it is not relevant to our discussion. Our attention is focused on the conditions $\delta > 0$ $R_e > R_{ecr}$ The perturbations may be viewed as the soft selfexcitation of an elementary oscillator which produces steady periodic oscillations with small, but finite amplitude $\propto (\mathrm{Re} - \mathrm{Recr})^{1/2}$ Nevertheless, equation (1.25) defines only the amplitude of the oscillations not the phase. The essential feature of such an oscillator is that it comprises of a single degree of freedom, which is contrary to steady laminar flow which is uniquely defined by boundary conditions and exhibits no property analogues to a spectrum of degrees of freedom.

As the values of Re is further increased the periodic motion itself may become unstable to small disturbances of the form $v(x,t)$ The instability of flow, with a velocity field taking the form $u(x)+v(x,t)$ where u represents the final value of the disturbances associated with (1.23) which, in turn, depends on (Re - Recr), may be investigated by the method of ordinary disturbances.

It is only necessary to investigate particular solutions of the linear equation with a perturbation $v(x,t)$ of the form $v = \exp(-i\omega t) f(x)$ 1.27 where f is a periodic function of time having a period $\frac{2\pi}{\omega_1}$ and to determine the frequency when $\omega = \omega_2$ with which as Re increases, there will first appear for Re = Recr a positive imaginary part. Now as t approaches extreme large values, quasi-periodic oscillations will occur with two periods $\frac{2\pi}{\omega_1}$ and $\frac{2\pi}{\omega_2}$ having two degrees of freedom . Hence it is possible to extrapolate a concept of intervals between critical Reynolds numbers which will decrease continuously and the oscillations which arise will be of higher and higher frequency and of smaller scale. Hence, for sufficiently large Reynolds number the motion will have many degrees of freedom and be very complex and disordered.

The discussion has illustrated the core of Landau's theory concerning the onset of turbulence. However, it is really difficult to assume it is rigorous and complete. It is founded on the assumption that a single perturbation will be induced at small positive values of Re - Recr but many disturbances will often exist for Re $>$ Recr and their interactions are of considerable importance. See [27] Eckhaus (1965). Furthermore, terms such as $|A|^6$ also play an important part as indicated by [28] Ponomarenko (1965). However, the most important defect of Landau's theory is that, so far, it has not been verified by direct calculations to any problem and the process of transition

to turbulence which it describes is in no way universal. Consequently, turbulent motion will occur as a result of instability with respect to finite disturbances, while at the onset it will contain a very large number of degrees of freedom.

Convection in a fluid layer heated from below and other similar problems have also been investigated from another direction [29] Yudovich (1966) and (1967). With the aid of the combination of the topological method of Krasnosel'skiy and the analytical method of Lyapunov - Schmidt. Yudovich illustrated that when Ra slowly increases and passes through the critical value Racr two new steady solutions of given periodicity in the (x,y) plane appeared; both these values having asymptotic expansions in powers of (Ra - Racr) Furthermore, the equilibrium solution turns out to be unstable for super-critical Ra numbers and the other two solutions are stable with respect to small disturbances of the same periodicity. However, the consideration of two different periodicities is required to explain the formation of hexagonal cells in convection.

Stationary cellular solutions arise with an amplitude which is proportioned to (Ra - Racr) subject to the constraint that the ratio $\frac{Ra - Racr}{Ra}$ is small. This fact is in agreement with the concept for $Ra > Racr$, there occurs softly excited oscillations spatially rather than temporarily orientated corresponding to the Landau theory. Additionally, cellular solutions of the non-linear Boussinesq equations were studied by Sorokin (1954), [30] Gorkov (1957), [31] Malkus and Veromis (1958), [32] Kuo (1961) and [33] Bisshopp (1962), [34] Stuart (1958) employed an approximate solution to equation (2.39) the so called 'shape assumption': that the character of the perturbations do not change with time, and coincide with unstable perturbations which appear at Ra = Racr. He derived, that $\gamma \sim (Ra - Racr)$ from linear perturbation

theory and δ is directly related to the eigenfunction which ascribe the neutrally stable infinitesimal perturbation. The Landau-Stuart approach is not exact and is only a first order approximation for Ra when it is first greater than Racr. The more exact methods of Gor'kov , Malkus and Veronis, Kuo, Bisshopp et al, predict a large number of distinct stationary solutions to be derived in the form of two dimensional waves which are proportional to $\cos(k_1 x + k_2 y)$ subject to the constraint $k_1^2 + k_2^2 = k^2_{cr}$ which (under particular boundary conditions) produces: square cells, hexagonal cells et sequ.

A general method for the construction of stationary solutions to the non-linear convection equations for moderate values of Ra > Racr, was developed by Schlüter, Lortz and Busse [35] (1965). This method employed an expansion in powers of a small parameter, ϵ, linked to the expansions employed by Gor'kov and by Malkus and Veronis for the construction of specific solutions; these take the form of

$$u(x) = \epsilon u^{(1)}(x) + \epsilon^2 u^{(2)}(x) + \cdots \quad T(x) = \epsilon T^{(1)}(x) + \epsilon^2 T^{(2)}(x) + + \quad 1.28a$$

$$Ra = Ra_{cr} + \epsilon Ra^{(1)} + \epsilon^2 Ra^{(2)} + + - - \quad 1.28b$$

Certainly that up to the second-order terms and according constraint upon ϵ, we will have $\epsilon \sim (Ra - Ra_{cr})$

By setting the coefficients of equal powers of ϵ on both sides of the system of Boussinesq equations and each time employ the boundary conditions of the problem we obtain linearized convection equations. For higher order terms in the series, a sequence of systems of inhomogenous partial differential equations is obtained. Employing certain existence conditions it is possible to define all the $Ra^{(m)}$ and subsequently $u^{(m)}(\bar{x})$ and $T^{(m)}(\bar{x})$, $m = 2, 3$. In many cases they may be determined uniquely with aid of the corresponding inhomogenous partial differential system. Finally we define a parameter ϵ from the equality

$$Ra - Ra_{cr} = \epsilon Ra^{(1)} + \epsilon^2 Ra^2 + + + \quad 1.29$$

This approach was employed by [36] Segel (1966) to obtain the solution of a simple non-linear partial differential equation. Schlüter et al (1965) studied the stationary solutions obtained if the zero order approximation $U^{(1)}(\tilde{x}), T^{(1)}(\tilde{x})$ is chosen proportional to the function

$$\Phi(x,y) = \sum_{n=-N}^{N} C_n \, EXP\left\{ i\left(k_1^{(n)} x + k_2^{(n)} y \right) \right\} \qquad 1.30$$

where $k_i^{(-n)} = -k_i^{(n)}$, $i = 1, 2$: and $C_{-n} = C_n^*$; $(k_1^{(n)})^2 + (k_2^{(n)})^2 = K^2$ and K is a constant

In this context the existence conditions for solutions of the second-order system namely $U^{(2)}$, $T^{(2)}$ reduce to the condition $Ra^{(1)} = o$. If we select $Ra^{(1)} = o$, then the system of equations $U^{(2)}$, $T^{(2)}$ has unique solutions for an arbitrary choice of functions for (1.30) in the zero-order approximation. Furthermore, Schlüter et al illustrated that the number of functions, $\Phi(x,y)$ from which it is possible to construct stationary solutions $U(x), T'(x)$ up to terms of all orders ϵ, appears to be infinite. Thus, all existence conditions can be easily confirmed in the 'regular case' in which all angles between neighbouring $\underline{k}$ vectors are equal with regular case including, rolls, square cells, and hexagons.

When Ra >> Racr the preceding expansion methods are no longer valid.

The most fruitful approach is the application of numerical methods employing a variety of approximations. The aim is to determine using various boundary conditions and values of Prandtl numbers, steady state Boussinesq equations for simple two dimensional rolls. These procedures were adopted by: Kuo (1961), [37] Herring (1963); (1964) [38] Deardoff (1964), [39] Fromm (1965), [40] Veronis (1966), [41] Busse (1967), [42] Roberts (1966) and [43] Schneck and [44] Veronis (1967). The results obtained by these workers are in accordance with the existing data on convective heat transfer for large enough

Rayleigh numbers, and for the mean characteristics of temperature and velocity fields under such conditions. However, one feature which appears from the observations, is that the vertical profile of the mean temperature at a large Ra differs markedly from that of the linear profile which is observed at Ra : Racr. As Ra is increased, a large region in the centre of the fluid layer attains a nearly isothermal state in the mean; the thickness of this region increases with increasing Ra, almost all the change in the mean temperature is concentrated in two thin thermal boundary layers near the boundaries of the flow. The temperature field for large values of Ra is characterised by a large mass of nearly isothermal fluid in the centre of the fluid, and comprising of a series mushroom-shaped isothermals. A further feature is that in the almost isothermal centre region a small positive vertical temperature gradient, which is a reversal of the normal temperature gradient, occurs, when Ra/Racr is greater by several units. The reversal of temperature gradient in the central region of a fluid layer at $\frac{Ra}{Ra_{cr}} = 16$ was observed experimentally by [45] Gille (1967) by interferometric measurements.

Turning now to the important question of the existence of a preferred mode of disturbance which is the only physically possible solution in a real fluid. The linear stability theory predicts that for the condition Ra > Racr there will be an infinite set of unstable infinitesimal disturbances with exponential growth rates corresponding to a range of values of the wave number, k, in the region of the value k = kcr at which instability will first appear. The most unstable disturbance will be naturally the most rapidly increasing and will correspond to a particular value of k, However, there will be an infinite set of such disturbances, since for any given k the horizontal form of a disturbance may be described

by an arbitrary function such as $\Phi(x,y)$ satisfying equation (1.20).

Experimental evidence shows that under each specific set of conditions there will always arise only a disturbance having a strictly defined form. In particular a division of the horizontal plane into a set of regular hexagonal cells, with and associated amplitude. The Landau theory does not explain why perturbations with several different values of k never arise in the fluid and also among all the possible perturbations only one with a particular form of $\Phi(x,y)$ is naturally observed. Calculations by [46] Segel (1962) partially explain the problem that in a number of particular cases non-linear interactions of disturbances differing in wave numbers may lead to a vigorous growth of disturbances of one particular wave number, with the suppression of the rest. In his work Segel, considered a simple "pair interaction" of two rolls independent of the y coordinate in a layer bounded both above and below by plane-free boundary conditions. The evolution of a disturbance having a velocity component

$$w(x,t) = w(\xi,\eta,\zeta,t) \text{ where } \xi = \frac{x}{d}\ \eta = \frac{y}{d}\ \zeta = \frac{z}{d} \qquad 1.31a$$

and will take the form of:

$$w(x,t) = A_1(t)\cos k\xi f_1(\zeta) + A_2(t)\cos l\xi f_2(\zeta) + \text{other small complements} \qquad 1.31b$$

Employing the methods of [47] Stuart (1960) and [48] Watson (1960) Segel deduced the first non-linear approximations the 'amplitude equations' for the functions A_1 and A_2 in the following form:

$$\frac{dA_1}{dt} = \gamma_1 A_1 - (\delta_1 A_1^2 + \beta_1 A_2^2) A_1 \qquad 1.32$$

$$\frac{dA_2}{dt} = \gamma_2 A_2 - (\beta_1 A_1^2 + \delta_2 A_2^2) A_2 \qquad 1.33$$

When $A_2 = 0$ or $A_1 = 0$ the equations (1.32) and (1.33) yield equations which are equivalent to Landau's equation (1.49). The above equations will yield the following steady state solutions:

$$A_1 = A_2 = 0 \qquad 1.34$$

$$A_1 = 0\,; \quad A_2 = \left(\frac{\gamma_2}{\delta_2}\right)^{1/2} \qquad 1.35$$

$$A_2 = 0\,; \quad A_1 = \left(\frac{\gamma_1}{\delta_1}\right)^{1/2} \qquad 1.36$$

$$A_1 = \left(\gamma_1\delta_2 - \gamma_2\delta_1\right)^{1/2}\left(\delta_1\delta_2 - \beta_1\beta_2\right)^{1/2} \qquad 1.37$$

$$A_2 = \left(\gamma_2\delta_1 - \gamma_1\beta_2\right)^{1/2}\left(\delta_1\delta_2 - \beta_1\beta_2\right)^{1/2} \qquad 1.38$$

The important physical case will occur with 1.39

$$\gamma_1 > 0,\ \gamma_2 > 0,\ \delta_1 > 0,\ \delta_2 > 0$$

It follows that if (1.35) or (1.36) exhibits a stability then (1.37) or (1.38) will not be stable. It follows, therefore, with a wide range of physical situations the final stability state will comprise of a single roll alone, having a definite wave number.

A greater analysis of the equations, when Ra is just above Racr, reveals that if the linear growth rate γ_1 of the first roll is more than twice the growth rate Y2 of the second roll then in the final equilibrium state only the first roll will be present. For the condition with $\gamma_2 < \gamma_1 < 2\gamma_2$ then the solutions of (1.35) and (1.36) are locally stable and whether the final state is either (1.35) or (1.36) will depend on the boundary conditions. In thermal convection problems with Ra just greater than Racr and the instability of both primary rolls with $\gamma_1 > 0, \gamma_2 > 0$ one of the two rolls will necessarily decay. This affords an explanation why for small Ra-Racr, out of a whole range of unstable disturbances, that only one single wavelength k is observed. However, a more general approach and explanation of the mechanism of the selection of a single preferred wave number from a whole spectrum of unstable wave numbers for Ra Racr is given by [49] Ponomarenko (1968).

A role of fundamental importance is the investigation of the

FIGURE Ia

Stability range of rolls at Rayleigh numbers close to critical

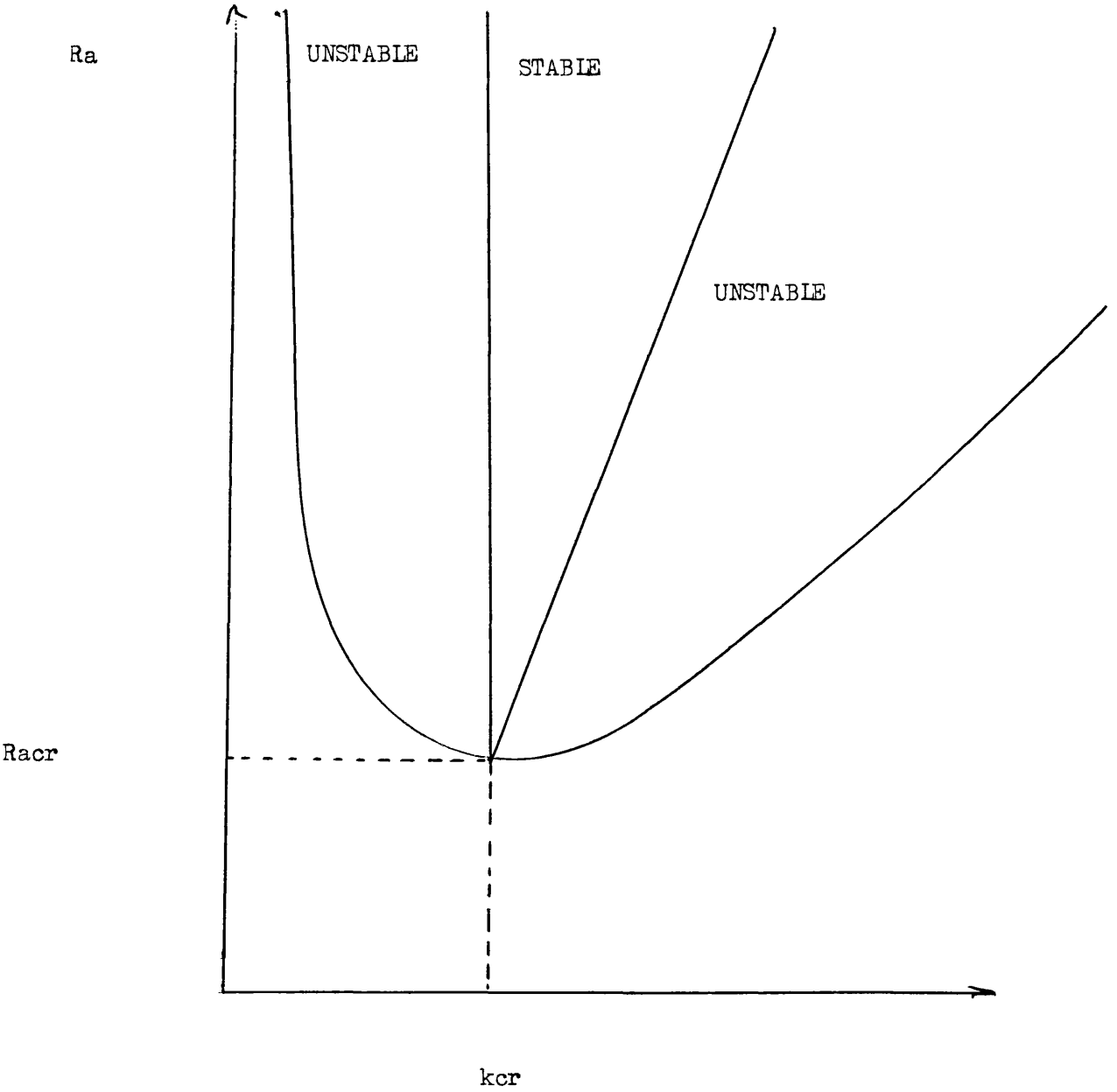

stability of the different steady solutions of the non-linear Boussinesq equations for Ra>Racr. One of the most complete investigations was conducted by Schlüter, Lortz and Busse (1965). These authors considered all the steady state solutions which arise from small perturbations of equation (1.30) at value just above the supercritical value of the Rayleigh number and investigated the stability of the finite amplitude cellular motions obtained. The following important conclusion was derived: that all the cellular solutions, with the exception of the simplest two dimensional rolls, which correspond to N = 1 in (1.30) are certainly unstable. However, for the exceptional case of the rolls with a given horizontal wave number k Schlüter et al showed that they are stable to all infinitesimal disturbances with same wave number k if only this wave number belongs to the band of unstable wave numbers. Finally, Schlüter et al investigated the stability of two dimensional rolls of finite amplitude to infinitesimal perturbations of horizontal wave number $k_1 \neq k$. They found that when Ra - Racr is small enough the rolls with wav e number $k < k_{cr}$, where k_{cr} is the wave number of the infinitesimal perturbation which is neutrally stable at Racr, cannot be stable to disturbances with arbitrary wave numbers. However, if k is greater than k_{cr} and $k - k_{cr}$ is small enough of the order of Ra - Rcr the rolls with wave number k are stable with respect to all possible infinitesimal perturbations. The full range of the stable two dimensional rolls for small enough values of the difference Ra - Racr > o found by the authors is illustrated in the figure (Ia). Schlüter, Lortz and Busse obtained their results by an expansion procedure in powers of a small parameter ϵ and are valid only for Rayleigh numbers in the region of the critical value. The general stability analysis for solutions of Boussinesq equations for

higher Rayleigh numbers is very complicated to carry out. But in the particular case of infinite Prandtl number the Boussinesq equations are considerably simplified, and the stability problem is possible to analyse mathmetically.

Employing numerical methods, Busse (1967) computed steady solutions of the Boussinesq equations with Prandtl number approaching very large values in the form of rolls for a wide range of Rayleigh numbers and investigated the stability of the solutions obtained with the aid of linear stability theory. He found that stable rolls are represented by a narrow elongated region on the (Ra, k) plane. The range of stable wave numbers for all Rayleigh numbers below 22, 600 is restricted to a small band, which is almost independent of the value of Ra, surrounding k_{cr}. At Ra = 22 600 all two dimensional solutions of the Boussinesq equations, subject to the condition Prandtl number is equal to infinity, becomes unstable see figure (Ib). There is agreement that the value of 22 600 is the same order of magnitude as the value of the Rayleigh number at which the second discrete transition in cellular convection was observed experimentally.

The foregoing theory always predicts that the only stable form of infinite amplitude cellular convection is in the form of two dimension rolls. However, another form which the convection may take is the form of regular hexagonal Bénard cells. The explanation why the theory does not predict the latter form of convection, is that other terms generally neglected in the Boussinesq approximation play a dominating role in practical experiments. (50) Palm (1960) was the first to point out that the usual Boussinesq equations for free convection do not afford a mathmetical explanation of the fundamental phenomena of hexagonal cellular convections. Experiments

FIGURE Ib

Stability region of rolls for a wide range of Rayleigh numbers with the Prandtl number equal to infinity

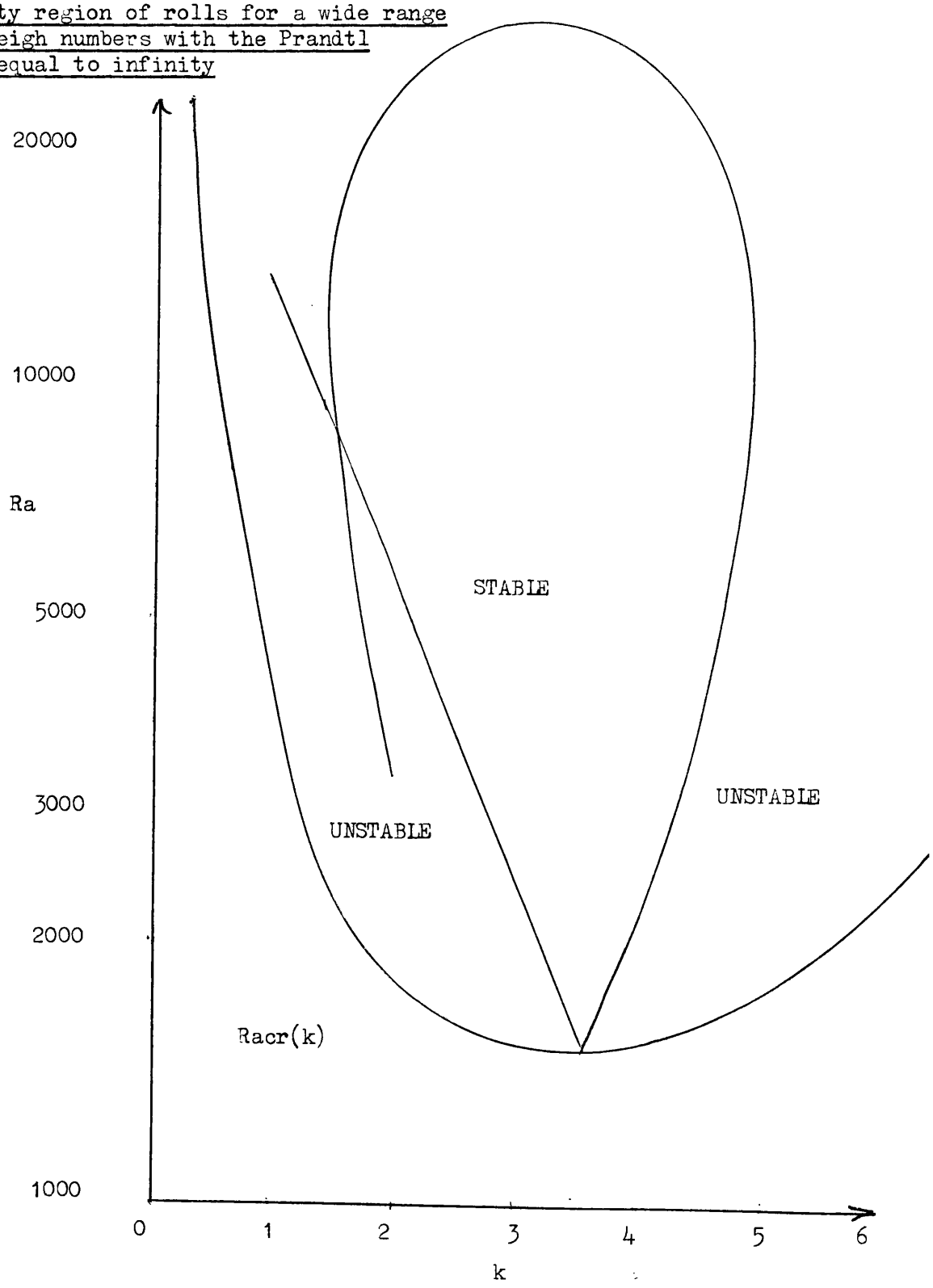

conducted by [51] Tippelskirch (1956) confirmed that the character of the circulation in the cells is a function of the dependence of the coefficient of viscosity on the temperature. With the condition

(i) $\frac{d\nu}{dT} < 0$ the fluid rises in the centre of the cells and sinks at the edges

(ii) $\frac{d\nu}{dT} > 0$ it rises on the edges and sinks at the centre.

Palm employed more complicated equations which also take account of the possible dependence of ν on T, and estimated the effect of this dependence on the value of Racr. Additionally, he assumed that at the initial time there arose, in the fluid, some 'basic disturbance' in the form of a roll, on which is then superimposed a weak 'background' of various other disturbances of small amplitude with the same and most unstable value of the wave-number vector k. In this instance the fundamental role will be played by "pair interactions" of this basic disturbance with other secondary order terms. Palm confined his attention to the study of the evolution of disturbances with vertical velocity

$$w(\underline{x},t) = u(\xi,\eta,\zeta,t) \qquad 1.40$$

where $\xi = \frac{x}{d}$, $\eta = \frac{y}{d}$ and $\zeta = \frac{z}{d}$ 1.41

and d is the depth of the fluid

Taking the form:

$$w(\xi,\eta,\zeta,t) = [A_1(t)\cos k\eta + A_2(t)\cos k_1\xi \cos k_2\eta]\, f(\zeta) \qquad 1.42$$

where $$k_1^2 + k_2^2 = k^2 \qquad 1.43$$

The disturbances with $k_1^2 + k_2^2 = k^2$ will be linked with the basic disturbance because quadratic combinations of these disturbances, which enter into the equations of fluid mechanics, may once again generate terms of the same form as the basic disturbance. At the commencement of his study Palm opposed the equation:

$$w(\xi,\eta,\zeta,t) = [A_1(t)\cos k\eta + A_2(t)\cos\left(\frac{\sqrt{3}k\xi}{2}\right)\cos\left(\frac{k\eta}{2}\right)]\, f(\zeta) \qquad 1.44$$

On the assumption that the interaction of any disturbances with the basic one under certain conditions, lead to the mutual amplification of both and as a result only these will play an important role in the convective pattern. The boundary conditions for simplicity, were selected as the unreal "free-free" case. Then letting $f(\zeta) = \sin A\zeta$ 1.45 Palm then deduced a system of differential equations for the amplitudes $A_1(t)$ and $A_2(t)$ Assuming that terms of order which are higher that the third in amplitudes may be ignored. The differential equations take the form of:

$$\frac{dA_1}{dt} = \gamma A_1 - \frac{1}{4}\sigma' A_2^2 - \delta_1 A_1^3 - (2\delta_2 - \delta_1/2) A_1 A_2^2 \qquad 1.46$$

$$\frac{dA_2}{dt} = \gamma A_2 - \sigma' A_1 A_2 - \delta_2 A_2^3 - (4\delta_2 - \delta_1) A_1^2 A_2 \qquad 1.47$$

Where $\gamma, \sigma', \delta_1$ and δ_2 are constant coefficients and $\gamma \sim (R_a - R_{acr})$ The variation of viscosity with temperature generates second order terms on the right side of the amplitude equations, whereas with differential equations of the previous work of Segel and Stuart (1962): (1.32) and (1.33) only first and third order terms are present. In the steady state differential equations (1.46) and (1.47) will reduce to

$$A_2 = \pm 2A_1 \qquad 1.48$$

which is the condition for the formation of hexagonal prismatic cells. Furthermore, Palm showed that for $\sigma' \neq 0$ only solutions, subject to this condition, will be stable for small perturbations of the respective amplitudes A_1, A_2 When thetime parameter approaches large values A_1, A_2 will also be the only acceptable solutions.

Further extensions and modifications were carried out on Palm's theory by the following workers: Segal and Stuart (1962), [52] Palm

and Ø̈iann (1964), [53] Segal (1964), [54] Busse (1967), [55] Palm, Ellingsen and Gjevik (1967) and [56] Davis and Segal (1968). The following conclusions of Palm's original work were found to be incorrect: the solutions of (1.46), (1.47) and (1.48) are stable for, in fact, only values of Ra - Racr that are not too large; Ra will be smaller than some value, say, Ra, where $Ra_1 > Racr$ which in turn depends on the "scale" σ' of the variation of viscosity. Furthermore, when $\sigma' \neq 0$ then for a small range of substantial values of Ra when $Ra_0 < Ra < Ra_{cr}$ where Racr - Rao is of the order of σ'^2 hexagonal steady motions of finite amplitude will exist, which are also stable to infinitesimal perturbations. Hence, the hexagonal convection cells are stable to all infinitesimal perturbations with the same horizontal wave numbers in the range $Ra_0 < Ra < Ra_1$ of Ra values; for $Ra > Ra_1$ the only stable solution of amplitude equations is that which corresponds to a convection pattern in the form of two dimensional rolls. Furthermore, the rolls are stable to all infinitesimal disturbances not only for $Ra > Ra_1$ but for a wider range $Ra > Ra_2$ where $Racr > Ra_2 > Ra_1$ All other forms of convection pattern are certainly unstable; hence for $Ra_0 < Ra < Ra_2$ only hexagons are stable, for $Ra_2 < Ra < Ra_1$ both hexagons and rolls are stable, and for $Ra > Ra_1$ only rolls are stable. When the Rayleigh number Ra is slowly increased the convection pattern commences growing at Racr and takes the form of stable hexagonal cells. At $Ra = Ra_1$ the hexagonal convection pattern becomes unstable and transforms into rolls, which are the only stable form at high Ra. With decreasing Rayleigh numbers the transition from rolls to hexagons occurs at $Ra = Ra_2$ when the rolls become unstable, and the convection decays after Ra = Rao has been passed. Thus, when the Rayleigh number initially increases slowly and then decreases slowly a hysteresis effect occurs. However, as

$\sigma' \to 0$ this causes the viscosity variations to disappear and all the values of Ra_0, Ra_1 and Ra_2 approach the value of Racr; the results then become identical with those of Schlüter, Lortz and Busse.

The influence of viscosity variation was obtained by Segel (1965) for a model where "free-free" boundary conditions were employed. Later Palm, Ellingsen and Gjevik (1967) considered all types of possible boundary conditions with permutations of rigid and free planes. They calculated all the critical values Ra_0, Ra_1 and Ra_2 for these cases. However, important work was conducted by Busse in 1962 and published in 1967 see Busse (1967). The method adopted by the author was a parametric expansion technique and accounted for not only the slight variation of viscosity with temperature, but of the thermal conductivity, the specific heat at constant pressure and the thermal expansion coefficient. He concluded that all the effects considered implied some stability situation. Davis and Segel (1968) showed for a fluid having independent properties, the hexagonal cell will appear for Ra sufficiently close to Racr, provided the boundary condition at the free upper surface allows for its deformation.

(57) Ponomarenko (1968) produced a very general approach to the problem of establishing hexagonal convection cells. He did not employ a specific form of dynamic equation, but concentrated on a dominant role which is played by the second order terms of the right hand side of the amplitude equations. The method employs the feature that these terms disappear for constant fluid properties and they make the equation for the amplitude of an isolated disturbance different from the Landau equation (1.25).

(58) Busse (1972) investigated the instability of convection rolls in a fluid layer heated from below having stress free boundaries,

for small Prandtl number. It is proposed that the two dimensional rolls which are initially set up become unstable to oscillatory three dimension disturbances when the amplitude of convective motion exceeds a particular critical value. It is proposed that the instability corresponds to the generation of vertical vorticity a mechanism which will operate in the case of a variety of roll-like motions.

The instability can manifest itself as wave travelling in either direction along the axis of the rolls or as a standing wave. The period of oscillations given in units of $\frac{d^2}{\chi}$ is

$$\tau_p = \frac{2}{\sqrt{3}k_2}\left\{\frac{Ra_c}{Ra_c - Ra}\right\}^{1/2} \qquad 1.49$$

The phenomenological picture of this type of instability compares well with the detailed observations by several workers of the oscillations of convection rolls in a layer of air. However, the authors stress the point that the oscillations occur essentially independently of depth which is a contradiction to earlier theoretical explanations. Busse (1972) also states the value of its smaller Prandtl number convection in mercury would probably afford a better opportunity for quantitative comparison with theory.

An important feature of the preceding analysis is that the oscillatory instability of rolls is caused solely by the action of hydrodynamic advection terms in the equations of motion. The mechanism of instability is thus independent of the release of gravitational energy which produces the convection of the rolls. The reason given is that any field of two dimensional vortices in the form of rolls can become unstable by the same mechanism of instability. The oscillatory instability of convection rolls is related at least phenomenologically to the non axisymmetric instability of Taylor vortices between concentric cylinders rotating at different speeds.

A number of observers, in particular, [59] Deardoff and Willis (1965), [60] Rossby H.T. (1969), [61] Krishna-Mutri (1970), [62] Busse and Whitehead (1974) and [63] Ahlers (1974), have also noted that beyond a particular Rayleigh number the convection flow is no longer steady. However, a number of problems arise with this phenomena. Krishna-Mutri (1970) asserts that for Prandtl number of the order of 50 the critical Rayleigh number approaches a constant value; but this fact is not in agreement with the findings of Busse and Whitehead (1974).

Experimental work has been carried out with liquid helium, by Ahlers (1974). He measured the total flux in a convection experiment and found there was a defined jump from steady flow to an unsteady flow with irregular time dependance. In addition, the white noise spectrum described by Ahlers (1974) may be the result of small regions of hot/cold fluid in the layer. They originate effectively in two thermal boundary layers close to each rigid horizontal boundary where the temperature gradient experiences the greatest deformation under extreme conditions observed in the turbulent area. The sporadic and random so called 'thermals' move rapidly throughout the cell, carrying a discrete amount of heat energy which is released at the upper thermode.

There are several theories which have been proposed to account for this phenomena. The first theory proposed by [64] Rossby (1969) was an adaption of a large Rayleigh number theory developed by [65] Howard (1963). Consider an instant of time say $t = o$, convection will have made the vertical temperature field uniform throughout the layer, however, not including two thin boundary layers adjacent to the horizontal boundaries. Now let T_1 be the 'uniform' temperature disturbance and T_2 be the temperature of the lower

interface; let $T_2 > T_1$ The diffusive boundary layer that will be initiated at each interface will have a width of $\delta(t_c) = \frac{d}{Pe^{1/2}(Kt_c)^{1/2}}$ where tc represents some characteristic interval. The temperature difference across the boundary layer will be $T_1 - T_2$ The uniform temperature difference itself will become unstable if

$$Ra_{cr} < \frac{(T_2-T_1)\alpha g \delta^3(t_c)}{\chi \nu} \qquad 1.50a$$

and convection will be developed in the boundary layer. This results in a 'sudden' instability as convection tends to increase the thickness of the layer, which will increase growth rate. Now a 'thermal' of temperature T_2 moves upward from the lower interface through the uniform temperature distribution T_1 Its momentum will destroy the boundary layer and the fluid will regain its initial configuration. This momentum will generate an oscillation of mean period τ which is of the order of the time delay required to build a new boundary layer and is given by

$$(\chi\tau)^{3/2}(T_2 - T_1) \sim 1 \qquad 1.50$$

from which we have:

$$\tau \sim (T_2 - T_1)^{-2/3} \qquad 1.51$$

This power dependance given by (1.51) is in good agreement with the experimental results of Rossby (1969).

The second approach was proposed by [66] Welander (1967). He considered a temperature fluctuation which is convected by the flow. To a first order approximation the temperature fluctuation will rotate within the roll with an average period which is approximately proportional to the convective time delay imposed by the velocity field. The temperature perturbation will have a velocity smaller when moving downwards than the convective flow velocity and the converse when moving upwards. Hence, the perturbation will, on balance, become greater on each rotation; however the process is also counteracted by heat and vorticity diffusion.

In the high Prandtl number limit Krishna-Murti has observed oscillations of the convection pattern which are similar in nature to the fluctuations predicted by Welander. However, [66] Willis and Deardoff (1970) state there is no fundamental difference between the fluctuations in liquids of high Prandtl number e.g. silicone oil $P \approx 57$ and air, having a Prandtl number of $P \approx 0{\cdot}7$ In addition, they studied the temperature fluctuations at low Prandtl number and have shown that the oscillations are independent of the depth. The measurements of Busse and Whitehead (1974) with large Prandtl number were as follows: they first observed an oscillatory instability whose general structure closely resembles the low Prandtl number case and they also observed that when the oscillations exceeded some level a transition occurred to a more irregular phenomenon which they termed 'spoke pattern'. The recent results of [67] Clever and Busse (1974) are important. In their comparison of an infinite array of two-dimensional parallel rolls to infinitesimal time dependent perturbations above a critical Rayleigh number they have proposed a number of instabilities. The two important ones are:-

(i) The Zig-Zag Instability

It has a special periodicity to the primary roll pattern and along the x axis. It also has a non-vanishing wave number component b along the y direction which is perpendicular to the primary structure. The growth rate and periodicity b of this instability vanishes at least as b^2 with vanishing b. Hence, this instability tends to reduce the effective wavelength of the rolls and represents a small shift in the roll pattern in the y direction.

(ii) The oscillatory instability

This instability has similar features the previous instability, however, it corresponds to a bending of the primary rolls that propogate with time along the roll axis.

Another approach was that of [68] Saltzmann (1962); the Boussinesq equations were replaced by a truncated set. He employed boundary conditions which were stress-free and considered only a two dimensional roll pattern. The stream function and the temperature perturbation take the form of:

$$\psi_1 = \left\{\frac{1+a^2}{a}\right\} x\sqrt{2}\sin\left(\frac{ay\pi}{d}\right)\sin\left(\frac{z\pi}{d}\right) \qquad 1.52$$

where $a = \frac{k}{\pi}$

$$\Theta_1 = \frac{\Delta T}{\pi} Ra\left\{Y\sqrt{2}\cos\left(\frac{ay\pi}{d}\right)\sin\left(\frac{z\pi}{d}\right) - z\sin\left(\frac{2\pi z}{d}\right)\right\} \qquad 1.53$$

Hence only three modes are retained (a) velocity potential and a temperature mode with a fundamental cellular wave number (b) a second temperature mode a second harmonic in z that has no horizontal periodicity and that contributes to the vertical mean flow. Substitution into (1.52) and (1.53) into the Boussinesq equation yields

$$x_t = P_r(y-x) \qquad 1.54$$

$$y_t = -xz + rx - y \qquad 1.55$$

$$z_t = xy - bz \qquad 1.56$$

where $r = \frac{Ra}{Ra_{cr}}$; $b = \frac{4}{1+a^2}$

The time has been made dimensionless with the scale which is the mean diffusion time of a temperature fluctuation across a cell. The only non-linear terms which have been retained in the model arise from the inertial term in the heat equation. The inertial term in the Navier-Stokes equation has also been ignored; this will naturally restrict the consideration to infinitely large Prandtl number fields i.e. $\mathcal{P} \gg \chi$ having a non-dimensional velocity not of the same order as the Prandtl number. With liquid metals such as mercury and gallium they are on the boundary of applicability.

Section (iii)

Crystal Growth Problems and Applications

The study of natural convection of enclosed fluid, subjected to a horizontal temperature gradient, has focused considerable attention. The majority of the work has been centred on geometry with a large aspect ratio. [69] Batchelor (1954) investigated, theorectically, the conduction dominated and transition areas. Further work carried out by [70] Elder (1965), experimentally, investigated the laminar boundary layer region and reported the existence of secondary and tertiary flows before the commencement of turbulence in boundary layers. The stability of the flow has been investigated by [71] Gill (1966); [72] Gill and Davey (1969) and more especially the heat transfer characteristics by Newel and [73] Schmidt (1970). The work has shed considerable light on the features of internal natural convection with imposed temperature gradients for large aspect ratios.

Workers in the field of crystal growth have brought to light a complementary stability problem, which occurs in the melt from which crystals are grown. The problem is centred upon internal natural convection, due to an imposed horizontal temperature difference; however, having aspect ratios which in some cases are less than unity.

Turning now to the production of crystals. There are essentially three general methods for melt growth, the horizontal normal freeze, zone melting and Czochralski technique. The method which will interest us here is the zone melting technique. Employing this technique, the material is contained in a horizontal rectangular box with dimensions 100 mm in length 30 or 20 mm in width and height. The material crystallizes out preferentially at one end of the melt due to an imposed temperature gradient. If crystals are grown from

melts other than pure elements, striations are often observed in the crystals at right angles to the growth axis. [74] Ueda (1961) reported the existence of resistive striations in melt-grown crystals and showed that the striation repeat distance is a function of the temperature crystal growth. Further workers [75] Cole and Winegard (1965), [76] Utech and Fleming (1966) and [77] Hurle (1966) demonstrated that there is a strong correlation between striations in crystals and temperature fluctuations in the melt. Temperature oscillations in mercury were first observed by [78] Bradshaw (1966) and reported by [79] Pamplin (1967). Furthermore, Hurle (1966) has demonstrated, under suitable constraints, the temperature fluctuations are sinusodial oscillations which can persist for long periods of time. Hurle has suggested that the oscillations are an example of the phenomenon of overstability which is discussed fully by Chandrasekhar (1961). Hurle (1966) and Utech and Fleming (1966) showed that the oscillations can be damped by a transverse magnetic field and this implies that the oscillations are hydrodynamic in character, rather than the early observations which ascribed the process as the periodic release of latent heat of fusion during solidification.

Further work has also been conducted to gain a fuller insight into the understanding of the nature of the oscillations. Hurle (1966) concluded, from employing liquid gallium as a working fluid, that a critical horizontal temperature is a prerequisite for initiating oscillations. Furthermore, the temperature decreased with increasing boat length andfrequency of the oscillations also decreased. [80] Johnson (1967), using liquid gallium as well, found that the frequency of the oscillations was proportional to one quarter power of the depth. Also the critical temperature by suitable experimental investigations,

increased as the square of the Hartmann number on the application of a transverse magnetic field. Further work was also conducted on the mean temperature field; however, any correlation with the oscillations was not recorded. Bradshaw (1966) was able to show that thermo solutal instability did not effect the oscillations, by varying the purity of mercury. He also found by severely reducing the width or boat length the oscillations could be eliminated. This feature has been confirmed tentatively by [81] Gill (1974). When the ratio of the width to the depth is equal to 0.58, both the Rayleigh number and the theoretical frequency becomes infinite. Therefore, oscillations are not possible if the ratio is less than 0.58.

[82] Skafel (1972) conducted the majority of his experiments with an annulus subjected to a radial heat flow. He measured the mean temperature profiles and the power spectra of oscillations just above threshold. Spatial correlation mea-surements suggested the existence of a progressive wave in the azimuthal direction. Observations of the mean temperature profiles in the annulus, at critical temperature gradients, see Skafel's table (1), the frequency varied, inversely with the depth.

[83] Hurle et al (1974) had studied convection in a rectangular box geometry containing molten gallium. This paper represents a comprehensive review of the phenomenon. From measurements of the frequency of the oscillations in depth ranges 5 to 6 mm and9 to 13.5 mm. They had concluded that the period of the oscillations was essentially constant; however, there was a marked dependance of the frequency of the oscillations on the boat length for lengths in the range 20 to 40 mm. The aspect ratio was varied between 0.21 to 0.52. Work was also conducted on the dependance of the critical temperature on the application of a transverse magnetic field. [84] Bolt (1975) also

carried out experiments in a box geometry system with mercury as the working fluid; however, with very small aspect ratios in the range 0.052 to 0.081. He concluded for depths ranging from 5 to 8 mm the frequency of the oscillations was proportional to the depth.

This section of the study is only a quantitative assessment of the various author's findings. At a later juncture a qualitative assessment of both the theoretical and all the experimental results will be conducted.

The knowledge of the flow regime in annuli and slots of similar Rayleigh numbers, but with aspect ratios in the region of unity or greater have been investigated theoretically; in particular the slot problem by Elder (1965) and the annular problem by [85] Thomas (1970).

Thomas employing numerical models obtained the following flow characteristics: (for small h)

(a) $\frac{\text{Rayleigh Number}}{\text{Aspect ratio}} < 400$ = Conduction region

(b) $\frac{\text{Rayleigh Number}}{\text{Aspect ratio}} > 30000$ = Boundary layer region

However, if h is greater than 5 the results are weakly dependent on the Prandtl number.

For an aspect ratio of 1; the following criteria are more relevant:

(a) Rayleigh number < 1000 = Conduction region

(b) Rayleigh number > 8000 = Boundary layer region

Thus for motion to be initiated and maintained, in a low aspect ratio cavity a higher Rayleigh number is always necessary.

Elder has confirmed experimentally for an aspect ratio greater or equal to unity and for a Rayleigh number less than 1000 the vertical temperature gradient is zero. However, in the interval of a Rayleigh

number greater than a 1000 but less than 100,000 there are larger temperature gradients in the proximity of the vertical walls and the flow away from the horizontal boundaries is concentrated mainly in the vertical boundary layers.

The interior has no effective motion and is coupled with a positive vertical temperature gradient having a constant value away from the horizontal boundaries for an aspect ratio greater than unity. In the region of a Rayleigh number of 100,000 secondary motion is induced, and the flow field remains laminar to a Rayleigh number of a very high order. The onset of turbulence is a function of the aspect ratio commencing at a lower Rayleigh number for larger aspect ratios. In conclusion, no reports of the regular temporal oscillations have been recorded for aspect ratios greater than or equal to unity.

CHAPTER II

Chapter II

Section (i)

Introduction to Basic State

The genesis of the theory lies in the pioneering work of Hadley (1735)[86] who proposed a single cell, thermally direct driven zonally symmetric model of the general circulation of the earth; such regions of circulation are now called Hadley circulations. Hart (1972)[87] in his paper "stability of thin non-rotating Hadley circulations" considered a simple parallel flow model with a small aspect ratio. The Hadley circulation was contained in a two dimensional box with rigid horizontal boundaries maintained at a temperature which increased linearly with the horizontal coordinate. The small aspect ratio implied that the vertical velocities were concentrated in narrow regions near the ends.

In the basic flow state several modes of energy transfer to and from the mean kinetic and potential energies were able to occur. The transverse disturbances, with symmetry normal to the shear vector, were always more unstable than the horizontal disturbances, with symmetry parallel to the shear vector. Hart obtained exact solutions for the neutral stability curves as a function of the Prandtl number.

Gill (1974), using the work of Hart as a foundation, derived a model for the explanation of thermal oscillations created spontaneously in a crystal growth melt. The reference frame considered was a right handed Cartesian system with the x axis pointing in the direction of an increasing horizontal temperature gradient. The fluid was constrained between two boundaries situated at a distance d apart.

The mechanism of the basic state could be described as follows: the horizontal buoyancy gradient generated a vorticity leading to a

shear strain; the velocity generated was a function of z alone. Then the end effects could be ignored for a cavity whose depth was small as compared with its length, i.e. a small aspect ratio. The basic flow pattern was a single convective roll. Then the velocity and temperature perturbation was superimposed on the basic flow, subject to the constraint $\frac{\partial}{\partial x} = 0$

From a complex potential $\omega = \phi + i\psi$ was defined a two variable stream function, namely $\psi = \psi(y,z)$

Application of three hydrodynamic equations: x component of momentum, vorticity equation, coupled with the temperature equation and an eighthorder differential equation expressed in terms of the stream function was derived. Then the eighth order differential equation was made non-dimensional by the introduction of non-dimensional values, the Prandtl and the Rayleigh numbers. An expression for the condition of marginal stability was determined. With either of the boundaries of rigid or free conducting, oscillatory instability was only possible for a Prandtl number less than 3. Finally, an expression for the frequency of oscillation was derived.

Gill concluded that the oscillations were primarily longitudinal in nature and could be explained in terms of a diffusion dominated inviscid model, Considering now the essential features of explanation of the oscillations. If a simple roll convection cell is envisaged, then the plane z will lie between fluid layers with opposing directions directions of movement along the x axis. However, molecular diffusion will occur across this plane, for liquids of low Prandtl number it will be almost instantaneous. The x momentum of the molecules will be conserved and a perturbation velocity is superimposed in opposition to the main convective flow and this advection induces a corresponding temperature perturbation. The particles are at their minimum temperature

when at their maximum elevation; whence the restoring force is a maximum at this depth. Now the fluid is effectively inviscid and simple harmonic motion is the result. The overall pattern is shown explicitly in Gill's diagram of a vertical section through the fluid transverse to the imposed temperature gradient.

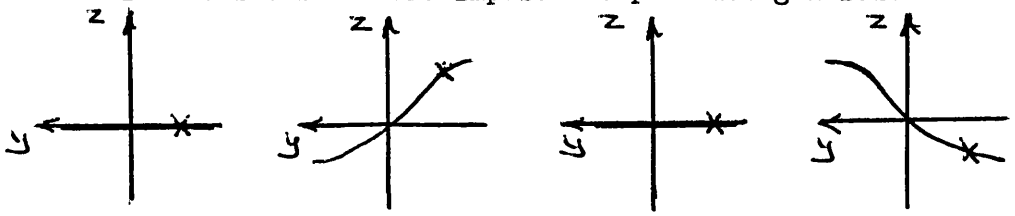

Successive positions (thick line) of the particles undergoing oscillations. Their equilibrium position is $z=0$ and the x axis is directed into the page. The fluid above $z=0$ is moving towards the reader and the cold wall. The fluid below $z=0$ is moving away from the reader

The oscillations in the rectangular boat are a function of the ratio of the width to the depth. His theory predicts a frequency, f, of oscillation of the order of f = $\sqrt{\frac{\alpha g T_x l_z}{\chi}} \quad \frac{l}{l^2+n^2}$

However, in the box geometry which is of finite dimensions the following constraints apply (88) Gill (1975)

(i) when the ratio of the width to the depth $\frac{W}{d}$ is less than 0.58 both Racr and the frequency σ becomes infinite

(ii) if the ratio of $\frac{W}{d}$ is less than 2.0 the disturbance wavelength is half the optimum value and the wavelength is selected by the geometry So $l \propto \frac{1}{W}$ and $n \propto \frac{1}{d}$ then

$$f \propto \frac{Wd^2}{W^2+d^2}$$

(iii) if $\frac{W}{d}$ is greater than the critical value of 2.0 then $\frac{l}{n}$ is fixed at the value for fastest growing wave and $n \propto \frac{1}{d}$ then

$$f \propto d$$

Section (ii)

The cylindrical Polar Model

The geometry of the system comprises of an annulus with a temperature difference maintained between the inner and outer cylindrical surfaces. The transformation between the cartesian and cylindrical coordinates are the following relationships:

$$x = r\cos\phi,\ y = r\sin\phi,\ z = z$$

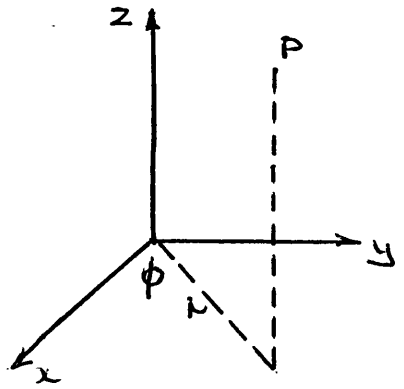

A typical point P is illustrated in the diagram opposite.

Turning now to the characteristics of the flow and ultimately equations governing the problem. The radial component points in the direction of an increasing temperature gradient. The horizontal buoyancy, due to Archimedian forces, will generate a vorticity leading to respective shear strains in the radial and vertical directions of U_r and U_z, and the advection by the associated velocity will generate a vertical temperature gradient T_z. When the aspect ratio is small, following the pattern of the Gill exposition, the vertical flow will be concentrated in the end regions. Naturally, for the theoretical model, the assumption is that R_i is very much smaller than R_o, which is not always true for the practical model. Nevertheless, it is possible to derive a positive correlation between theory and experiment and estimate the region, where agreement between theory and experiment diverges.

The shear is a function of both r and z; hence it follows that the velocity, in the steady state, will be $(U'(z,r), 0, 0)$ whence the velocity vector is

$$\underline{v} = U'(z,r)\hat{r} + 0\hat{\phi} + 0\hat{z} \qquad 2.1$$

where $\hat{r}$, $\hat{\phi}$ and $\hat{k}$ are unit vectors in polar coordinates. This is assuming one convective roll. In the steady state the temperature equation is given by:

$$\frac{DT}{Dt} = U' T_r \qquad 2.2$$

Measurements of horizontal temperature profiles have shown that the horizontal temperature gradient is not uniform across a cell length. Hurle et al (1974) experimented with heat flow which was slightly off axis by covering one half of each thermode with mica strips. The use of an off axis heat flow wasfound to give rise to very stable oscillations. This accounted for the authors early experimental success that the more carefully the experiment was set up the less successful were they in obtaining stable oscillations. They concluded that the basic flow from figure (11) of their results, was a single convective loop with liquid metal rising at the hot thermode and flowing along the boat and descending at the cold thermode. The curvature of the isotherms in horizontal planes is due to insulating the vertical side walls of the boat.

Also measurements of the horizontal temperature profiles, in the annulus see Skafel (1972) figure 12, have shown that the horizontal temperature gradient to be larger than $\frac{\Delta T}{L}$ near the end walls, but to be approximately linear over the central portion with a value smaller than $\frac{\Delta T}{L}$. However, in our derivation we shall assume that T_r is a constant. The continuity equation will not be satisfied exactly, however, letting $\nabla . \underline{q} = 0$ will be a good approximation.

The momentum equation, in cylindrical polars, for the r th component will yield:

$$0 = -\frac{1}{\rho} P_r + \nu \nabla^2 U' - \nu \frac{U'}{r^2} \qquad 2.3$$

where $\nabla^2 \equiv \frac{\partial^2}{\partial r^2} + \frac{1}{r}\frac{\partial}{\partial r} + \frac{\partial^2}{\partial \phi^2} + \frac{\partial^2}{\partial z^2}$ 2.4

with the application of (2.4)(2.3) becomes

$$0 = -\frac{1}{\rho} P_r + \nu \left\{ U'_{rr} + \frac{1}{r} U'_r + U'_{zz} - \frac{U'}{r^2} \right\} \quad 2.5$$

Differentiating partially with respect to z

$$0 = -\frac{1}{\rho} P_{zr} + \nu \left\{ U'_{rrz} + \frac{1}{r} U'_{rz} + U'_{zzz} - \frac{U'_z}{r^2} \right\} \quad 2.6$$

The z is the component of the momentum equation:-

$$0 = -\rho g - P_z \quad 2.7$$

Differentiating partially with respect to r yields

$$0 = -g \rho_r - P_{rz} \quad 2.8$$

From (2.6) and (2.8) we obtain:

$$-\frac{g}{\rho} P_r = \nu \left\{ U'_{rrz} + \frac{1}{r} U'_{rz} + U'_{zzz} - \frac{U'_z}{r^2} \right\} \quad 2.9$$

Retaining the variation in ρ

$$\frac{d\rho}{\rho} = -\alpha \, dT \quad 2.10$$

or

$$\frac{1}{\rho} \rho_r = -\alpha T_r \quad 2.11$$

Whence, from (2.9) and (2.11) the following partial differential equation is obtained:

$$U'_{rrz} + \frac{1}{r}U'_{rz} + U'_{zzz} - \frac{U'_z}{r^2} = \frac{\alpha g T_r}{\nu} \qquad 2.12$$

Integrating with respect to z we have:

$$U'_{rr} + \frac{1}{r}U'_r + U'_{zz} - \frac{U'_z}{r^2} = \frac{\alpha g T_r z}{\nu} \qquad 2.13$$

This is the fundamental partial differential equation, of the flow characteristics. The solution will be of the form:

$U' = \Omega(z)\,\Pi(r)$ using the Bernoulli trial solution method and substituting into (2.13) gives:

$$\Pi_{rr}\Omega + \frac{\Pi_r\Omega}{r} - \frac{\Pi\Omega}{r^2} + \Omega_{zz}\Pi = 0 \qquad 2.14$$

for the kernel solution

Then transforming $$\frac{\Pi_{rr}}{\Pi} + \frac{1}{r}\frac{\Pi_r}{\Pi} - \frac{1}{r^2} + \frac{\Omega_{zz}}{\Omega} = 0 \qquad 2.15$$

Now let $\frac{\Omega_{zz}}{\Omega} = -k^2$ (where k is a separation constant) 2.16

The solution of(2.16) will be of the form:

$$\Omega = A\sinh kz + B\cosh kz \qquad 2.17$$

Now if the independent variable in the remainder of (2.15) is changed to kr, where k is the separation constant, the resulting equation is

$$r^2\Pi_{rr} + r\Pi_r + (k^2r^2 - 1)\Pi = 0 \qquad 2.18$$

with a general solution of

$$\Pi = C J_1(kr) + D Y_1(kr) \qquad 2.19$$

where J_1 is the Bessel function of the first kind of order J_1 and Y_1 is the Bessel function of the second kind of order 1. From (2.19) and (2.17) the kernel solution will be

$$U = (C J_1(kr) + D Y_1(kr))(A \sinh kz + B \cosh kz) \qquad 2.20$$

Turning now to the particular integral:

$$\frac{1}{(r^2D^2 + rD + r^2D^2 - 1)} \left[\frac{\alpha g T_r z r^2}{\nu}\right] \qquad 2.21$$

Let D and $\mathfrak{D}$ denote the operators $\frac{d}{dr}$, $\frac{d}{d\sigma}$ respectively, these relations may be expressed as

$$rD = \mathfrak{D} \quad ; \quad r^2D = \mathfrak{D}(\mathfrak{D} - 1)$$

The particular integral (21) may be converted to

$$\frac{\alpha g T_r}{\nu} \cdot \frac{1}{(\mathfrak{D}(\mathfrak{D}-1) + \mathfrak{D} + r^2D^2 - 1)} [z e^{2\sigma}] \qquad 2.22$$

where $r = e^{\sigma}$

Expanding by the binomial theorem:

$$\frac{\alpha g T_r e^{2\nu}}{3\nu}\left\{1+\frac{t^2D^2}{3}\right\}[z] \qquad 2.23$$

Particular integral = $\frac{\alpha g T_r t^2 z}{3\nu}$

The general solution will take the form of

$$u=\frac{\alpha g T_r t^2 z}{3\nu}+\sum_k^1\left\{C_k J_1(kr)+D_k Y_1(kr)\right\}\left\{A\sinh kz+B\cosh kz\right\} \qquad 2.24$$

The values of k, which are not necessarily integers and the other constraints will have to meet the requirements of the boundary conditions.

The fluid is constrainted in the finite space between two concentric cylinders r = Ro and r = Ri and the planes $z=\pm\frac{d}{2}$ Then for rigid boundaries, which do not, however, satisfy the full viscous conditions the following criteria will hold:

$u = 0$ where r = Ro or Ri for all values of z

$u=0$ when $z=\pm\frac{d}{2}$ for all values of r such as that Ro > r > Ri

Then the velocity equation is:

$$u=\frac{\alpha g T_r (r-R_o)(r-R_i)z}{3\nu}-\sum_k^1 C_k\left\{\frac{J_1(kr)}{J_1(kR_o)}-\frac{Y_1(kr)}{Y_1(kR_o)}\right\}\frac{\sinh kz}{\sinh\left(k\frac{d}{2}\right)} \qquad 2.25$$

It will vanish for r = Ro, and r = Ri provided

$$J_1(kR_o)Y_1(kR_i) - J_1(kR_i)Y_1(kR_o) = 0 \qquad 2.26$$

The roots of this equation fix the permissible values of k. Finally, it vanishes when $u = 0$ for $z = \pm \frac{d}{2}$ provided

$$\sum_k C_k \left\{ \frac{J_1(kr)}{J_1(kR_o)} - \frac{Y_1(kr)}{Y_1(kR_o)} \right\} = \frac{\alpha q \tau_r (r-R_o)(r-R_i) d}{4\gamma} \qquad 2.27$$

The coefficient C_k can be expressed in the form of a definite integral. Thus, if we write

$$u^* = \frac{J_1(kr)}{J_1(kR_i)} - \frac{Y_1(kr)}{Y_1(kR_i)} \qquad 2.28$$

The following integral is now valid:

$$2\pi \int_{R_i}^{R_o} f(r)\, u^* r\, dr = L C_k \qquad 2.29$$

It is assumed that the arbitrary function f(r) can be expressed in a series of Bessel-Fourier coefficients.

The fluid will commence, from rest with a configuration of $u = f(r)$

where $$L = \pi \int_{R_i}^{R_o} u^{*2} r \, dr = \frac{\pi R_o}{2k} \left\{ u^*_{k,} u^*_r \right\}_{r=R_o} \qquad 2.30$$

and L is a constant derived from the theory of Lommel integrals

But $$\left(u^*_r\right)_{r=R_o} = k \left\{ \frac{J_1'(kR_o)}{J_1(kR_i)} - \frac{Y_1'(kR_o)}{Y_1(kR_i)} \right\} \qquad 2.31$$

and with transendental equation (2.26) and (2.31) becomes:

$$\left(u^*_r\right)_{r=R_o} = k \frac{Y_1(kR_o)}{Y_1(kR_i)} \left\{ \frac{J_1'(kR_o)}{J_1(kR_o)} - \frac{Y_1'(kR_o)}{Y_1(kR_o)} \right\} \qquad 2.32$$

Then with the aid of the general relationship
$J_1(x) Y_1'(x) - J_1'(x) Y_1(x) = \frac{1}{x}$ (2.32) becomes:

$$\left(u^*_r\right)_{r=R_o} = - \frac{1}{R_o J_1(kR_o) Y_1(kR_i)} \qquad 2.33$$

Likewise

$$\left(u^*_r\right)_{r=R_o} = R_o \left\{ \frac{J_1'(kR_o)}{J_1(kR_i)} - \frac{Y_1'(kR_o)}{Y_1(kR_i)} \right\} + \frac{J_1(kR_o)}{k \left[J_1(kR_i) \right]^2 Y_1(kR_i)}$$

Hence it follows from (2.33) and (2.34)

$$L = \pi R_o^2 \left\{ \frac{J_1'(kR_o)}{J_1(kR_i)} - \frac{Y_1'(kR_o)}{Y_1(kR_i)} \right\}^2 - \frac{\pi}{2k^2 \left(J_1(kR_i) Y_1(kR_i) \right)^2} \qquad 2.35$$

or $$L = \pi \left[\frac{r^2}{2} \left\{ \frac{J_1'(kr)}{J_1(kR_i)} - \frac{Y_1'(kr)}{Y_1(kR_i)} \right\} \right]_{R_i}^{R_o} \qquad 2.36$$

Then $C_k = \frac{\alpha q T_0}{4\nu} \int_{R_i}^{R_o} \frac{(r-R_i)(r-R_o)\, d\, u^* r\, dr}{L}$ 2.37

or $C_k = \frac{\alpha q T_0}{r 2\pi i \nu} \int_{R_i}^{R_o} \left[\frac{J_1(kr)}{J_1(kR_o)} - \frac{Y_1(kr)}{Y_1(kR_o)} \right] H(r-R_i)(r-R_o)\, d\, dr$ 2.38

$$\Big/ \left[r^2 \left\{ \frac{J_1'(kr)}{J_1(kR_i)} - \frac{Y_1'(kr)}{Y_1(kR_i)} \right\}^2 \right]_{R_i}^{R_o}$$

yielding for the final expression of C_k the following integral

$$C_k = M \int_{R_i}^{R_o} \left\{ \frac{J_1(kr)}{J_1(kR_i)} - \frac{Y_1(kr)}{Y_1(kR_i)} \right\} r\,(r-R_i)(r-R_o)\, d\, dr \qquad 2.39$$

where M is a constant compounded of numerator and denominator of (2.39). The technique adopted follows the more detailed treatment given in [89] Riemann and [90] Rayleigh (1894).

The initial step in calculating the value of C_k would be the estimation, by employing truncated Bessel and Neumann series, to determine the values of the separation constant k. These values of k will not necessarily be integral in value. This feature is indirect contrast to a Fourier series. Hence, the velocity will be in the form of an infinite series whose coefficients will be composed from Fourier-Bessel coefficients and whose terms are of descending magnitude.

The roots of the Bessel function of order unity and the Neumann function of order unity were determined by [91] M. Mahon's method (1895). The S roots, in order of magnitude of the transendential

equation:

$$\frac{Y_1'(x)}{J_1'(x)} - \frac{Y_1(\rho x)}{J_1(\rho x)} = 0 \qquad 2.40$$

where $\rho > 1$ is given by the following truncated expressions:

$$\alpha_1^s = \delta + \frac{p}{s} + \frac{q - p^2}{\delta^3} + \frac{r - 4pq + 2p^3}{\delta^5} \qquad 2.41$$

where

$$\delta = \frac{s\pi}{\rho - 1}, \quad p = \frac{m-1}{8\rho}, \quad q = \frac{4(m-1)(m-25)(\rho^3-1)}{3(8\rho)^3(\rho-1)}$$

$$r = \frac{32(m-1)(m^2-114m+1073)(\rho^5-1)}{5(8\rho)^3(\rho-1)} \quad \text{and} \quad m = 4n^2 \qquad 2.42$$

Now equation (2.40) is identical to the transendential equation (2.26). The values of x and ρx will be replaced by KR_i, and KR_o, where R_i and R_o are the respective internal and external radii. Computer program number 1 was used to calculate the appropriate values of K. For 5 different values of the inner radius. The outer radius was fixed at 40 mm. The values are tabulated in Table 1.

The initial value of the first root is not correct. By the application of linear interpolation it can be calculated if required.

It is not possible to evaluate analytically expression (2.39). There is a possibility by, employing truncated Bessel and Neumann series, and integrating term by term or alternatively, with numerical integration techniques such as Newton-Cotes, Romberg, Gauss or Chenshaw-Cotes to evaluate (2.39) approximately. However, this evaluation is a considerable computation task and then with the aid of (2.25) to determine the velocity. The mathematical difficulties are obviously great with this approach. The next section is centred on introducing approximations to reduce the mathematical complexity, but still obtaining meaningful results.

TABLE I

Bessel-Neuman Roots

Inner Radius 10 mm

Root Number	Value of K
1	4.27581
2	2.23214
3	3.18255
4	4.21343
5	5.25448
6	6.29826
7	7.3432
8	8.38875
9	9.4347
10	10.4809
11	11.5273
12	12.5738
13	13.6204
14	14.6671
15	15.7139
16	16.7607
17	17.8076
18	18.8545
19	19.9014
20	20.9484

Inner Radius 13.75 mm

Root Number	Value of K
1	3.10968
2	1.62337
3	2.31458
4	3.06432
5	3.82144
6	4.58055
7	5.34051
8	6.10091
9	6.8616
10	7.62247
11	8.38348
12	9.14458
13	9.90577
14	10.667
15	11.4283
16	12.1896
17	12.951
18	13.7124
19	14.4738
20	15.2352

Inner Radius 17.5 mm

Root Number	Value of K
1	2.44332
2	1.27551
3	1.8186
4	2.40768
5	3.00256
6	3.59901
7	4.19611
8	4.79357
9	5.39126
10	5.98908
11	6.58702
12	7.18503
13	7.7831
14	8.38122
15	8.97983
16	9.57756
17	10.1758
18	10.774
19	11.3723
20	11.9705

Inner Radius 21.25 mm

Root Number	Value of K
1	2.01215
2	1.05042
3	1.49767
4	1.98279
5	2.47269
6	2.96389
7	3.45562
8	3.94765
9	4.43986
10	4.93219
11	5.4246
12	5,91708
13	6.40961
14	6.90218
15	7.39478
16	7.8874
17	8,38005
18	8.87271
19	9.36538
20	9.85807

Inner Radius 25 mm

Root Number	Value of K
1	1.71032
2	.892856
3	1.27302
4	1.68537
5	2.10179
6	2.5193
7	2.93728
8	3.3555
9	3.77388
10	4.19236
11	4.61091
12	5.02952
13	5.44817
14	5.86685
15	6.28556
16	6.70429
17	7.12304
18	7.5418
19	7.96058
20	8.37936

Section (iii)

Reduced cylindrical polar model

A physical system comprising of an annulus with a temperature maintained between the inner and outer cylindrical surfaces, having a very small aspect ratio and deep in a cavity, the shear will be a function of z alone. The velocity, in the steady state of flow, will be, therefore, reduced to

$$(U'(z), 0, 0) \qquad 2.43$$

The velocity vector for a single convective roll will be given by:

$$\underline{q} = U'(z)\hat{i} \qquad 2.44$$

The constraint upon the equation of continuity will be the same as in Section (ii). The momentum equation, in cylindrical polars for the r th component will now be

$$0 = -\frac{1}{\rho} P_r + \nu \nabla^2 U' - \frac{U'}{r^2} \qquad 2.45$$

Following the same procedure as with the previous section we obtain the following third order differential equation:

$$\nu U'_{zzz} - \frac{\nu}{r^2} U'_z = \alpha g T_r \qquad 2.46$$

The temperature equation is also given by

$$U' T_r = \chi \Theta_{zz} \qquad 2.47$$

When r approaches large values which correspond physically to the 'centre' of a fluid with unbounded sides, equation (2.46) and (2.47) reduce to the Gill equations (1.3) and (1.4). The solution of (2.46) can be found as follows:

kernel solution: $$m^2 - \frac{1}{r^2} = 0 \qquad 2.48$$

Then $$U' = A\,EXP(\tfrac{z}{r}) + B\,EXP(-\tfrac{z}{r}) \qquad 2.49$$

where A and B are arbitrary constants.

The particular integral is

$$\frac{\alpha g T_r z}{(D^2 - \frac{1}{r^2})\nu} + \frac{C}{\nu(D^2 - \frac{1}{r^2})} \qquad 2.50$$

By suitable application of operator D methods, the particular integral is

$$-\frac{\alpha g T_r r^2 z}{\nu} + \frac{C r^2}{\nu} \qquad 2.51$$

Hence the complete solution is

$$U' = A\,EXP(\tfrac{z}{r}) + B\,EXP(-\tfrac{z}{r}) - \frac{\alpha g T_r r^2 z}{\nu} + \frac{C r^2}{\nu} \qquad 2.52$$

Integrating equation (2.52) twice and substituting into equation (2.47) it is possible to obtain an expression for Θ in terms of Z and r namely

$$\Theta = \frac{A T_r r^2}{\chi} EXP(\tfrac{z}{r}) + \frac{B T_r r^2}{\chi} EXP(-\tfrac{z}{r}) - \frac{\alpha g T_r^2 r^2 z^3}{6} + \frac{C r^2 z^2}{2} + D'z + E' \qquad 2.53$$

where C, D and E are arbitrary constants.

Equation (2.52) has three constants namely A, B and C. By suitable choice of boundary conditions the values of the constants can be enumerated. The following physical constraints will be employed.

(a) Rigid conducting boundaries conditions

$$U' = 0 \qquad z = \pm \frac{d}{2} \qquad \textcircled{H} = 0 \qquad 2.54a$$

(b) Free conducting boundaries

$$U'_z = 0 \qquad z = \pm \frac{d}{2} \qquad \textcircled{H} = 0 \qquad 2.54b$$

(c) Rigid free conducting

$$U'_z = 0 \quad z = \frac{d}{2} \;, \; U' = 0 \quad z = -\frac{d}{2} \quad \textcircled{H} = 0 \qquad 2.54c$$

Any of the boundary conditions will yield two simultaneous equations having three unknown. The continuity integral

$$\int_{-d/2}^{d/2} U' \, dz = 0 \qquad 2.54d$$

gives the final linear equation. The linear equations may then be solved simultaneously for A, B and C.

The work of Gill was centred, as was Harts work, on rigid and free conducting boundaries. The Gill equations will now be compared with the reduced cylindrical model.

(a) Rigid conducting boundaries

(i) Gill Equations

velocity $$U = \frac{\alpha q T_x}{\sqrt{b\nu}} \left[z^3 - \frac{z d^2}{4} \right] \qquad 2.55$$

shear $$U_z = \frac{\alpha q T_x}{\sqrt{b\nu}} \left[3z^2 - \frac{d^2}{4} \right] \qquad 2.56$$

(ii) Reduced cylindrical Polar Model

Employing the continuity integral and zero slip at $z=\pm\frac{d}{2}$ the following linear simultaneous equations are obtained in matrix form:

$$\begin{bmatrix} 2r\sinh E & 2r\sinh E & Fd \\ \exp -E & \exp E & F \\ \exp E & \exp -E & F \end{bmatrix} \begin{bmatrix} A \\ B \\ C \end{bmatrix} = \begin{bmatrix} 0 \\ -\frac{Gd}{2} \\ \frac{Cr d}{2} \end{bmatrix} \qquad 2.57$$

where $E = \frac{d}{2r}$ $F = \frac{r^2}{\nu}$ $G = \frac{\alpha g T_r r^2}{\nu}$

solving (2.57) by the usual matrix methods the following values are obtained for the constants:

$$A = \frac{\alpha g T_r r^2 d}{\nu}\left\{\frac{2r\sinh E - d\cosh E}{8r\sinh^2 E - 2d\sinh E}\right\} \qquad 2.58$$

$$B = \frac{\alpha g T_r r^2 d}{\nu}\left\{\frac{-2r\sinh E + d\cosh E}{8r\sinh^2 E - 2d\sinh E}\right\}$$

and $c = o$.

Substituting the constants, first derived, into (2.52) the following relationships for the velocity and shear are respectively:

$$U = \frac{\alpha g T_r r^2 d}{\nu}\left\{\left(\frac{2r\sinh E - d\cosh E}{4r^2\sinh E - 2d\sinh 2E}\right)\sinh\left(\frac{z}{r}\right) - \frac{z}{d}\right\} \qquad 2.59$$

$$u_2' = \frac{\alpha g T_r r d}{\nu}\left[\left(\frac{2r\sinh E - d\cosh E}{4r\sinh^2 E - 2d\sinh 2E}\right)\cosh\left(\frac{z}{r}\right) - \frac{1}{d}\right] \quad 2.60$$

(b) Free conducting boundaries

(i) Gill Equations

Velocity $$u = \frac{\alpha g T_x}{2\nu}\left\{\frac{z^3}{3} - \frac{2d^2}{4}\right\} \quad 2.61$$

Shear $$u_z = \frac{\alpha g T_z}{2\nu}\left\{z^2 - \frac{d^2}{4}\right\} \quad 2.62$$

(ii) Reduced cylindrical Polar Model

This juncture employing the continuity integral and zero shear at boundaries $z = \pm \frac{d}{2}$ a similar triad of linear simultaneous equations are obtained (the constants are the same as in the previous section)

$$\begin{bmatrix} 2r\sinh E & 2r\sinh E & Fd \\ \frac{\exp E}{r} & -\frac{\exp -E}{r} & 0 \\ \frac{\exp -E}{r} & -\frac{\exp E}{r} & 0 \end{bmatrix}\begin{bmatrix} A \\ B \\ C \end{bmatrix} = \begin{bmatrix} 0 \\ G \\ G \end{bmatrix} \quad 2.63$$

solving matrix equation (2.63) the following values for A, B and C are obtained:

$$A = \frac{\alpha g T_r r^2 \sinh E}{\nu \sinh 2E}, \quad B = -\frac{\alpha g T_r r^2 \sinh E}{\nu \sinh 2E}$$

and C = o

The respective velocity and shear equations are:

$$u' = \frac{\alpha g T_r r^3}{\nu}\left\{\frac{2\sinh E}{\sinh 2E}\cosh\left(\frac{z}{r}\right) - \frac{z}{r}\right\} \quad 2.64$$

$$u'_z = \frac{\alpha q T_r l^2}{\nu}\left\{\frac{2\sinh E}{\sinh 2E}\cosh\left(\frac{z}{r}\right) - 1\right\} \qquad 2.65$$

(c) Rigid-Free conducting boundaries

At $z = d/2$ the shear is zero while at $z = -d/2$ the velocity will be zero.

(i) Gill Equations

Velocity $$u = \frac{\alpha q T_x}{2\nu}\left\{\frac{z^3}{3} - \frac{z^2 d}{8} - \frac{z d^2}{8} + \frac{d^3}{196}\right\} \qquad 2.66$$

Shear $$u_z = \frac{\alpha q T_x}{2\nu}\left\{z^2 - \frac{zd}{4} - \frac{d^2}{8}\right\} \qquad 2.67$$

(ii) Reduced cylindrical Polar Model

The matrix equation is given by:-

$$\begin{bmatrix} 2r\sinh E & 2r\sinh E & Fd \\ \exp -E & \exp E & F \\ \frac{\exp E}{r} & -\frac{\exp -E}{r} & 0 \end{bmatrix}\begin{bmatrix} A \\ B \\ C \end{bmatrix} = \begin{bmatrix} 0 \\ -\frac{Gd}{2} \\ 0 \end{bmatrix} \qquad 2.68$$

The constants are:

$$A = \frac{\alpha q T_r l^2}{\nu}\left\{\frac{\frac{d^2\exp -E}{2r} + 2r\sinh E - d\exp E}{2\sinh E\cosh E - \frac{d}{r}\cosh 2E}\right\}$$

$$B = \frac{\alpha q T_r l^2}{\nu}\left\{\frac{\frac{d^2\exp E}{2r} - 2r\sinh E + d\exp -E}{2\sinh E\cosh E - \frac{d}{r}\cosh 2E}\right\}$$

$$C = \frac{\alpha q T_r l^2}{\nu}\left\{\frac{-2d\sinh E\cosh E + 4r\sinh^2 E}{2\sinh E\cosh E - \frac{d}{r}\cosh 2E}\right\}$$

The respective velocity and shear equations are:

$$u_1' = \frac{\alpha g T_1 t^2}{\nu}\left\{\frac{\frac{d^2}{2r}\exp\left(-E+\frac{2}{r}\right) + \frac{d^2}{2r}\exp\left(E-\frac{z}{r}\right) + 4r\sinh E\cosh\left(\frac{z}{r}\right)}{2\sinh E\cosh E - \frac{d}{r}\cosh 2E}\right\}$$

$$+ \frac{\alpha g T_1 t^2}{\nu}\left\{\frac{-d\exp\left(E+\frac{z}{r}\right) + d\exp\left(-E-\frac{z}{r}\right) - 2d\sinh E\cosh E + 4r\sinh^2 E}{2\sinh E\cosh E - \frac{d}{r}\cosh 2E}\right\} \quad 2.69$$

$$u_2' = \frac{\alpha g T_1 r}{\nu}\left\{\frac{\frac{d^2}{2r}\exp\left(-E+\frac{z}{r}\right) - \frac{d^2}{2r}\exp\left(E-\frac{z}{r}\right) + 4r\sinh E\sinh\left(\frac{z}{r}\right)}{2\sinh E\cosh E - \frac{d}{r}\cosh 2E}\right\}$$

$$- \frac{\alpha g T_1 r}{\nu}\left\{\frac{d\exp\left(E+\frac{z}{r}\right) + d\exp\left(-E-\frac{z}{r}\right)}{2\sinh E\cosh E - \frac{d}{r}\cosh 2E}\right\} \quad 2.70$$

Naturally, velocity equations having the velocity as zero at the rigid boundaries do not satisfy the full viscous boundary conditions, so thin stoke layers are required adjacent to the boundaries in order to satisfy the non-slip criteria. These layers will have a thickness $\left(\frac{\rho}{\sigma\omega}\right)^{1/2}$ according to Hart (1972). This thickness for rigid boundaries is of the order of $\frac{1}{40}$ the depth for mercury when it is used as the working fluid.

CHAPTER III

Chapter III

Section (i)

Stability Characteristics and Perturbed Equations

Hart (1972) has enumerated the stability of the basic flow state in a box geometry. The stability characteristics were solved numerically using the Galerkin approach. This method converted a set of ordinary differential equations into a matrix eigenvalue problem. The results were applied to: rigid, conducting and insulating boundaries. The results were extended for a broad spectrum of Prandtl number values 10^{-3} to 10^{2} For liquid metals, P is very small and the results for the lower end of the spectrum were naturally relevant.

For transverse modes Hart proposed the following energy characteristics in the basic state:-

(i) the conversion of potential energy into kinetic energy

(ii) the energy extracted from the mean velocity field

(iii) the viscous kinetic energy dissipation

The following criteria were indicative of this type of stability:

(i) when the conversion of potential to kinetic energy was greater than the energy of the mean velocity field the instability was convective in nature,

(ii) when the energy of the mean velocity field was greater than the conversion of potential to kinetic energy the instability was of shear character.

For longitudinal modes the energy was extracted out of the flow; while the transverse modes, in some cases, may have converted kinetic energy into shear flow.

For low values of P the first form of instability to arise was a 'transverse mode' which was not oscillatory in character. The

oscillatory disturbances were longitudinal 'even' modes. The longitudinal implied motion in the Hart box geometry which was independent of x coordinate and the 'even' symmetry about the line $z=0$. These modes are labelled L and E in Hart's (1972) figure (5).

Turning now to the formation of the perturbed equations. In the box geometry of Hart (1972) the longitudinal modes are subject to the constraint $\frac{\partial}{\partial x} = 0$ While the transverse modes are subject to an analogue constraint $\frac{\partial}{\partial y} = 0$ Consider a perturbation in the anullii of the reduced cylindrical polar model; let the velocity perturbations be u', v', w' respectively in the three coordinates, and Θ' the temperature perturbation. These are subject to the Boussinesq approximations, the respective velocity and temperature equations will be:

$$\underline{U}' = (U' + u', v', w') \qquad 3.1$$

$$T = T_r + \Theta_{(z)} + \Theta' \qquad 3.2$$

The perturbation equations will be valid, provided that the flow pattern is approximated by the equations (2.46) and (2.47). This condition is certainly true in the middle of a cavity with a small aspect ratio. It also follows, for small values of ϕ that

$$\frac{\partial}{\partial x} \simeq \frac{\partial}{\partial r} \quad \text{and} \quad \frac{\partial}{\partial y} \simeq \frac{1}{r}\frac{\partial}{\partial \phi} \qquad 3.3$$

Then the perturbation velocity and temperature can adopt two forms:

$$u' = u'(\phi, z, t) \qquad 3.4a$$

$$v' = v'(\phi, z, t) \qquad 3.4b$$

$$w' = w'(\phi, z, t) \qquad 3.4c$$

$$\theta' = \theta'(\phi, z, t) \qquad 3.4d$$

or

$$u' = u'(r, z, t) \qquad 3.5a$$

$$v' = v'(r, z, t) \qquad 3.5b$$

$$w' = w'(r, z, t) \qquad 3.5c$$

$$\theta' = \theta'(r, z, t) \qquad 3.5d$$

The former perturbations will generate longitudinal modes which are subject to the constraint $\frac{\partial}{\partial r} = 0$ the latter form of perturbation will generate transverse modes. However, in the Hart (1972) box geometry there was no generation of transverse oscillary modes. There are two possible explanations: the side walls of the box stabilized this form of oscillation or alternatively, the measuring apparatus employed by experimental observers was not sensitive enough to detect their presence. In Skafel (1972) measurements of the mean temperature field corresponded to the box geometry. However, he noted small amplitude fluctuations with a wide frequency band were present. These small amplitude fluctuations could have been the result of shear flow instability, but they did not inhibit the thermal

oscillations occurring. Furthermore, the measured temperature fields, in the work of Skafel (1972) and Hurle et al (1974) concluded that a single circulation was present; whereas if transverse modes were present secondary circulations would appear, indicative of shear instability. The experimental work conducted by Hurle et al indicated that lines of constant phase will have a tendency to be parallel to the lines of flow and supports the view that the former type of perturbation equations (3.4a - d) will dominate, and in the cylindrical mode will have $\frac{\partial}{\partial r} = 0$

It is now possible to introduce a Stoke's stream function, ψ such at the current function will be connected to the flow in the plane by the following partial differential equations:

$$v' = -\psi_z \quad ; \quad w' = \frac{1}{r}\psi_\phi \qquad 3.6$$

Naturally, the stream function will satisfy the equation of continuity. The new velocity $\underline{q}$ with the perturbation velocity, will now be given by

$$\underline{q} = (U' + u')\hat{r} + v'\hat{\phi} + w'\hat{k} \qquad 3.7$$

where $\hat{r}$, $\hat{\phi}$ and $\hat{k}$ represent unit vectors in the radial, azimuthal and z directions respectively. The vorticity is defined by

$$\underline{\omega}' = \nabla \times \underline{q} \qquad 3.8$$

or expressing the vorticity in a more perspicuous form, we have in determinant notation:

$$\frac{1}{r}\begin{vmatrix} \hat{r} & r\hat{\phi} & \hat{z} \\ 0 & \frac{\partial}{\partial\phi} & \frac{\partial}{\partial z} \\ U'+u' & rv' & w' \end{vmatrix} = \underline{\omega} \qquad 3.9$$

(Neglecting the variation in r). Expanding determinant (3.9)

$$\underline{\omega} = \frac{1}{r}\left\{ (w'_\phi - rv'_z)\hat{r} + r(U'_z+u'_z)\hat{\phi} - (U'_\phi - u'_\phi)\hat{k} \right\} \qquad 3.10$$

However, $U'_\phi = 0$ and replacing v and u by the Stoke's stream function, the vorticity, in a succinct form is:

$$\underline{\omega} = \frac{1}{r}\left\{ \left(\frac{1}{r}\psi_{\phi\phi} + r\psi_{zz}\right)\hat{r} + (U'_z+u'_z)r\hat{\phi} - \hat{k}u_\phi \right\} \qquad 3.11$$

Now the fundamental vorticity equation is:

$$\nabla\rho \times \frac{Dq}{Dt} + \rho\left\{ \underline{\omega}_t - \nabla\times(q\times\underline{\omega}) \right\} = -g\nabla\rho\times\hat{k} + \mu\nabla^2\underline{\omega} \qquad 3.12$$

considering each term of (2.8) individually

The first term $\nabla\rho \times \frac{Dq}{Dt}$ is of second order and will be ignored.

The second term yields:

$$\rho\underline{\omega}_t = \rho\left\{ \frac{\partial}{\partial t}\left(\frac{1}{r^2}\psi_{\phi\phi} + \psi_{zz}\right)\hat{r} + \frac{\partial}{\partial t}\left(U'_z + \frac{1}{r}u'_z\right)\hat{\phi} - \frac{1}{r}\frac{\partial}{\partial t}(u_\phi)\hat{k} \right\} \qquad 3.13$$

The next term $\nabla\times(q\times\underline{\omega})$ will also provide a second order contribution and will be neglected.

The term $-g\nabla\rho\times\hat{k}$ yields:

$$-g\rho_r\hat{\phi} - \frac{1}{r}g\rho_\phi\hat{r} \qquad 3.14$$

The final term is $\mu\nabla^2 \underline{\omega}'$ each of the components with its appropriate direction, in cylindrical coordinates, will be

$$\nabla^2\omega'_r - \frac{\omega'_r}{r^2} - \frac{2}{r^2}\omega'_{\phi\phi} \qquad 3.15a$$

$$\nabla^2\omega'_\phi - \frac{\omega'_\phi}{r^2} + \frac{2}{r}\omega'_{r\phi} \qquad 3.15b$$

$$\nabla^2\omega'_z \qquad 3.15c$$

From the r th component of the vorticity equation (3.12) and with the above considerations, and neglecting the perturbation term u'_z we have

$$\nabla^2\psi_t = -\frac{1}{(r\rho)}g\rho'_\phi + \nu\nabla^4\psi - \frac{\nu}{r^2}\nabla^2\psi \qquad 3.16$$

Now $$f_\phi = -\alpha\rho T_\phi = -\alpha\rho\theta'_\phi \qquad 3.17$$

From (3.16) and (3.17)

$$\nabla^2\psi_t = \frac{\alpha g}{r}\theta'_\phi + \nu\nabla^4\psi - \frac{\nu}{r^2}\nabla^2\psi \qquad 3.18$$

where $\nabla^2 = \frac{1}{r^2}\frac{\partial^2}{\partial\phi^2} + \frac{\partial^2}{\partial z^2}$ the reduced Laplacian operator.

The energy equation, to first order considerations, may be written as:

$$\theta'_t + (U'+u')T_r + w\,\Theta_z = \chi(\Theta_{zz} + \nabla^2\theta') \qquad 3.19$$

and the unperturbed temperature equation

$$U'T_r = \chi\,\Theta_{zz} \qquad 3.20$$

Subtracting (3.10) from (3.19)

$$\theta'_t + u'T_r + \frac{1}{r}\psi_\phi \cdot \Theta_z = \chi \nabla^2 \theta' \qquad 3.21$$

Examination of the r th component of the Navier-Stokes equation gives:

$$u'_t + \frac{v'}{r}u'_\phi + w'(u'_z + U'_z) - \frac{v'^2}{r} = \left\{ -\frac{1}{\rho}P_r \right. \qquad 3.22$$
$$\left. + \nu(\nabla^2 u' + U'_{zz} - \frac{U'+u'}{r^2} - \frac{2}{r^2}v'_\phi \right\}$$

Now ignoring the perturbation in P_r i.e. p is satisfying the unperturbed state viz:-

$$0 = -\frac{1}{\rho}P_r + \nu U'_{zz} - \nu \frac{U'}{r^2} \qquad 3.23$$

The perturbation velocity which is superimposed on the basic state is small in magnitude in comparison to the basic state, thus terms such as v'^2 may be neglected as second order. Also we shall choose to ignore the product terms

$$\frac{v'}{r}u'_\phi \qquad \text{and} \quad w'u'_z$$

Introducing the Stoke's stream function equation (3.22) now becomes:

$$u'_t + \frac{1}{r}\psi_\phi U'_z = \nu\left\{ \nabla^2 u' - \frac{U'}{r^2} + \frac{2}{r^2}\psi_{z\phi} \right\} \qquad 3.24$$

Equations (3.16), (3.19) and (3.24) are the fundamental equations which govern the flow. Now equation (3.18), the vorticity equation,

expresses Θ in terms of ψ. Differentiating partially, the temperature equation (3.21), with respect to ϕ

$$\Theta'_{t\phi} + u'_{\phi} T_r + \frac{1}{r} \psi_{\phi\phi} \Theta_z = \chi \frac{\partial}{\partial \phi} \nabla^2 \Theta' \qquad 3.25$$

Substituting into equation (3.16) for Θ then (3.25) becomes:

$$-\frac{\alpha g T_r u_{\phi}}{r} = \left\{ \left(\frac{\partial}{\partial t} - \chi \nabla^2 \right) \left(\frac{\partial}{\partial t} - \nu \nabla^2 \right) \nabla^2 \psi \right. \qquad 3.26$$

$$\left. + \frac{\alpha g}{r^2} \Theta_z \psi_{\phi\phi} + \frac{\nu}{r^2} \left(\frac{\partial}{\partial t} - \chi \nabla^2 \right) \nabla^2 \psi \right\}$$

Differentiating the reduced Navier-Stokes equation (3.24) with respect to ϕ and substituting for u_{ϕ} from equation (3.26) the resulting equation is:

$$\left(\frac{\partial}{\partial t} - \nu \nabla^2 \right)^2 \left(\frac{\partial}{\partial t} - \chi \nabla^2 \right) \nabla^2 \psi + \frac{\nu}{r^2} \left(\frac{\partial}{\partial t} - \chi \nabla^2 \right) \left(\frac{\partial}{\partial t} - \nu \nabla^2 \right) \nabla^2 \psi$$

$$+ \frac{\alpha g}{r^2} \left(\frac{\partial}{\partial t} - \nu \nabla^2 \right) \Theta_z \psi_{\phi\phi} = \left\{ \frac{\alpha g}{r^2} u'_z T_r \psi_{\phi\phi} - 2 \frac{\alpha g}{r^3} T_r \nu \psi_{\phi\phi z} \right\} \qquad 3.27$$

Solutions of the form $\psi = \exp \sigma t \sin(r l \phi) \hat{\psi}(z)$ 3.28

may be found for (3.27) which on substitution, yield an eight order differential equation. The value of σ is real for all positive Rayleigh numbers. The transition from stability to instability will occur through the marginal state. The equations governing the marginal state are obtained when σ_r approaches zero, and this limiting value is then substituted into the problem governing equations.

Section (ii)

Non-Dimensional Forms

The next step is to convert equation (3.27) into non-dimensional form. However, there is a requirement first to examine the parameters upon which the flow is dependent and by suitable substitution of non-dimensional qualities, reduce (3.28) into non-dimensional form. Turning to the physical properties of the model. Steady free convection in a gravitational field is characterized by five parameters: thermal diffusivity, kinematic viscosity, temperature difference, characteristic length, and, the product of gravitational acceleration and volume coefficient of expansion. From these parameters we can form two dimensional qualities which are the Prandtl number and the Rayleigh number.

(a) Prandtl Number

This is a measure of the relative importance of the heat conduction and the viscosity of the fluid and is defined as

$$P = \frac{\text{kinematic viscosity}}{\text{thermal diffusivity}}$$

This ratio P is an index of the capacity of the fluid to diffuse momentum as compared with its capacity to diffuse heat energy. Also this ratio between the two most significant relaxation times in a real fluid is very important. In low Prandtl number fluids, the heat diffuses significantly faster than vorticity which is a typical situation in liquid metals, in which the effective transport of heat energy is electronic in nature.

(b) Rayleigh Number

The basic velocity field varies directly with the volume coefficient α, and the temperature gradient T_x and indirectly with the viscosity i.e. $\frac{\alpha}{\nu} T_x$ and with g as an

additional factor. Since U is the third integral of U_{zzz} the dimension d^3 will also appear. The vertical distribution Θ_z results from a balance of the convection by the velocity field and conduction in a vertical direction. Consider an elemental volume having a base area $\delta x \delta z$ and forming a parallelopipedon in the y direction. The nett influx of heat, due to convection is

$$-U \delta T \delta z = -U T_x \delta x \delta z \qquad 3.29$$

in the limit as the base area approaches an infinitesimal value. The nett outflow, due to conduction

$$-d\left\{\chi T_z dx\right\} = -\chi T_{zz} dz dx \qquad 3.30$$

Thus Θ_{zz} depends on $\frac{U T_x}{\chi}$ which is proportional to

Thus $$\frac{U T_x}{\chi} \propto \frac{\alpha g d^3 T_x^2}{\nu \chi} \qquad 3.31$$

Now taking a non-dimensional ratio of the vertical flux to the horizontal as:

$$d\left\{\frac{\Theta_{zz}}{T_x}\right\} = \frac{\alpha g T_x d^4}{\nu \chi}$$

Hence, the Rayleigh number = $\frac{\alpha g T_x d^4}{\nu \chi}$ 3.32

The Rayleigh number represents the balance between the properties governing the natural convection. Alternatively, it can also be viewed as the ratio: energy liberated by buoyancy to the energy dissipated by heat conduction and viscous drag.

From these two non-dimensional parameters we can form another the Grashof, and the three are related as follows:

Grashof number = Rayleigh x Prandtl 3.33

Low values of this number imply that the transport energy is almost entirely by conduction - a molecular process. Conversely, high values correspond to convective regions and the larger this number the stronger is the convective current.

Now two flows are similar if the Prandtl and Grashof numbers are the same. However, convective heat transfer, created by gravity forces, is also characterized by another number the Nusselt number, and is a function of the Prandtl and Grashof numbers alone:

$$N = f(P, G_r) \qquad 3.34$$

There is naturally no Reynolds number for free convection, due to there being no characteristic velocity parameter, and the onset of turbulence is determined by the magnitude of the Grashof number which becomes very large. Hence the stability characteristics associated with equation (3.27) will be dependent upon:

$$P = \frac{\nu}{\chi}$$

$$R_a = \frac{\alpha g T_x d^4}{\nu \chi} \qquad 3.35$$

However, at this juncture before equation (3.27) is transformed into non-dimensional form it is convenient to review the operator notation and to define a series of ancillary non-dimensional quantities. The operators are listed as follows:

$$\nabla^2 = \frac{1}{r^2}\frac{\partial^2}{\partial \phi^2} + \frac{\partial^2}{\partial z^2} \qquad 3.36$$

$$\frac{\partial}{\partial t} - \nu\nabla^2 = \sigma - \nu\left[\frac{d^2}{dz^2} - l^2\right] \qquad 3.37$$

$$d^2(\nu\chi)^{-1/2}\left(\frac{\partial}{\partial t} - \nu\nabla^2\right) = \sigma_* - P^{1/2}\nabla_x^2 \qquad 3.38$$

$$d^2\chi^{-1}\left(\frac{\partial}{\partial t} - \chi\nabla^2\right) = P^{1/2}\sigma_* - \nabla_x^2 \qquad 3.39$$

$$d^2\nabla^2 = \nabla_*^2 \qquad 3.40$$

$$\nabla_x^2 = \frac{d^2}{dz_x^2} - l_x^2 \qquad 3.41$$

Similarly, the non-dimensional quantities are:

$$z_x = \frac{z}{d}\,; \quad \sigma_x = \sigma d^2(\nu\chi)^{-1/2}\,; \quad l_x = l\,d \qquad 3.42$$

$$\text{(i)}\ U_z' = -\frac{d^2 U_z'}{\chi Ra}\,; \quad \text{(ii)}\ T_z = \frac{\Theta}{Ra\,T_r} \qquad 3.43$$

Relationship 3.43 (i) is the non-dimensional shear. The necessity for the negative sign is that $T_r > 0$ and $U_z < 0$ on the central plane $z = 0$ The latter relationship 3.43 (ii) is the non-dimensional vertical temperature gradient which is dependent on the vertical and horizontal temperature gradients.

By transforming equation (3.27) into non-dimensional form it is possible to introduce a dependance on the Rayleigh and Prandtl numbers.

Multiplying each term of equation (3.27) by $d^6(\nu\chi^2)^{-1}$

(i) Left hand terms:

$$(a)\ d^6(\nu\chi^2)^{-1}\left(\frac{\partial}{\partial t}-\nu\nabla^2\right)^{-1}\left(\frac{\partial}{\partial t}-\chi\nabla^2\right)\nabla^2\psi = (\sigma_*-P^{1/2}\nabla_*^2)^2(\nabla_*^2-P^{1/2}\sigma_*)\nabla_*^2\hat{\psi}$$

$$(b)\ d^6(\nu\chi^2)^{-1}\nu\left(\frac{\partial}{\partial t}-\chi\nabla^2\right)\left(\frac{\partial}{\partial t}-\nu\nabla^2\right)\nabla^2\psi = l_*^2P^{1/2}(\sigma_*-P^{1/2}\nabla_*^2)(\nabla_*-P^{1/2}\sigma_*)\nabla_*^2\hat{\psi}$$

$$(c)\ d^6(\nu\chi^2)^{-1}\nu\left(\frac{\partial}{\partial t}-\nu\nabla^2\right)\underbrace{\alpha g\,\Theta_2\,\psi\phi}_{\uparrow 2} = l_*^2R_a^2P^{1/2}(\sigma_*-P^{1/2}\nabla_*^2)T_2\hat{\psi}$$

(ii) Right hand terms:

$$(a)\quad \underbrace{-d^6(\nu\chi^2)^{-1}\chi^{-1}\alpha g\,u_2\,T_\nu\,\psi\phi}_{\uparrow 2} = -l_*^2R_a^2u_2\hat{\psi}$$

$$(b)\quad \underbrace{-2d^6(\nu\chi^2)^{-1}\alpha g\,T_\nu\,\psi_z\phi}_{\nu^{-1}\uparrow 3} = -\frac{2l_*^2R_aP}{\uparrow}\frac{d}{dz}(\hat{\psi})$$

Term (ii)(b) is only of order Ra. The Rayleigh number is usually greater than 10^3 when critical oscillations occur and certainly higher with a liquid metal such as gallium. The other terms containing the Rayleigh number are of order Ra^2; hence the contribution from this term is minor and may be ignored. Then the reduced non-dimensional equations:

$$(\sigma_*-P^{1/2}\nabla_*^2)^2(\nabla_*^2-P^{1/2}\sigma_*)\nabla_*^2\hat{\psi} + l_*^2R_a^2u_2\hat{\psi} +$$

$$l_*^2R_a^2P^{1/2}(\sigma_*-P^{1/2}\nabla_*^2)T_2\hat{\psi} + l_*^2P^{1/2}(\sigma_*-P^{1/2}\nabla_*^2)(\nabla_*^2-P^{1/2}\sigma_*)\nabla_*^2\hat{\psi}$$

$$= 0 \qquad 3.44$$

Equation (3.44) is the fundamental equation upon which the model rests.

The first approximation for small P estimates the frequency of the oscillation. However, it is possible to express σ_* as an infinite

series $$\sigma_* = \sigma_0 + P^{1/2}\sigma_1 + P^{3/2}\sigma_2 + + \qquad 3.45$$

and in the interior of the fluid, in the same manner,

$$\hat{\psi} = \psi_0 + P^{1/2}\psi_1 + P^{3/2}\psi_2 + + \qquad 3.46$$

By employing the next order of approximation it is possible to determine whether the oscillation is unstable or stable. Substitution into (3.45) ψ_1 will satisfy:

$$\sigma_0^2 \nabla_*^4 \psi_1 + \lambda_*^2 Ra\, W_2 \psi_1 + 2\sigma_0(\sigma_1 - \nabla_*^2)\nabla_*^4 \psi_0$$

$$- \sigma_0^3 \nabla_*^2 \psi_0 + \sigma_0^2 \lambda_*^2 Ra^2 T_2 \psi_0 + \lambda_*^2 \sigma_0 \nabla_*^4 \psi_0 = 0 \qquad 3.47$$

Now drawing upon the theory of partial differential equations and in particular Green's functions, the concept of a self adjoint operator is used. The 'wave diffusion' operator is in itself self adjoint. The operator acting on ψ_1 in (3.47) is self adjoint, for free conducting boundaries, and this condition is obtained by multiplying (3.47) by ψ_0 and integrating over the non-dimensional depth:

$$2\sigma_1 \int_{-1/2}^{1/2} \left\{ (\psi_0'')^2 + 2\lambda_*^2 (\psi_0')^2 + \lambda_*^4 \psi_0^2 \right\} dz_* =$$

$$-2\int_{-1/2}^{1/2} \left\{ (\psi_0''')^2 + 3\lambda_*^2 (\psi_0'')^2 + 3\lambda_*^4 (\psi_0')^2 + \lambda_*^6 \psi_0^2 \right\} dz_*$$

$$- \sigma_0^2 \int_{-1/2}^{1/2} \left\{ (\psi_0')^2 + \lambda_*^2 \psi_0^2 \right\} dz_*$$

$$- \sigma_0 \int_{-1/2}^{1/2} \left\{ (\psi_0'')^2 + 2\lambda_*^2 (\psi_0')^2 + \lambda_*^4 \psi_0^2 \right\} dz_* - \lambda_*^2 Ra_*^2 \int_{-1/2}^{1/2} T_2 \psi_0^2 \, dz \qquad 3.48$$

The first term on the right hand side represents the viscous dissipation. The second and the third terms represent the

destabilizing effect due to the finite diffusion time, whereas the former of the two terms represents the dominating influence. The final term represents the stabilizing effect of the stable vertical temperature gradient.

Section (iii)

Stability Solutions

It is possible to derive solutions for (3.44) by replacing T_z and U_z by constants $\bar{T}_z$ and $\bar{U}_z$ which may be looked upon as weighted mean values. This strategem has been employed by Faller (1969) with advective instability in geophysical flows with downstream gradients of density. A negative downstream gradient, with positive vertical shear, leads to a weak convective phenomenon termed, advective instability. The parameter that modifies the convective instability is a function of two weighted mean values $\bar{P}_x$ the downstream gradient and $\bar{U}_z$ the vertical shear.

Hence, using an analogue approach to Faller it is possible to replace U_z and T_z in equation (3.44) by their weighted mean values, it will yield solutions which are sinusoidal in z. A feature associated with the basic state flow pattern is that the depth of the fluid approaches half a wavelength. This feature is certainly true with rigid boundaries, then it is possible to rewrite the operator

$$\nabla_x^2 = -\pi^2 - l_x^2 = -k^2 \qquad 3.49$$

The two modifications will reduce (3.44) to an algebriac expression viz:-

$$(\sigma_x + P^{1/2}k^2)^2(k^2 + P^{1/2}\sigma_x)k^2 + l_x^2 R_a^2 P^{1/2}(\sigma_x + P^{1/2}k^2)\bar{T}_z$$

$$+ l_x^2 R_a^2 \bar{U}_z + l_x^2 P^{1/2}(\sigma_x + P^{1/2}k^2)(\sigma_x + P^{1/2}k^2)k^2 = 0 \qquad 3.50$$

A solution of the form $\sigma_x = \sigma_r + i\sigma_i$ will be examined,

where σ_r is the growth rate and σ_i is the frequency of oscillation. Now when σ_r is less than zero, the disturbances decay with time, while with σ_r greater than zero the disturbances grow with time. However, with the boundary condition $\sigma_r = 0$ the disturbances will neither grow or decay and this condition is termed marginal stability. Then it follows that $\sigma_x = i\sigma_i$

Expanding each term of (3.50) we obtain

(a) $-k^4\sigma_i^2 + 2k^6P^{1/2}i\sigma_i + Pk^8 - ik^2P^{1/2}\sigma_i^3 - 2k^4P\sigma_i^2 + ik^6P^{3/2}\sigma_i$

(b) $l_x^2 R_a^2 \bar{u}_z$

(c) $il_x^2 R_a^2 P^{1/2}\bar{T}_z\sigma_i + l_x^2 R_a^2 Pk^2\bar{T}_z$

(d) $-\sigma_i^2 l_x^2 P^{1/2}k^2 + 2iPl_x^2k^4\sigma_i + l_x^2P^{3/2}k^6$

Grouping the real and imaginary parts:

Real Part

$$\sigma_i^2 = \frac{Pk^8 + l_x^2R_a^2\bar{u}_z + l_x^2R_a^2P\bar{T}_zk^2 + l_x^2k^6P^{3/2}}{k^4 + 2k^4P} \qquad 3.51$$

Imaginary Part

$$\sigma_i^2 = \frac{2k^6P^{1/2} + k^6P^{3/2} + l_x^2R_a^2P^{1/2}\bar{T}_z + 2Pl_x^2k^4}{k^2P^{1/2}} \qquad 3.52$$

Expressions (3.51) and (3.52) combine to give $Ra = Ra_{ms}$ which is the conditional for marginal stability.

$$R_{a_{ms}}^2 = \frac{2k^8 + 4k^8P + 4k^6l_x^2P^{1/2} + 2k^8P^2 + 4k^6l_x^2P^{3/2} + 2l_x^4Pk^4}{l_x^2\left(\bar{u}_z - \bar{T}_zk^2P - \bar{T}_zk^2 - \bar{T}_zk^2P^{1/2}l_x^2\right)} \qquad 3.53$$

Stable solutions of (3.53) will be found for Ra Ra_{ms} and unstable solutions follow for the converse mutatis mutandis. Sinusoidal instability is only possible for

$$\bar{U}_z > \bar{T}_z k^2 \left(1 + P + P^{1/2} J_x^2\right) \qquad 3.54$$

To derive meaningful expressions for the solutions of the non-dimensional shear and temperature gradient a weighted integral, arising from energy considerations, is used. Then the non-dimensional shear is evaluated from the integral

$$\bar{U}_z = \frac{\int_{-1/2}^{1/2} U_{zx} W(z_x) dz_x}{\int_{-1/2}^{1/2} W(z_x) dz_x} \qquad 3.55$$

where $W(z_x) = \cos^2 \pi z_x$ An analogue integral for the non-dimensional temperature gradient is also similar in form to (3.55). The relationship connecting the non-dimensional temperature gradient will be:

$$\frac{d^2}{dz_x^2} \{T_z\} = \frac{d^2 U_z}{\chi Ra} \qquad 3.56$$

Integral (3.55) is used for the evaluation of the non-dimensional shear and the analogous integral for the non-dimensional temperature gradient, for constant radial coordinate. The integrals have been calculated in appendix III.

The respective values for the various models are tabulated below.

Rigid conducting boundaries

(a) Reduced polar model

Non-dimensional shear

$$\bar{u}_z = \frac{2r^2}{d^2}\left\{\frac{4r\sinh E - 2d\cosh E}{8r\sinh^2 E - 2d\sinh 2E}\right\}\frac{\sinh E}{1+\frac{\pi^2}{E^2}} \qquad 3.57$$

where $E = \frac{d}{2r}$

Non-dimensional temperature gradient

$$\bar{T}_z = \frac{r^2}{2\pi d^2}\left\{\frac{4r\sinh E - 2d\cosh E}{8r\sinh^2 E - 2d\sinh 2E}\right\}\frac{\sinh E}{1+\frac{\pi^2}{E^2}} \qquad 3.58$$

(b) Gill values

Non-dimensional shear

$$\bar{u}_z = (2\pi)^{-2}$$

Non-dimensional temperature gradient

$$\bar{T}_z = (2\pi)^{-4}$$

Free conducting boundaries

(a) Reduced polar model

Non-dimensional shear 3.59

$$\bar{u}_z = \frac{r^2}{d^2}\left\{1 - \frac{\tanh E}{E} + \frac{4E\sinh E}{4E^2+4\pi^2}\right\}$$

Non-dimensional temperature gradient

$$\bar{T}_z = \frac{r^2}{(2\pi d)^2}\left\{1 - \frac{\tanh E}{E} + \frac{4E\sinh E}{4E^2+4\pi^2}\right\} \qquad 3.60$$

(b) Gill values

Non-dimensional shear

$$\bar{u}_z = \frac{1}{(2\pi)^2}\left\{1+\frac{\pi^2}{3}\right\}$$

Non-dimensional temperature gradient

$$\bar{T}_z = \frac{1}{(2\pi)^4}\left\{1+\frac{\pi^2}{3}\right\}$$

Rigid-Free conducting boundaries

(a) Reduced polar model

Non-dimensional shear

$$\bar{u}_z = \frac{2r^2}{d^3}\left\{\frac{d^2\sinh E}{r} - 4r\sinh E + 2d\cosh E\right\}\sinh E \Big/ \left\{4\sinh E\cosh E - \frac{2d}{r}\cosh 2E\right\} \qquad 3.61$$

$$+ \frac{2r^2}{d^3}\left\{\frac{-d^2\sinh E}{r} + 4r\sinh E - 2d\cosh E\right\}\frac{\sinh E}{1+\frac{\pi^2}{E^2}} + \frac{r^2}{d^2}$$

(b) Non-dimensional temperature gradient

$$\bar{T}_z = \frac{\bar{u}_z}{(2\pi)^2} \qquad 3.62$$

Gill values

Non-dimensional shear

$$\bar{u}_z = \frac{1}{4\pi^2}\left[\frac{\pi^2}{12}+1\right]$$

Non-dimensional temperature gradient

$$\bar{T}_z = \frac{1}{16\pi^4}\left[\frac{\pi^2}{12}+1\right]$$

For large values of r the following truncated series for $\cosh E$ and $\sinh E$ can be used

$$\sinh E \simeq E + \frac{E^3}{6} \qquad 3.63$$

$$\cosh E \simeq 1 + \frac{E^2}{2} \qquad 3.64$$

Then expression (3.57) becomes:

$$\bar{u}_z = \frac{1}{4}\left\{\frac{4\left(E+\frac{E^3}{6}\right) - 4E\left(1+\frac{E^2}{2}\right)}{8\left(E+\frac{E^3}{6}\right)\left(E+\frac{E^3}{6}\right) - 8E\left(1+\frac{E^2}{2}\right)\left(E+\frac{E^3}{6}\right)}\right\}\frac{E+\frac{E^3}{6}}{E^2+\pi^2} \qquad 3.65$$

Then (3.65) becomes:

$$\bar{u}_z = \frac{1}{4}\left\{\frac{\frac{8E^4}{3}}{\frac{8E^4}{3}}\right\}\frac{1}{E^2+\pi^2} \longrightarrow \frac{1}{4\pi^2} \qquad 3.66$$

$r \to \infty$

Relationship (3.66) is identical to the Gill value for the non-dimensional shear for rigid conducting boundaries.

Likewise, with the same approximations, (3.59) becomes:

$$\bar{u}_z = \frac{1}{4E^2}\left\{1 - \frac{E+\frac{E^3}{6}}{E(1+\frac{E^2}{6})} + \frac{4E(E+\frac{E^3}{6})}{4E^2+4\pi^2}\right\} \qquad 3.67$$

or

$$\bar{u}_z = \frac{1}{4E^2}\left\{1 - 1 + \frac{E^2}{2} - \frac{E^2}{6} + \frac{4E^2(1+\frac{E^2}{6})}{4E^2+4\pi^2}\right\} \qquad 3.68$$

$$\lim_{E\to 0} \bar{u}_z = \frac{1}{12} + \frac{1}{4\pi^2} \qquad 3.69$$

Relationship (3.65) is identical to the Gill value for the non-dimensional shear for free conducting boundaries.

The truncated expansions of $\cosh E$ and $\sinh E$ when E is approaching zero removed the dependance of the non-dimensional shear and temperature gradient upon the depth of the fluid and the radial coordinate. The limiting values are also in agreement with the Gill values for the rectangular configuration. However, it should be noted that the Gill model proposes that the fluid is unbounded both in the x and y directions.

Equations (3.57) to (3.62) were programmed on a computer see appendix I program 2. This was to determine the convergence of the reduced polar model non-dimensional shear and temperature gradient as compared with the Gill values. The range of the depth was four equal increments commencing at 7 mm and terminating at 10 mm. It was taken that the inner cylinder radius was small and the radial value commenced at 10 mm and was incremented in equal steps of 10 mm

to a maximum of 50 mm. These respective depth and range variations encompassed the proposed experimental values. The results are quoted as a ratio: the Gill value divided by the reduced polar model. The results are tabulated in Table 2 and all the measurements where appropriate are in mm.

TABLE Ia

Boundary Conditions : Rigid-Rigid

Depth	Radial Distance	Ratio
7	10	1.012
"	20	1.003
"	30	1.015
"	40	1.015
"	50	0.999
8	10	1.016
"	20	1.004
"	30	1.002
"	40	1.001
"	50	1.001
9	10	1.021
"	20	1.005
"	30	1.002
"	40	1.001
"	50	1.001
10	10	1.025
"	20	1.006
"	30	1.003
"	40	1.002
"	50	1.001

TABLE Ib

Boundary Conditions: Free-Free

Depth	Radial Distance	Ratio
7	10	1.035
"	20	1.009
"	30	1.038
"	40	1.001
"	50	1.001
8	10	1.046
"	20	1.012
"	30	1.005
"	40	1.003
"	50	1.001
9	10	1.057
"	20	1.015
"	30	1.007
"	40	1.004
"	50	1.002
10	10	1.071
"	20	1.018
"	30	1.008
"	40	1.004
"	50	1.003

TABLE Ic

Boundary Conditions : Rigid-Free

Depth	Radial Distance	Ratio
7	10	1.024
"	20	1.007
"	30	1.002
"	40	1.001
"	50	1.001
8	10	1.031
"	20	1.009
"	30	1.001
"	40	1.031
"	50	0.958
9	10	1.039
"	20	1.010
"	30	1.005
"	40	1.002
"	50	1.001
10	10	1.048
"	20	1.012
"	30	1.004
"	40	1.005
"	50	1.003

From these results it is clear that the reduced polar model agrees well with the Gill model.

Section (iv)

Non-dimensional velocity and shear equations

At this juncture this appears to be a slight digression from the main theme. However, the comparison between the two theories will throw further light on the nature of the problem, especially the velocity field.

Rigid-Conducting

Reduced cylindrical coordinates

$$u = \frac{1}{4E^2}\left\{\left(\frac{2E\cosh E - 2\sinh E}{4\sinh^2 E - 2E\sinh 2E}\right)\sinh 2Ez_* + z_*\right\} \qquad 3.70$$

$$s = \frac{1}{2E}\left\{\left(\frac{2E\cosh E - 2\sinh E}{4\sinh^2 E - 2E\sinh 2E}\right)\cosh 2Ez_* + \frac{1}{2E}\right\} \qquad 3.71$$

Gill

$$u = \frac{z_*}{24} - \frac{z_*^3}{6} \qquad 3.72$$

$$s = \frac{1}{24} - \frac{z_*^2}{2} \qquad 3.73$$

Free-conducting

$$u = \frac{1}{4E^2}\left\{z_* - \frac{\sinh 2Ez_*}{2E\cosh E}\right\} \qquad 3.74$$

$$s = \frac{1}{4E^2}\left\{1 - \frac{\cosh 2Ez_*}{\cosh 2E}\right\} \qquad 3.75$$

$$u = \frac{z_*}{8} - \frac{z_*^3}{6} \qquad 3.76$$

$$s = \frac{1}{8} - \frac{z_*^2}{2} \qquad 3.77$$

Rigid-Free Conducting

Reduced cylindrical coordinates

$$U = -\frac{1}{16E^3}\left\{\frac{2E^2\exp -E + 2\sinh E - 2E\exp E}{2\sinh E\cosh E - 2E\cosh E}\right\}\exp 2EZ_x$$

$$-\frac{1}{16E^3}\left\{\frac{2E^2\exp E - 2\sinh E + 2E\exp -E}{2\sinh E\cosh E - 2E\cosh E}\right\}\exp -2EZ_x$$

$$+\frac{1}{16E^3}\left\{\frac{2E^2\exp -E + 2\sinh E - 2E\exp E}{2\sinh E\cosh E - 2E\cosh E}\right\}\exp -E$$

$$+\frac{1}{16E^3}\left\{\frac{2E^2\exp E - 2\sinh E + 2E\exp -E}{2\sinh E\cosh E - 2E\cosh E}\right\}\exp E$$

$$+\frac{1}{8E^2} + \frac{Z_x}{4E^2} \qquad 3.78$$

$$S = -\frac{1}{8E^2}\left\{\frac{2E^2\exp -E + 2\sinh E - 2E\exp E}{2\sinh E\cosh E - 2E\cosh E}\right\}\exp 2EZ_x$$

$$+\frac{1}{8E^2}\left\{\frac{2E^2\exp E - 2\sinh E + 2E\exp -E}{2\sinh E\cosh E - 2E\cosh E}\right\}\exp -2EZ_x$$

$$+\frac{1}{4E^2} \qquad 3.79$$

Gill

$$U = -\frac{Z_x^3}{6} + \frac{Z_x^2}{16} + \frac{Z_x}{16} - \frac{1}{192} \qquad 3.80$$

$$S = -\frac{Z_x^2}{2} + \frac{Z_x}{8} + \frac{1}{16} \qquad 3.81$$

Equations (3.76) to (3.81) were programmed on a computer see appendix II program number 3.

The following spectrum of values were used:

(a) depth of fluid commencing at 7 mm to 10 mm with increments of 1 mm

(b) the radial distance commencing at 15 mm to 35 mm with increments of 5 mm

(c) the vertical depth in the fluid commencing at - 0.5 to 0.5 with increments of 0.125.

The results are quoted overleaf, for typical values; radial distance of 15 mm depth 9 mm.

TABLE 2

Boundary Conditions : Rigid-Rigid

Depth in fluid	Velocity		Shear	
	Polar Model	Gill	Polar Model	Gill
- 0.5	-2.4×10^{-5}	0	-8.23×10^{-2}	-8.33×10^{-2}
- 0.375	-6.8×10^{-3}	-6.84×10^{-3}	-2.83×10^{-2}	-2.86×10^{-2}
- 0.25	-7.75×10^{-3}	-7.81×10^{-3}	1.04×10^{-2}	1.042×10^{-2}
- 0.125	-4.84×10^{-3}	-4.88×10^{-3}	3.36×10^{-2}	3.39×10^{-2}
0	0	0	4.13×10^{-2}	4.17×10^{-2}
0.125	4.84×10^{-3}	4.88×10^{-3}	3.36×10^{-2}	3.39×10^{-2}
0.25	7.75×10^{-3}	7.81×10^{-3}	1.04×10^{-2}	1.04×10^{-2}
0.375	6.8×10^{-3}	6.84×10^{-3}	-2.83×10^{-2}	-2.86×10^{-2}
0.5	2.3×10^{-5}	0	-8.23×10^{-2}	-8.33×10^{-2}

TABLE 3

Boundary Conditions : Free-Free

Depth in fluid	Velocity		Shear	
	Polar Model	Gill	Polar Model	Gill
- 0.5	-4.02×10^{-2}	-4.17×10^{-2}	0	0
- 0.375	-3.68×10^{-2}	-3.81×10^{-2}	5.29×10^{-2}	5.47×10^{-2}
- 0.25	-2.76×10^{-2}	-2.87×10^{-2}	9.05×10^{-2}	9.38×10^{-2}
- 0.125	-1.47×10^{-2}	-1.53×10^{-2}	1.13×10^{-1}	1.17×10^{-2}
0	0	0	1.21×10^{-1}	1.25×10^{-1}
0.125	1.47×10^{-2}	1.53×10^{-2}	1.13×10^{-1}	1.17×10^{-1}
0.25	2.76×10^{-2}	2.87×10^{-2}	9.05×10^{-2}	9.38×10^{-2}
0.375	3.68×10^{-2}	3.81×10^{-2}	5.29×10^{-2}	5.47×10^{-2}
0.5	4.02×10^{-2}	4.17×10^{-2}	0	0

TABLE 4

Boundary Conditions : Rigid-Free

Depth in fluid	Velocity		Shear	
	Polar Model	Gill	Polar Model	Gill
- 0.5	0	2.794×10^{-9}	-1.24×10^{-1}	-1.25×10^{-1}
- 0.375	-1.09×10^{-2}	-1.11×10^{-2}	-5.37×10^{-2}	-5.47×10^{-2}
- 0.25	-1.41×10^{-2}	-1.43×10^{-2}	2.46×10^{-4}	0
-0.125	-1.15×10^{-2}	-1.17×10^{-2}	3.85×10^{-2}	3.91×10^{-2}
0	-5.1×10^{-3}	-5.21×10^{-3}	6.14×10^{-2}	6.25×10^{-2}
0.125	3.22×10^{-3}	3.26×10^{-3}	6.90×10^{-2}	7.03×10^{-2}
0.25	1.15×10^{-2}	1.17×10^{-2}	6.13×10^{-2}	6.25×10^{-2}
0.375	1.79×10^{-2}	1.82×10^{-2}	3.84×10^{-2}	3.91×10^{-2}
0.5	2.05×10^{-2}	2.08×10^{-2}	5.72×10^{-6}	0

It can be seen from the three tables that there is close agreement between the velocity and shear as predicted by the polar model values when compared to the Gill values.

Skafel's measurements of the mean temperature field looked much the same as the box geometry. Skafel used mercury as the fluid and studied convection more particularly in an annulus with the temperature difference maintained between the inner and outer cylindrical surfaces. Certainly, the experimental agreement between the mean temperature field, supports the values obtained in the three tables.

Figures 2 and 3 illustrate the variation of velocity and shear with depth as the reduced polar model and the Gill model are in close agreement only when a single curve is drawn. These figures are self-explanatory.

FIGURE 2

VELOCITY VARIATION FOR DIFFERENT CONDITIONS OF BOUNDARY WITH DEPTH

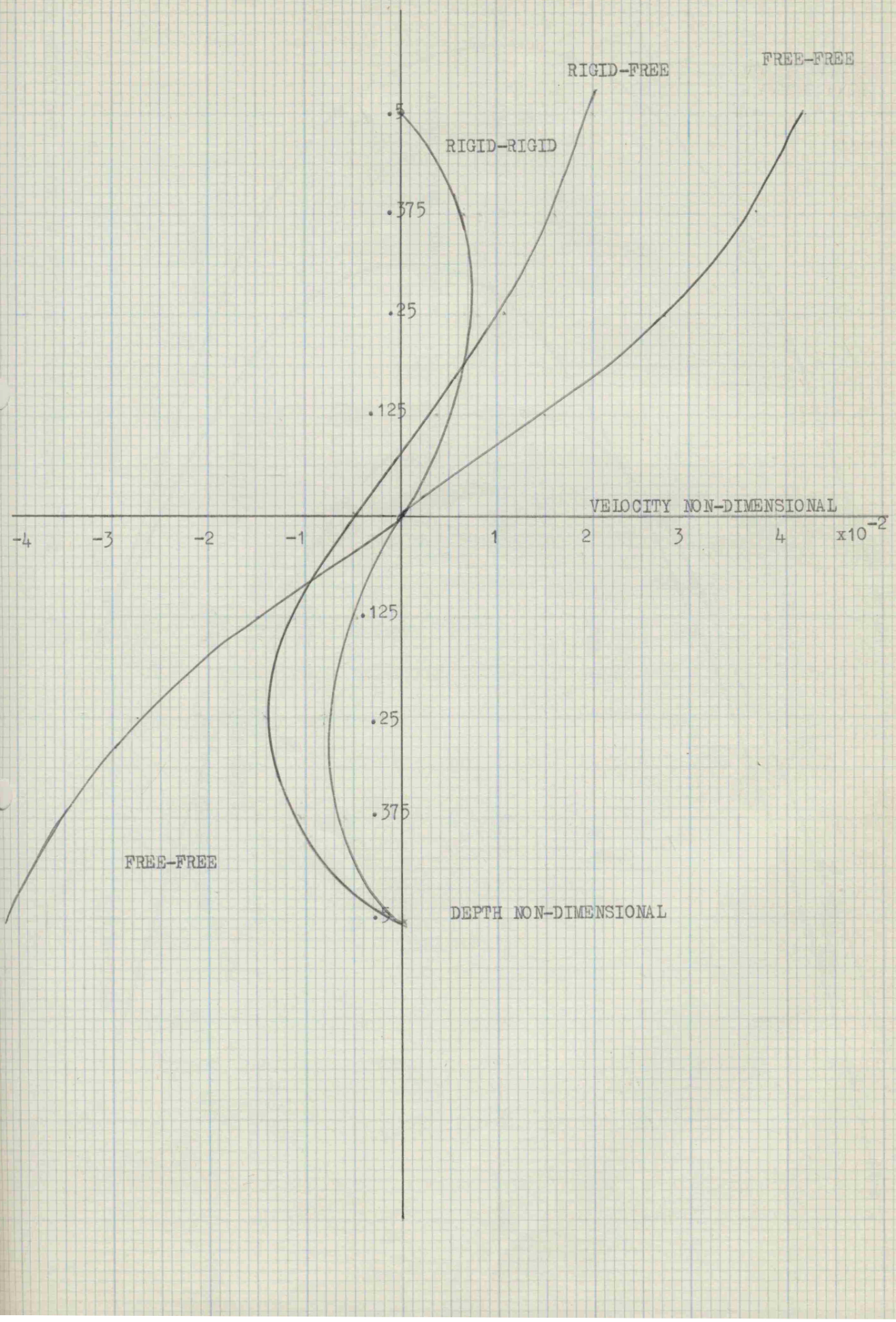

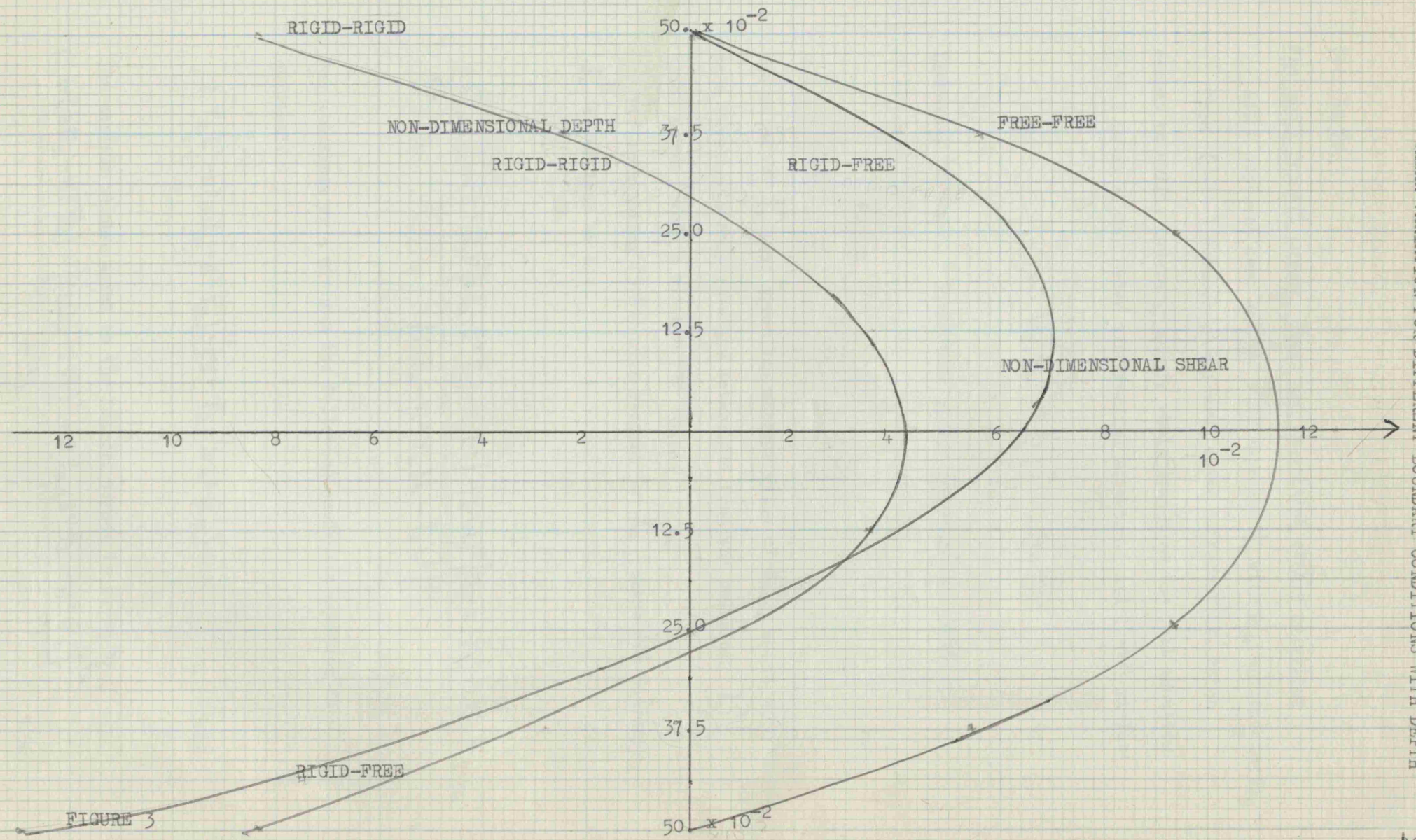

FIGURE 3

SHEAR VARIATION FOR DIFFERENT BOUNDARY CONDITIONS WITH DEPTH

Section (v)

The small Prandtl number limit and associated stable solutions

Let P approach zero and $\hat{\psi}$ will approach ψ_0 with σ_* approaching σ_0

Then (3.44) reduces to a fourth order differential, which cannot be valid, however, in the whole domain as the full equation (3.44) is an eighth order differential equation. And (3.44) yields:

$$\sigma_0^2 \nabla_*^4 \psi_0 + l_*^2 R_a^2 u_z \psi_0 = 0 \qquad 3.82$$

Likewise, the small P limit also yields for equation (3.53)

$$R_{a_{ms}}^2 = \frac{2k^8}{l_*^2 (\bar{u}_z - \bar{T}_z k^2)} \qquad 3.83$$

The value of l_*^2 that gives the minimum value of $R_{a_{ms}}^2$ which corresponds to a wavelength propogated is determined from the value of l_*^2 which makes (3.83) a minimum for $R_{a_{ms}}^2$

Differentiating (3.83) with respect to l_*^2 where for convenience l_*^2 is written as L.

$$\frac{dR_{a_{ms}}^2}{dL} \propto 4(\pi^2+L)^3\left\{(\bar{u}_z - \pi^2\bar{T}_z) - \bar{T}_z L^2\right\} - (\pi^2+L)^4\left\{(\bar{u}_z - \pi^2 T_z) - 2T_z L\right\} \qquad 3.84$$
$$\left\{(\bar{u}_z - \pi^2\bar{T}_z)L - \bar{T}_z L^2\right\}^2$$

For a maximum or a minimum the following quadratic equation is obtained:

$$2\bar{T}_z L^2 - L(6\bar{u}_z - \pi^2\bar{T}_z) - (\pi^4\bar{T}_z - 2\pi^2\bar{u}_z) = 0 \qquad 3.85$$

The minimum value, which is the logical choice is given by

$$L = \frac{(3\bar{u}_z - \pi^2\bar{T}_z) - \left\{(3\bar{u}_z - \pi^2\bar{T}_z)^2 + 8\bar{T}_z(\pi^4\bar{T}_z - \pi^2\bar{u}_z)\right\}^{1/2}}{4\bar{T}_z} \qquad 3.86$$

The non-dimensional frequency, in the small P limit is given by

$$\sigma_0^2 = \frac{l_x^2 R_{ams}^2 \bar{U}_z}{k^4} \qquad 3.87$$

or

$$\sigma_0^2 = \frac{2k^6 + l_x^2 R_{ams}^2 \bar{T}_z}{k^2} \qquad 3.88$$

Having determined the weighted mean values of the non-dimensional shear and temperature gradient it is now possible to estimate with the aid of (3.60) the value of P, below which, oscillations are possible. Stable solutions of (3.59) will be found for Ra less than Ra_{ms} and unstable solutions for the converse follow mutatis mutandis. Hence, sinusoidal instability is only possible for:

$$\bar{U}_z > \bar{T}_z k^2 (1 + P + P^{1/2} l_x^2) \qquad 3.89$$

The values of $\bar{U}_z$ and $\bar{T}_z$ have been already evaluated; hence employing the small P limit values of l_x^2 and k^2 it is possible to estimate the upper limit for P when oscillations cease. A computer program was written (see appendix I program 4) to calculate the non-dimensional shear, non-dimensional temperature gradient, Prandtl number, Rayleigh number, non-dimensional frequency and wavelength for a depth of 10 mm, aspect ratio of 0.333 and at a radial distance of 25 mm. The results, with the appropriate boundary conditions, are tabulated below.

Rigid conducting

Polar Model

Shear	Temperature Gradient	Prandtl Number
2.516×10^{-2}	6.356×10^{-4}	3.71×10^{-1}

Rayleigh Number	Frequency	Wavelength
1.042×10^{3}	2.189×10^{1}	3.728

Gill Model

Shear	Temperature Gradient	Prandtl Number
2.526×10^{-2}	6.381×10^{-4}	2.11

Rayleigh Number	Frequency	Wavelength
1.040×10^{3}	2.189×10^{1}	3.728

Free conducting

Polar Model

Shear	Temperature Gradient	Prandtl Number
1.0735×10^{-1}	2.712×10^{-3}	3.711×10^{-1}

Rayleigh Number	Frequency	Wavelength
5.045×10^{2}	2.189×10^{1}	3.728

Gill Model

Shear	Temperature Gradient	Prandtl Number
1.085×10^{-1}	2.743×10^{-3}	2.11

Rayleigh Number	Frequency	Wavelength
5.016×10^{2}	2.189×10^{1}	3.728

Rigid-Free

Polar Model

Shear	Temperature Gradient	Prandtl Number
4.569×10^{-2}	1.154×10^{-3}	3.711×10^{-1}

Rayleigh Number	Frequency	Wavelength
7.733×10^{2}	2.188×10^{1}	3.728

Gill Model

Shear	Temperature Gradient	Prandtl Number
4.609×10^{-2}	1.164×10^{-3}	2.11

Rayleigh Number	Frequency	Wavelength
7.69×10^{2}	2.188×10^{1}	3.128

In all three cases: rigid-rigid, free-free, and rigid-free, for the reduced polar model instability is only possible for P less than 0.3711. This value is certainly greater than all the well known molten metals. The largest value is of mercury 0.0264. For a value of P larger than 0.3711 it can be seen from the denominator of (3.59) viz:

$$\overline{U}_z - \overline{T}_z \left(k^2 P + k^2 + k^2 P^{1/2} J_x^2 \right) \qquad 3.90$$

that the stabilizing effect of the vertical temperature becomes too great for the oscillations to occur.

A further computer program (see appendix I program 5) was constructed. Employing the rigid-conducting boundary criteria, the

following variations were carried out in a cyclic pattern.

(i) the outer radius fixed at 40 mm

(ii) the inner radius varied for four values, namely, 10 mm, 13.75 mm, 21.25 mm, 25 mm

(iii) the depth of the fluid varied at each radius from 7 mm to 10 mm in steps of 1 mm

(iv) the radial distance at each depth stepped from $R = Ri + 1mm$ to $\frac{Ro + Ri}{2}$ in steps of 10 mm

At each increment the following information was printed out: depth of fluid, aspect ratio, radial distance, Rayleigh number, frequency, wavelength, Prandtl number

There was a variation in the Rayleigh number and the respective minimum and maximum values are listed below with the additional printed variables.

(i) depth	aspect ratio		radial distance
7 mm	2.667×10^{-1}		2.475×10^{1} mm
Rayleigh number	**frequency**	**Wavelength**	**Prandtl number**
1.03533×10^{3}	2.1829×10^{1}	3.72817	3.72524×10^{1}

(ii) depth	aspect ratio		radial distance
1×10^{1} mm	3.333×10^{-1}		1.1×10^{1} mm
Rayleigh number	**frequency**	**Wavelength**	**Prandtl number**
1.04511×10^{3}	2.18286×10^{1}	3.72817	3.72524×10^{1}

The work of Skafel (1972) revealed an important feature, namely, that the vertical temperature gradient varies. Following similar lines to Gill (1974) a final program to calculate the characteristics

of the initially marginal stable disturbance for varying values of T_z and the corresponding value of Ra and the ratio of the wavelength to the depth associated with the value of l_* which minimumizes Ra was written. The value of σ_i was also calculated. The boundary conditions were: Rigid-Rigid, Rigid-Free, and Free-Free and in the three cases for conducting boundaries. The results are displayed in figures: 4a, 4b and 4c. From the graphs it is interesting to note that the most marked change in the Rayleigh number occurs with the rigid-rigid conducting case. This mainly is due to the relatively smaller values of the non-dimensional shear and temperature gradient in comparison to the other boundary conditions, and they appear in the denominator of expression (3.89). Furthermore, with rigid boundaries the temperature gradient commences growing at the point where the fluid motion is more strongly inhibited by viscosity; conversely at a non-rigid, stress-free or free boundary the motion can commence much more easily.

CHAPTER IV

FIGURE (4a)

VARIATION OF RAYLEIGH NUMBER WITH TEMPERATURE GRADIENT FOR DIFFERENT BOUNDARY CONDITIONS

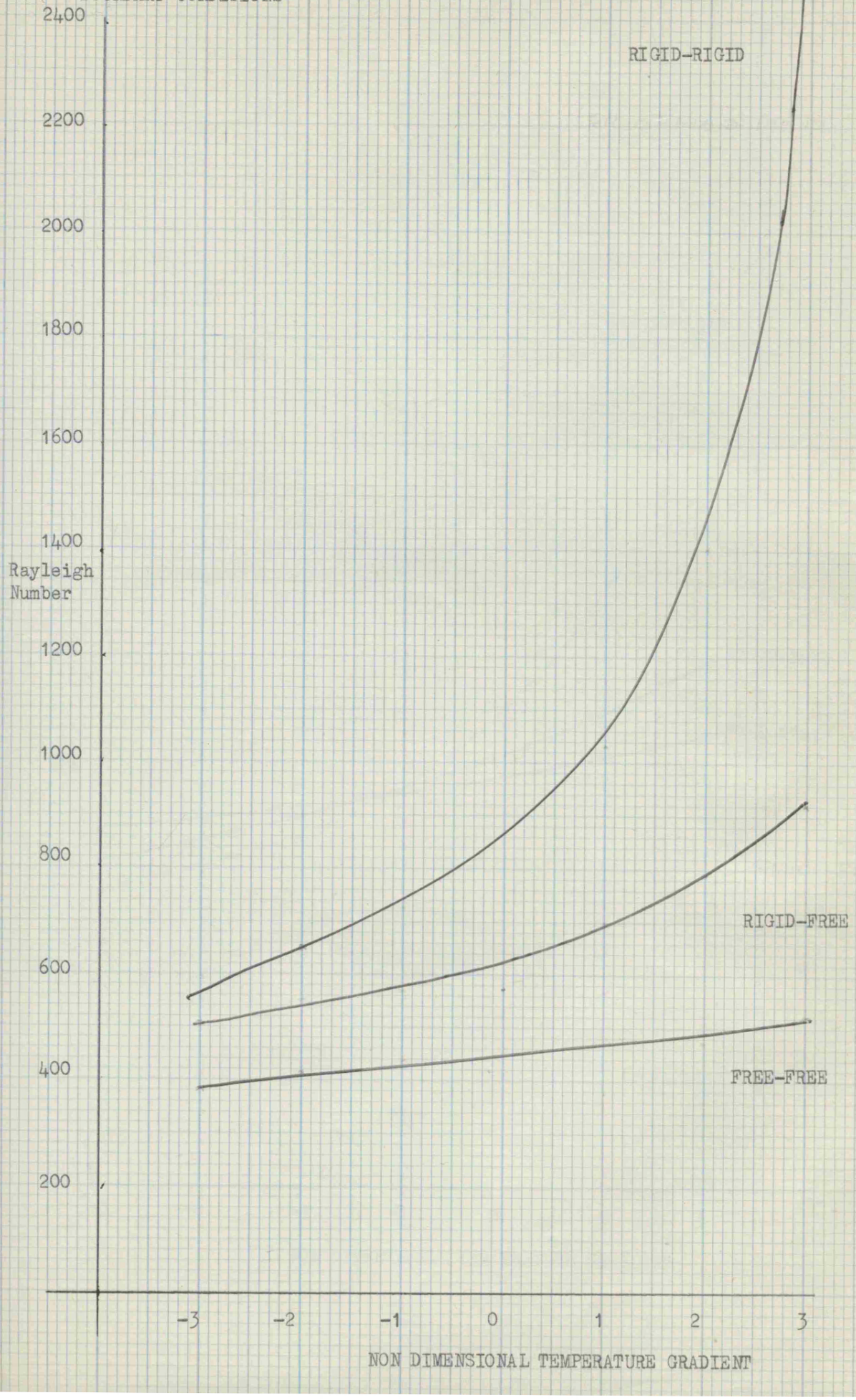

FIGURE (4b)

VARIATION OF THEORETICAL FREQUENCY WITH TEMPERATURE GRADIENT FOR DIFFERENT BOUNDARY CONDITIONS

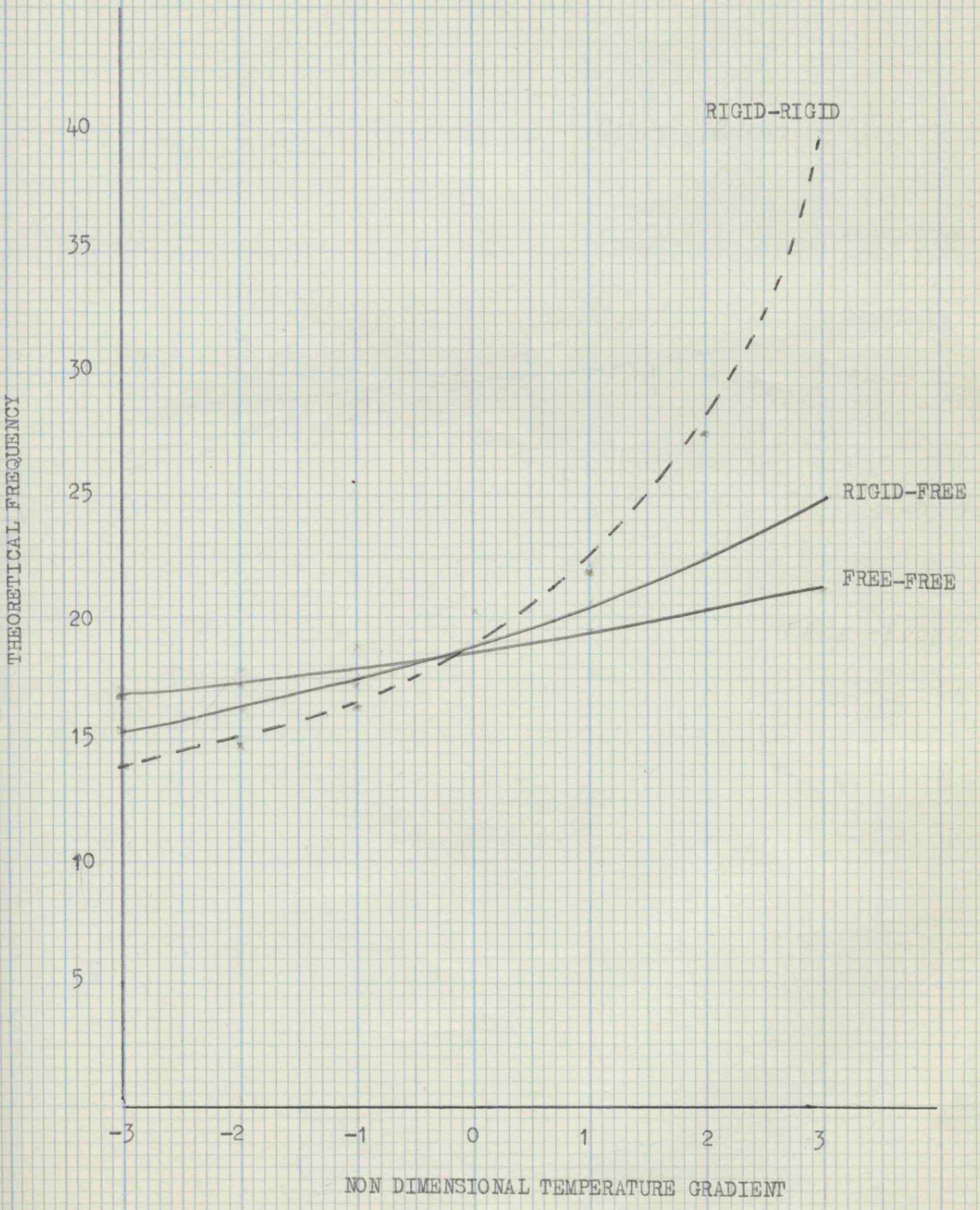

FIGURE (4c)

VARIATION OF WAVE LENGTH IN THE AZIMUTHAL DIRECTION WITH TEMPERATURE GRADIENT FOR DIFFERENT BOUNDARY CONDITIONS

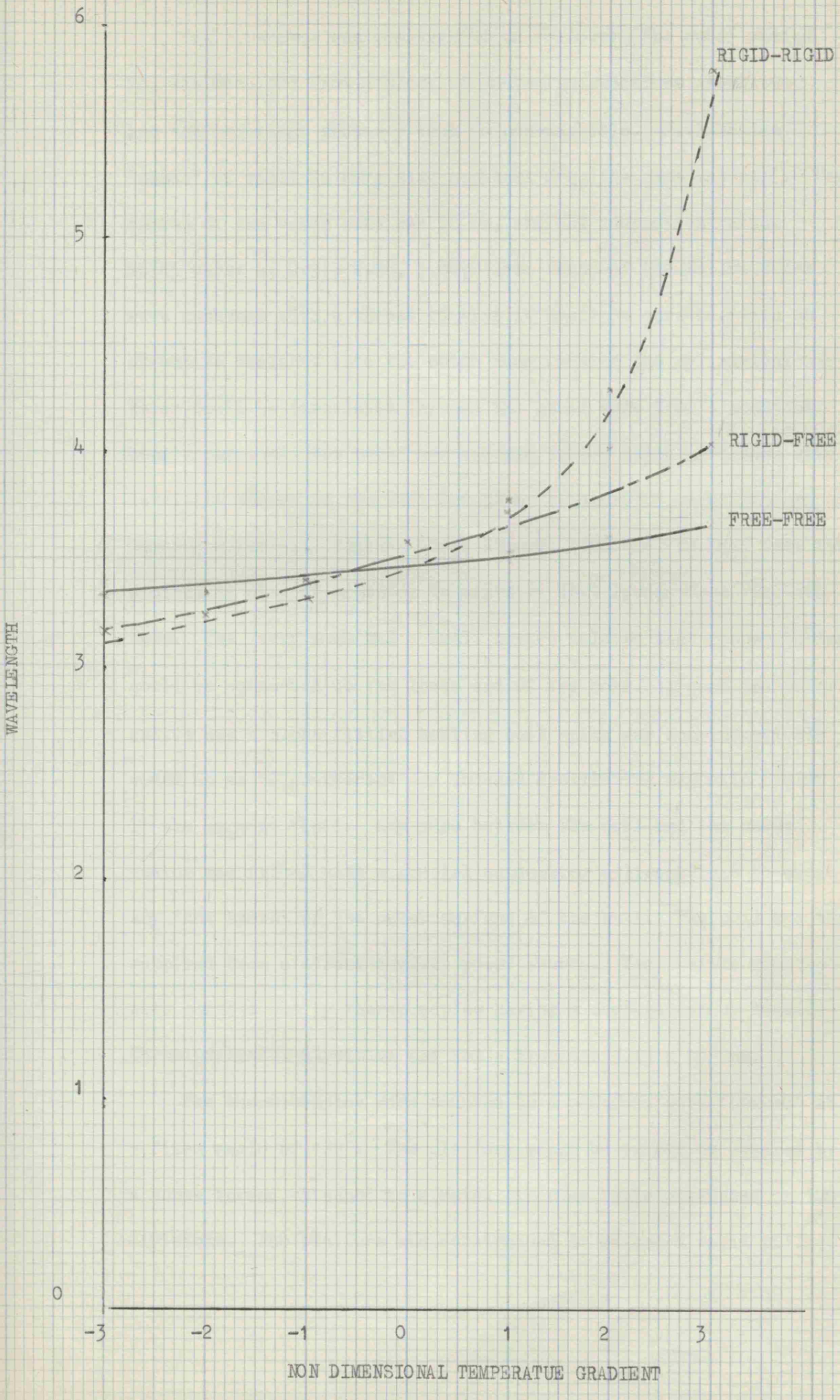

(i) Experimental Apparatus

The apparatus was constructed as follows: The outer radius Ro, was machined from a block of austensitic stainless steel; it has the important property that is non-magnetic. Five hollow 'cones' of radii Ri were also machined from the same material. The radius of the outer cone was 40 mm, and the respective ratios Ro/Ri were: 4, 2.91, 2.28, 1.88, 1.66. Each of the hollow cones were machined with a thread so that it could be screwed, with an effective sealant, into the outer cone forming the cylindrical bath. Water could be circulated through the inner cone from a constant head apparatus. The bath was screwed into a large iron mass with levelling screws on the base and it in turn rested on a platform of damping material. Between the cast iron mass and the bath base was a circular disc of asbestos to minimize heat losses from the bath base. The lower mass had a small centre hole so that rubber tubing could be connected to the lower end of the cone. Around the outer radius was a close fitting heating coil which was non-inductively wound so as to counteract any induced oscillating magnetic fields in the working fluid. Any gaps between the coil and the outer radius was filled with a special conducting silicone fluid to avoid any 'hot spots' on the outer surface of the bath. The coil was then supplied from a direct current power source. Temperature measurements were carried out by thermocouples having a composition of Nickel-Chromium/Nickel-Aluminium and had a diameter 3.15×10^{-1} mm.

The thermocouples were mounted on a platform each 'spaced' at a fixed angle of 120°. The platform could be raised or lowered by a screw thread attached to a metal circular scale graduated in 100 divisions. The platform was constrained to move on a rigid pillar,

with a keyway, to ensure only movement in the vertical direction. A rotation of 360 degrees raised or lowered the platform 1mm. This movement was for variation the z direction.

The platform could also be rotated through an angle of 120^{o}. This rotation corresponded to variation in the azimuthal direction. Finally, each of the thermocouples was mounted on a micrometer screw one revolution of a knurled nut, which has 10 divisions indented on its outer periphery, corresponds to a movement of 1 mm in the radial direction.

These respective movements were used to measure any spatial differences occurring in the working fluid. However, another modification was also used namely a radial probe. This comprised of an arm on which the thermocouples were mounted at equal intervals; and the temperature fluctuations measured along a radial line.

The whole of the apparatus was enclosed in a transparent, plastic, rectangular box with a fan mounted in the top of one corner. From a lower corner was an outlet pipe so that any fumes, generated in the apparatus, could be driven into the external atmosphere.

The output from the thermocouples was taken via screened cables to a three channel recorder. The temperature difference across the cell was measured by means of thermocouples in contact with the respective cones. The outputs of these latter thermocouples were connected to a Comark electronic thermometer, graduated to 10^{-1} deg. C.

The depth of mercury was set by introducing a calculated mass into the bath, however, no allowance was made in the experiments for the slight increase in depth due to the surface tension effect at the sides of the bath.

At an early stage in the experimental observations it was decided that all temperature measurements should be made within the mercury

and never in contact with the outer and inner cones. This would avoid any spurious end-effects due to thermal transfer processes and local convective instabilities.

The majority of experiments were conducted with the thermocouple junctions just 1 mm below the surface.

A sequence of experiments was conducted for each annulus. These were designed to determine the critical Rayleigh number required to initiate temperature oscillations and the nature of the oscillations with increasing temperature gradient. When the structural state was found within the cell, a series of measurements were taken to determine how the temperature oscillations varied with radial position. Experiments frequently showed a regular amplitude modulation, especially in the structural state. This modulation had been noted by other workers, Bolt (1975) [84] and Caldwell (1974) [92]. The latter worker noted the modulation, shown in one of his diagrams, as a typical characteristic, possibly being created by the movement of the convection cells, relative to his temperature measuring thermistor. The former worker found during a series of experiments employing a differential thermometer the results indicated a rhythmic rise and fall of amplitude inferring a wavelength.

The recorder channels were calibrated by employing a standard cell with a suitable potentiometer constructed from high stability resistors and each channel calibrated in steps up to a full scale deflection of 1 mv.

Finally, the paper drive speed at a selected setting was also measured. The calibrated value found was employed in all the frequency calculations.

The required depth of mercury was obtained by placing a calculated mass into the bath. The following masses were employed:

Ratio $\frac{Ro}{Ri}$	Mass (Kg)
1.6	4.149×10^{-2}
1.88	4.887×10^{-2}
2.28	5.507×10^{-2}
2.91	6.004×10^{-2}
4.00	6.383×10^{-2}

Each respective mass corresponded to a depth of 1 mm. Since the initial and subsequent incremental masses were measured to 10^{-5}kg the mercury depth was known to a high degree of accuracy. Special care, however, was taken to adjust the bath so that the base lay in a horizontal plane by means of spirit levels.

Turning now to the next section which comprises of the experiment results and observations. These have been presented in increasing order of cell length Ro - Ri. At each stage the apparatus had to be dismantled to insert the new core. The new bath was levelled and the recorder recalibrated at each stage. As the depth of fluid increased the temperature difference across the cell was reduced. Likewise, with increasing cell lengths a corresponding decrease in temperature difference also occurred. This explains why it is not possible to always maintain the same temperature differences in all the experiments. Hence, both the temperature difference and the Rayleigh number are quoted in each of the following tables. The oscillations were not sinusodial but with harmonics superimposed. This is why a comment column is included in each table. This procedure is confirmed by the results illustrated in figures (12) and (13).

(ii) Results and Discussion

TABLE 5

Results for critical Rayleigh number with aspect ratio.

$\frac{Ro}{Ri}$ = 1.6 Ro - Ri = 15 mm

Aspect ratio	Temp. difference	Critical difference	Comments
	Deg. C.	Rayleigh Number	
0.267	14.4	876	Small oscillations mainly harmonics small amplitudes
0.333	12.0	1762	Fundamental with mainly harmonics small amplitudes
0.400	10.5	3211	Fundamental with large amplitudes (structural state)
0.467	9.0	5114	Fundamental with harmonics small amplitudes
0.533	8.1	7733	Small amplitude oscillations mainly harmonics
0.600	6.25	1533	Small amplitude harmonic oscillations

TABLE 6

Structured State Results

$\frac{Ro}{Ri}$ = 1.6, Aspect ratio = 0.4 (Measured amplitudes peak to peak)

(a) Horizontal position of probes = 3.75 mm from outer radius

Rayleigh Number	Frequency Hz	Amplitude Deg. C.	Comments
4435	0.083	0.7	Narrow spectrum
6881	0.091	1.25	Narrow spectrum small second harmonic
8258	0.091	1.25	Narrow spectrum with second harmonic
9482	0.092	1.5	Narrow spectrum with second harmonic

(b) Horizontal position of probe = 7.5 mm from outer radius

3976	0.083	0.625	Narrow spectrum
6729	0.093	1.00	Narrow spectrum second harmonic present
8253	0.100	1.00	Narrow spectrum
9940	0.104	1.75	Narrow spectrum with small harmonic

$\frac{Ro}{Ri}$ = 1.6, Aspect ratio = 0.4 (Measured amplitudes peak to peak)

(c) Horizontal position of probe = 11.25 mm from outer radius

Rayleigh Number	Frequency Hz	Amplitude Deg. C.	Comments
4281	0.101	0.625	Narrow spectrum
5200	0.943	1.25	Narrow spectrum
7035	0.102	1.375	Narrow spectrum small distortion
8716	0.104	1.625	Narrow spectrum
9635	0.106	2.1	Narrow spectrum

FIGURE NUMBER 5

AMPLITUDE VARIATION WITH ASPECT RATIO FOR $\frac{Ro}{Ri}$ = 1.6 AND TEMPERATURE GRADIENT = 2.00 deg. C. mm^{-1}

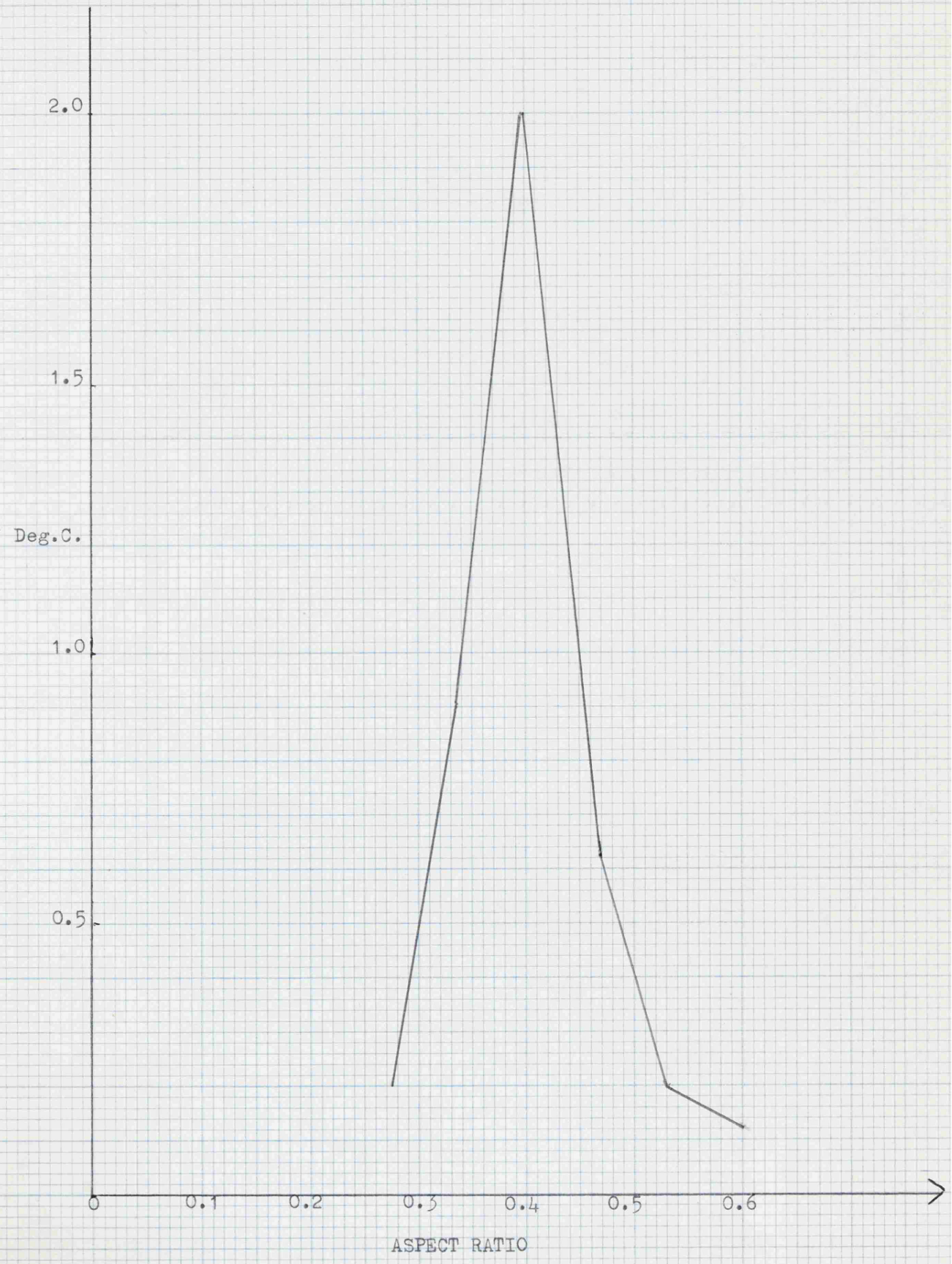

TABLE 7

Amplitude Variation with aspect ratio for $\frac{Ro}{Ri}$ = 1.6 and temperature gradient = 2.00 deg. C. mm^{-1}

Aspect Ratio	Amplitude Deg. C.	Comments
0.267	0.20	Harmonics
0.333	0.80	Fundamental with harmonics
0.400	2.0	Fundamental very small second harmonic
0.467	0.62	Fundamental large harmonics
0.533	0.20	Harmonics no fundamental
0.600	0.125	Harmonics no fundamental

TABLE 8

Results for critical Rayleigh number with aspect ratio

$\frac{Ro}{Ri}$ = 1.88, Ro - Ri = 18.75 mm

Aspect Ratio	Temp. difference Deg. C.	Critical difference Rayleigh number	Comments
0.213	19.6	942	Narrow spectrum with harmonics
0.267	11.95	1416	Harmonics with 0.5 deg. C. peak to peak amplitude
0.320	10.75	2630	Irregular wave form 0.5 deg. C. peak to peak amplitude
0.373	8.5	3839	Narrow spectrum second harmonics peak to peak amplitude 0.2 deg. C.
0.384	8.00	4059	Narrow spectrum with harmonics
0.400	8.02	4780	Narrow spectrum with small harmonics (structural state)
0.427	6.48	5026	Harmonics peak to peak 0.5 deg. C.
0.480	6.00	7436	Harmonics very small amplitudes
0.533	4.5	8474	Harmonics very small amplitudes

TABLE 9

Structured State results

$\frac{Ro}{Ri}$ = 1.88 Aspect ratio 0.400, Ro - Ri = 18.75 mm = Amplitudes measured peak to peak

(a) Horizontal position of probes = 9.38 mm from outer radius

Rayleigh Number	Frequency Hz	Amplitude Deg. C.	Comments
6571	0.061	0.7	Narrow spectrum
11948	0.0769	0.85	Narrow spectrum small second harmonic
15651	0.0806	2.1	Narrow spectrum
16427	0.0909	1.75	Narrow spectrum very small second harmonic

(b) Horizontal position of probes = 12.5 from outer radius

5974	0.059	0.6	Narrow spectrum
10454	0.0714	0.7	Narrow spectrum
14135	0.0746	1.25	Narrow spectrum small second harmonic
16250	0.0769	2.6	Narrow spectrum

FIGURE NUMBER 6

AMPLITUDE VARIATION WITH ASPECT RATIO FOR $\frac{Ro}{Ri}$ = 1.88 AT TEMPERATURE

GRADIENT = 1.44 deg. C. mm^{-1}

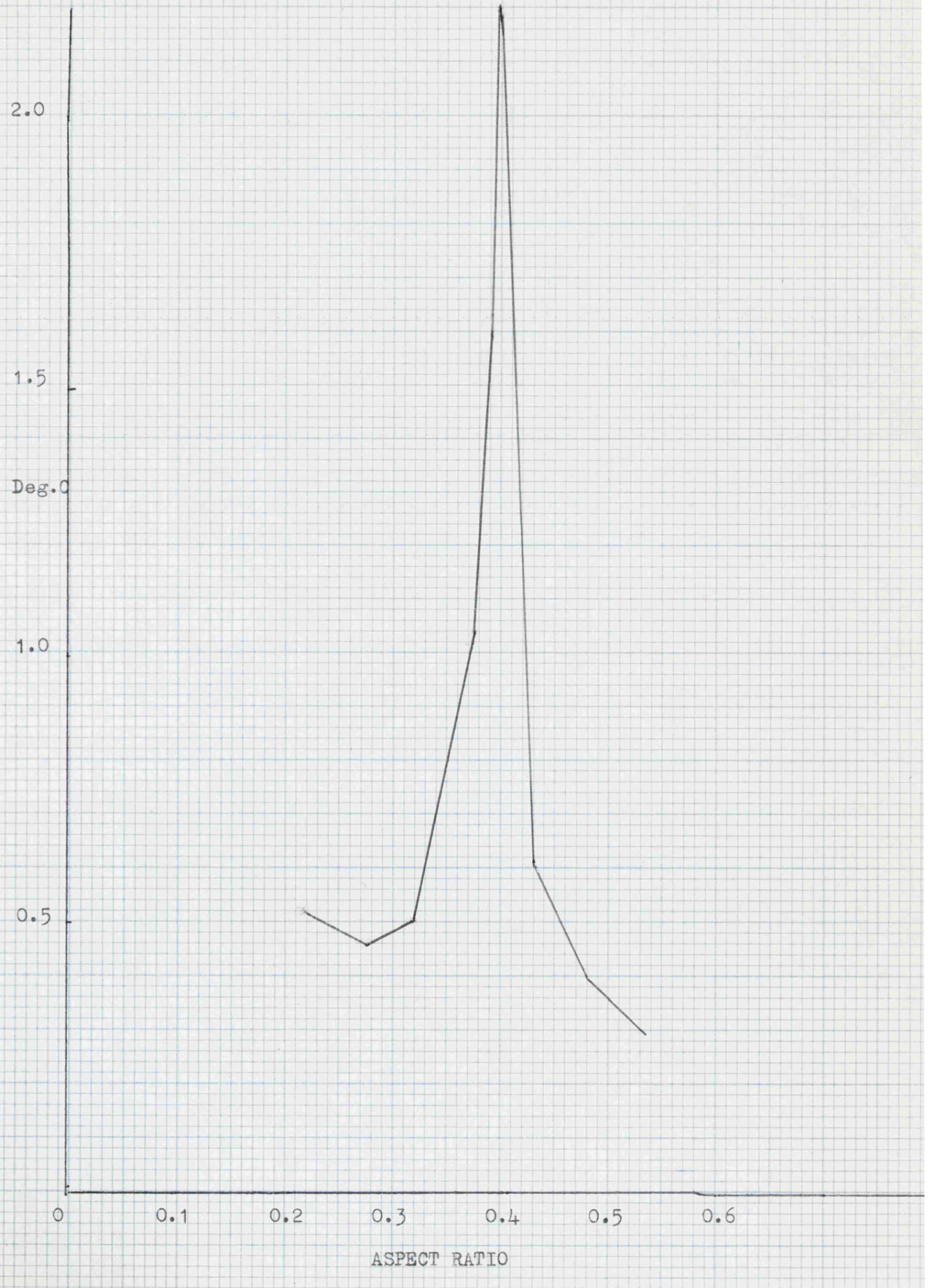

TABLE 10

Amplitude variation with aspect ratio for $\frac{Ro}{Ri}$ = 1.88, Ro - Ri = 18.75 mm and temperature gradient = 1.44 deg. C.mm^{-1}

Aspect Ratio	Amplitude Deg. C.	Comments
0.213	0.51	Narrow spectrum very small harmonics
0.267	0.48	Harmonics
0.320	0.5	Harmonics
0.373	1.1	Narrow spectrum with harmonics
0.384	1.6	Narrow spectrum with second harmonic
0.400	2.2	Narrow spectrum very small harmonic
0.427	0.6	Very irregular wave form
0.480	0.4	Irregular wave form
0.533	0.3	Very irregular wave form

TABLE 11

Results for critical Rayleigh number with aspect ratio

$\frac{Ro}{Ri}$ = 2.28, Ro - Ri = 22.5 mm

Aspect Ratio	Temp. difference Deg.C.	Critical difference	Frequency Hz	Amplitude and Comments Peak to Peak Deg. C.	
0.179	19.0	788	0.194	0.25	Narrow spectrum
0.200	10.00	1096	0.200	0.28	Narrow spectrum (Structured state)
0.222	13.1	1278	0.100	0.25	Narrow spectrum (Structured state) with harmonics
0.311	9.0	3394	0.133	0.3	Irregular wave form amplitude Narrow peaks
0.356	8.5	5476	0.091	0.2	Irregular wave form amplitude
0.422	5.5	7033	0.100	0.3	Irregular wave form amplitude Narrow peaks
0.400	6.3	6490	0.100	0.25	Narrow spectrum (Structured state)
0.444	5.0	7835	0.110	0.2	Irregular wave form amplitude

TABLE 12

Structured State results

Ro / Ri = 2.28, Ro - Ri = 22.5 mm

Horizontal position of probes = 11.25 mm from outer radius amplitudes are measured peak to peak

Aspect ratio = 0.200

Rayleigh Number	Frequency Hz	Amplitude Deg. C.	Comments
1197	0.0813	0.51	Narrow spectrum
1450	0.101	1.21	Narrow spectrum
1548	0.0908	1.15	Narrow spectrum
1710	0.1042	1.60	Narrow spectrum
1870	0.0952	1.00	Narrow spectrum with harmonics

Aspect ratio = 0.422

21910	0.0667	0.50	Narrow spectrum small harmonics
27550	0.0733	0.70	Narrow spectrum harmonics
29211	0.0744	1.10	Fundamental with second harmonics
33265	0.0833	0.90	Fundamental with harmonics

FIGURE NUMBER 7

AMPLITUDE VARIATION WITH ASPECT RATIO FOR $\frac{Ro}{Ri}$ = 2.28 FOR FIXED TEMPERATURE GRADIENT 1.20 deg. C.mm^{-1}

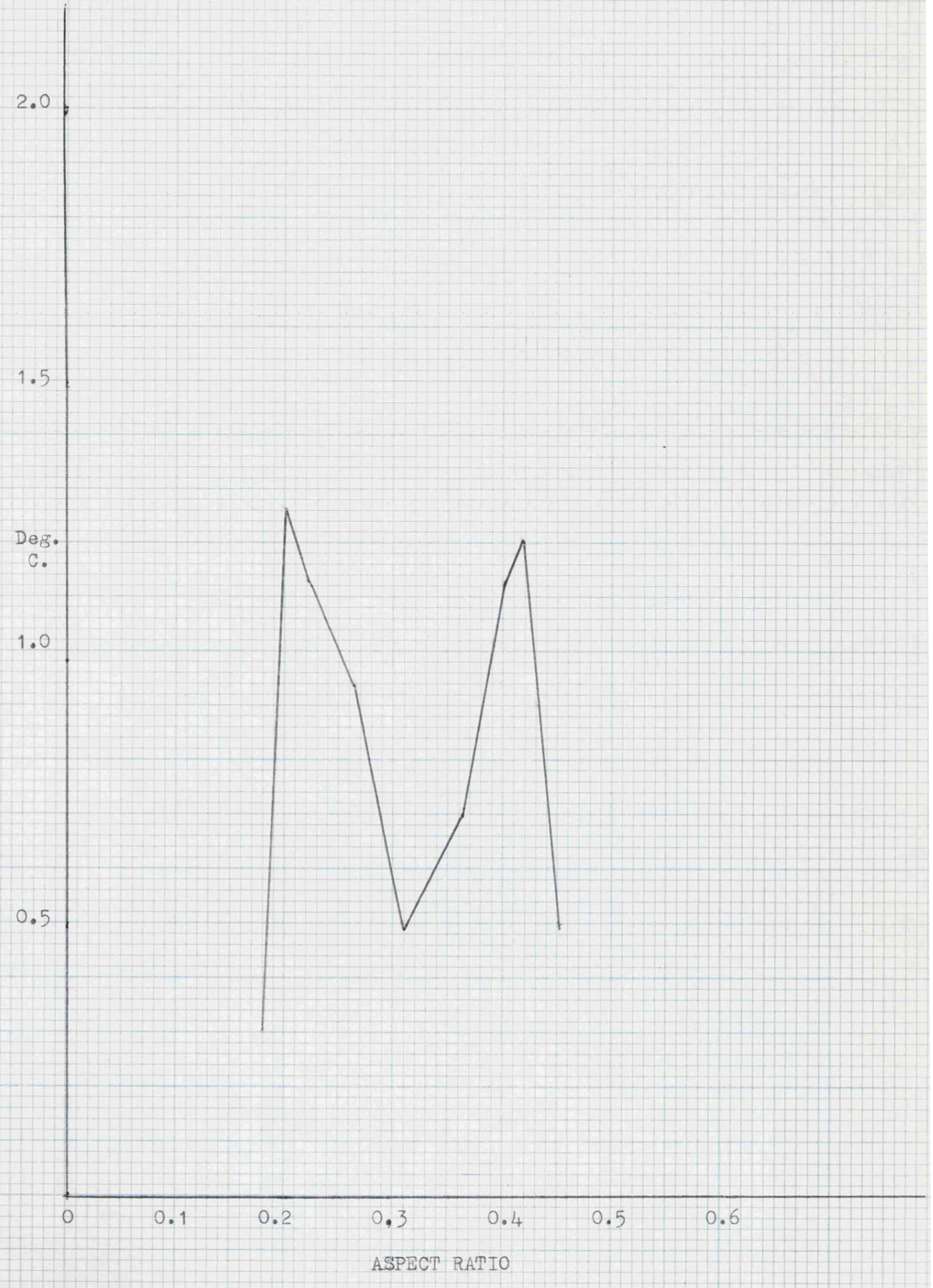

TABLE 13

Amplitude variation with aspect ratio for $\frac{Ro}{Ri}$ = 2.28, Ro - Ri = 22.5 mm and temperature gradient = 1.2 deg. C. mm^{-1}

Aspect Ratio	Amplitude Deg. C.	Comments
0.179	0.3	Second harmonic
0.200	1.25	Narrow spectrum
0.222	1.125	Narrow spectrum with harmonics
0.267	0.910	Irregular wave form
0.311	0.5	Irregular wave form
0.356	0.7	Narrow spectrum large harmonics
0.400	1.125	Narrow spectrum harmonics
0.422	1.20	Narrow spectrum small harmonics
0.444	0.5	Irregular wave form

TABLE 14

Results for critical Rayleigh number with aspect ratio

$\frac{Ro}{Ri}$ = 2.91, Ro - Ri = 26.25 mm

Aspect Ratio	Temp. difference	Critical difference Rayleigh Number	Comments
0.1520	18	615	Irregular wave form small amplitude
0.1910	13.4	1138	Narrow spectrum small harmonic frequency = 0.926 Hz peak to peak amplitude = 0.35 deg. C. (structured state)
0.2000	12.2	1250	Narrow spectrum small harmonic frequency= 0.0100 Hz peak to peak amplitude = 0.30 deg. C. (structured state)
0.229	10.9	1923	Irregular wave form with frequency 0.0833 Hz small amplitude
0.267	10.45	3400	A small harmonic with narrow spectrum fundamental frequency 0.111 Hz small amplitude 0.2 deg.
0.305	8.5	4696	Harmonic frequencies amplitude 0.2 deg. C.
0.343	7	6195	Narrow spectrum with harmonic amplitude 0.2 deg. C. frequency = 0.111 Hz
0.3810	6.1	8230	Narrow spectrum with harmonics (structured state) amplitude 0.25 deg. C.
0.4000	5.5	9015	Irregular wave form with small amplitude

TABLE 15

Structured State results

$\frac{Ro}{Ri}$ = 2.91, Ro - Ri = 26.25 mm Aspect ratio = 0.1910

Amplitudes measured peak to peak

Horizontal position of probes = 13.125 mm from outer radius

Rayleigh Number	Frequency Hz	Amplitude Deg. C.	Comments
1686	0.126	0.9	Narrow spectrum
1940	0.0833	1.125	Narrow spectrum small second harmonic
2360	0.0926	1.20	Narrow spectrum small harmonics
2782	0.1064	1.53	Narrow spectrum very small harmonics
3035	0.1082	1.48	Narrow spectrum small harmonics

TABLE 16

Structured State results

$\frac{Ro}{Ri}$ = 2.91, Ro - Ri = 26.25 mm aspect ratio = 0.2000

a) Horizontal position of probe = 6.56 mm from outer radius

b) Horizontal position of probe = 13.13 mm from outer radius

c) Horizontal position of probe = 19.69 mm from outer radius

Amplitudes measured peak to peak

Rayleigh Number	Frequency Hz			Amplitudes Deg. C.		
	a	b	c	a	b	c
1639	0.137	0.139	0.141	0.25	0.20	0.24
2562	0.167	0.165	0.165	0.625	0.4	0.5
3074	0.111	0.101	0.120	0.7	0.5	0.4
3330	0.111	0.111	0.982	1.0	0.6	0.5

TABLE 17

Structured State results

$\frac{Ro}{Ri}$ = 2.91, Ro - Ri = 26.25 mm aspect ratio = 0.3810

Amplitudes measured peak to peak

Horizontal position of probes = 13.125 mm from outer radius

Rayleigh Number	Frequency Hz	Amplitude Deg. C.	Comments
13490	0.0707	0.27	Narrow spectrum
25631	0.0606	0.75	Irregular wave form with harmonics
33725	0.0714	0.6	Irregular wave form with harmonics
40470	0.0902	0.51	Narrow spectrum with harmonics

FIGURE NUMBER 8

AMPLITUDE VARIATION WITH ASPECT RATIO FOR $\frac{Ra}{Ri}$ = 2.91 FOR FIXED TEMPERATURE GRADIENT = 0.8381 deg.C mm^{-1}

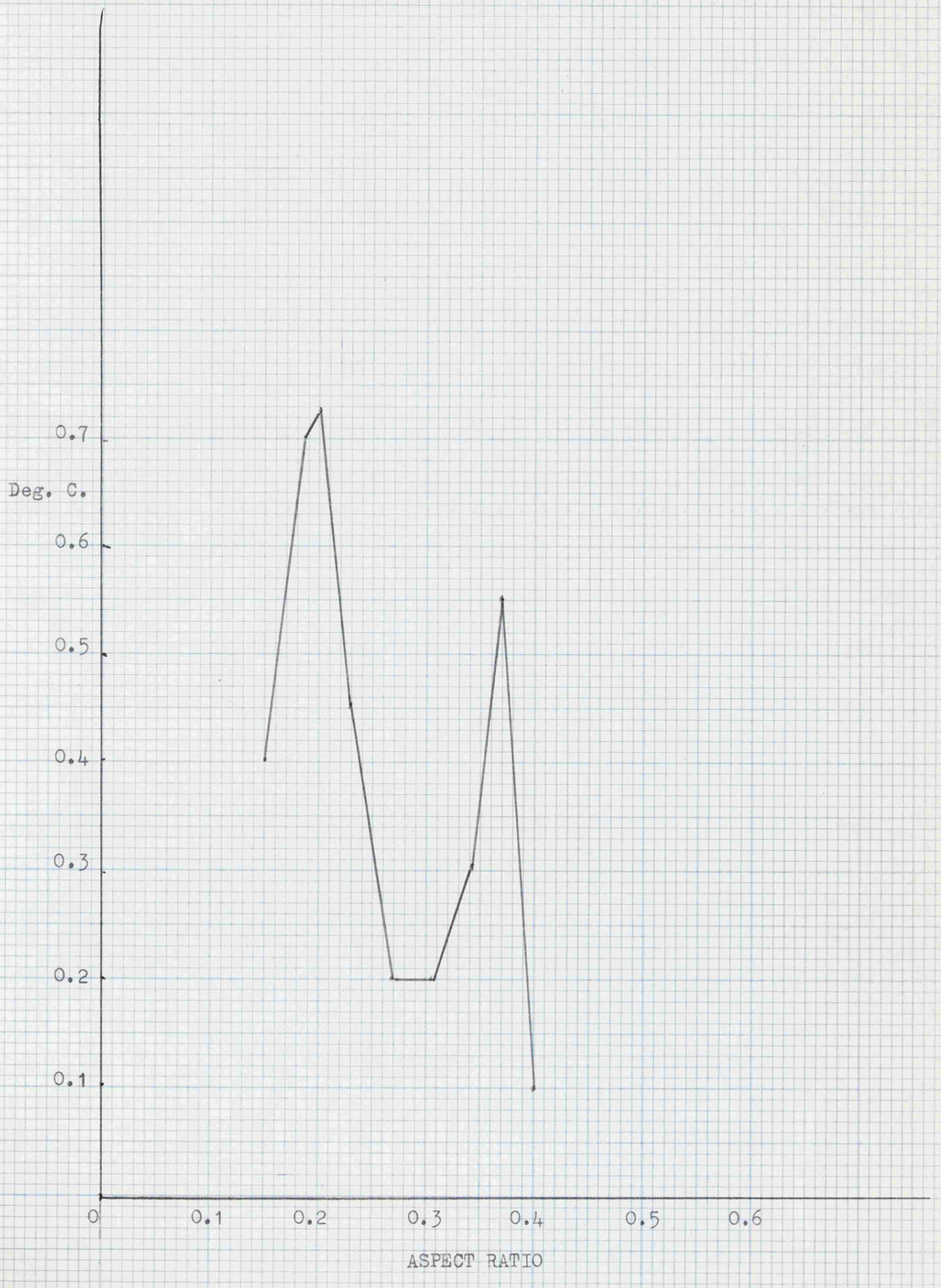

TABLE 18

Amplitude variation with aspect ratio for $\frac{Ro}{Ri}$ = 2.91, Ro - Ri = 26.25 mm and a temperature gradient = 0.8381 deg. C. mm^{-1}

Aspect Ratio	Amplitude Deg. C.	Comments
0.1520	0.4	Irregular wave form
0.1910	0.7	Narrow spectrum
0.2000	0.75	Narrow spectrum very small harmonics
0.229	0.45	Irregular wave form
0.267	0.2	Harmonics
0.305	0.2	Irregular wave form
0.343	0.3	Irregular wave form
0.3810	0.55	Narrow spectrum harmonics
0.400	0.1	Irregular wave form small amplitude

FIGURE 9

CRITICAL TEMPERATURE VARIATION WITH ASPECT RATIO FOR $\frac{Ro}{Ri} = 4$

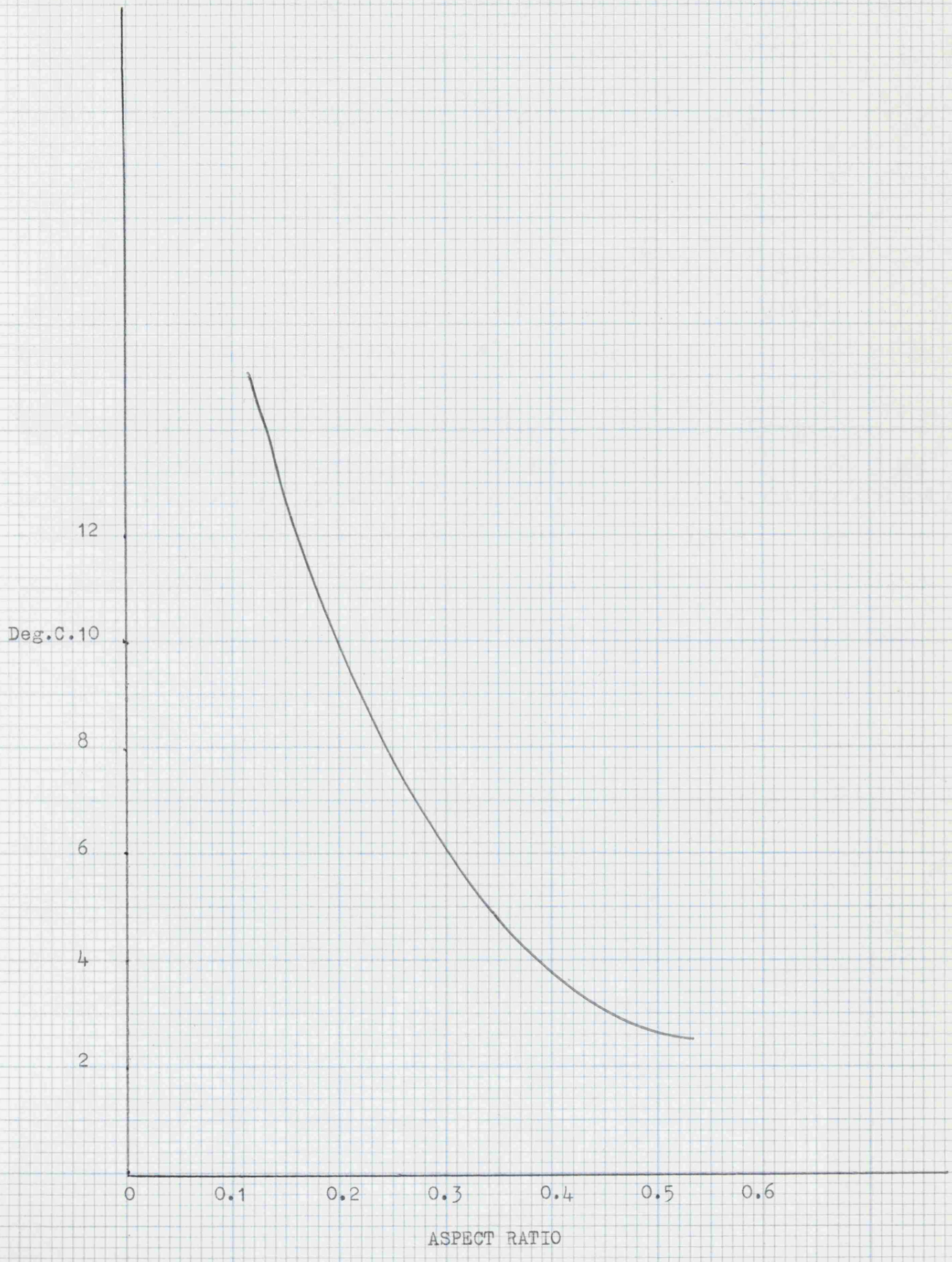

TABLE 19

Results for critical Rayleigh number with aspect raio

$\frac{Ro}{Ri}$ = 4, Ro - Ri = 30 mm

Aspect ratio	Temp. difference Deg. C.	Critical difference Rayleigh Number	Comments
0.167	11.15	822	Harmonics
0.20	10.1	1530	Narrow spectrum harmonics 0.709 Hz (structured state)
0.230	7.5	2126	Narrow spectrum with harmonics
0.27	7	3383	Harmonics irregular wave form
0.3	6.2	4800	Harmonics
0.333	5.5	6490	Harmonics
0.466	3.9	6737	Narrow spectrum small harmonics
0.4	3.5	8563	Narrow spectrum structured state
0.433	3	10110	Narrow spectrum with harmonics
0.46	2.9	13145	Narrow spectrum with harmonics
0.5	2.75	16427	Irregular wave form small amplitude

TABLE 20

Structured State results

$\frac{Ro}{Ri}$ = 4, Ro - Ri = 30 mm aspect ratio = 0.200

Amplitudes measured peak to peak

Horizontal position of probes = 15 mm from outer radius

Rayleigh Number	Frequency Hz	Amplitude Deg. C.	Comments
1835	0.1333	0.5	Narrow spectrum
2600	0.1667	0.6	Narrow spectrum
3213	0.2063	0.8	Narrow spectrum very small harmonics
4437	0.2063	1.2	Narrow spectrum with harmonics
Aspect ratio = 0.400			
28138	0.0463	0.6	Narrow spectrum
45251	0.0463	2.1	Narrow spectrum
53812	0.0492	1.9	Narrow spectrum very small harmonics
59927	0.0508	1.2	Narrow spectrum small harmonics

FIGURE NUMBER 10

AMPLITUDE VARIATION WITH ASPECT RATIO FOR $\frac{Ro}{Ri}$ = 4 FOR FIXED TEMPERATURE

GRADIENT = 0.6677 deg. C. mm^{-1}

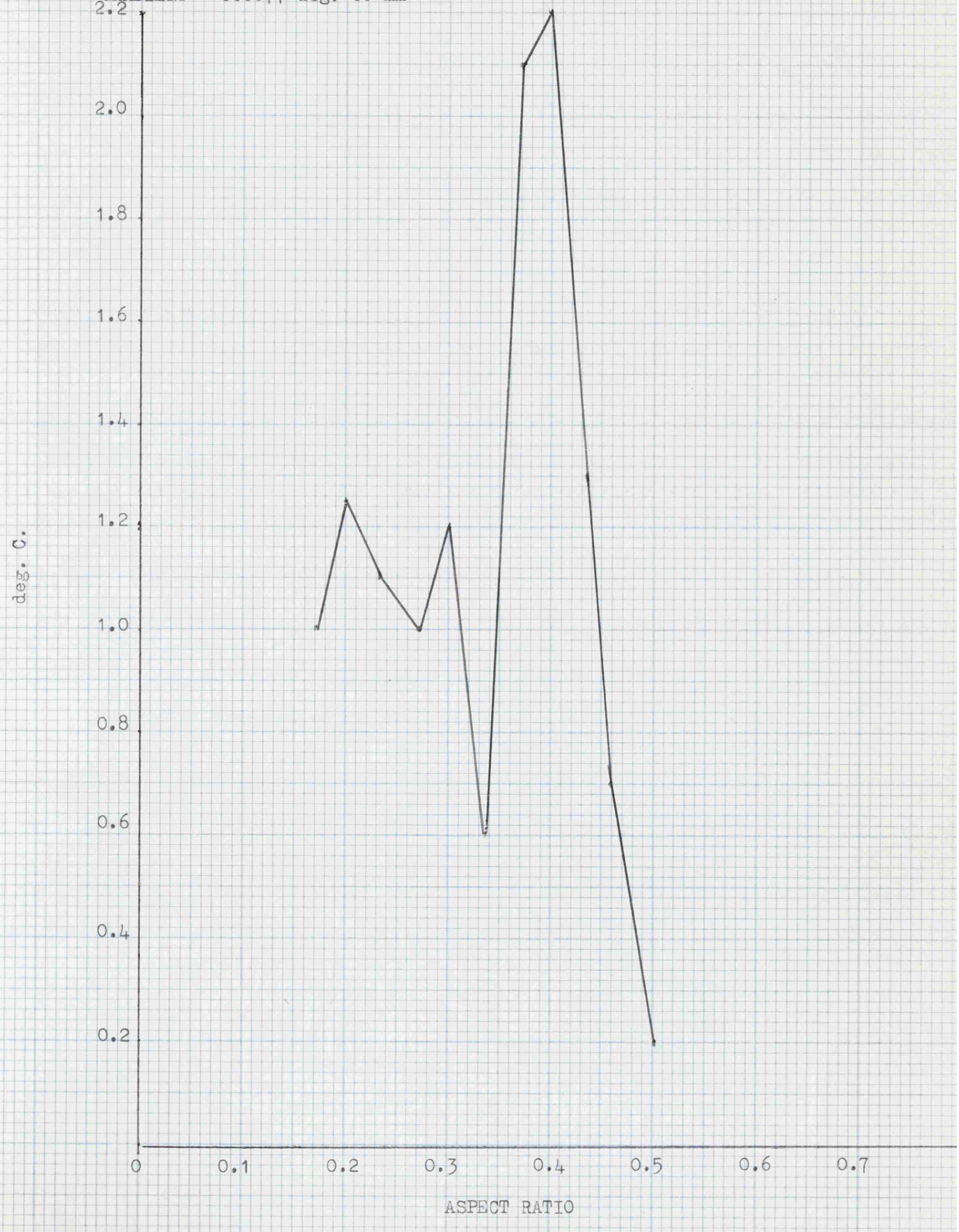

TABLE 21

Amplitude variation with aspect ratio for $\frac{Ro}{Ri} = 4$, Ro - Ri = 30 mm

and a temperature gradient = 0.6677 deg. C. mm^{-1}

Aspect Ratio	Amplitude	Comments
0.167	1.0	Mainly harmonics
0.2	1.25	Narrow spectrum with small harmonics
0.23	1.1	Narrow spectrum with harmonics
0.22	1.0	Harmonics with irregular wave form
0.3	1.2	Harmonics with irregular wave form
0.333	0.6	Harmonics
0.366	2.1	Narrow spectrum with harmonics
0.4	2.2	Narrow spectrum
0.433	1.3	Narrow spectrum with harmonics
0.46	0.7	Harmonics
0.5	0.2	Irregular wave form small amplitude

FIGURE 11

CRITICAL RAYLEIGH NUMBER WITH ASPECT RATIO

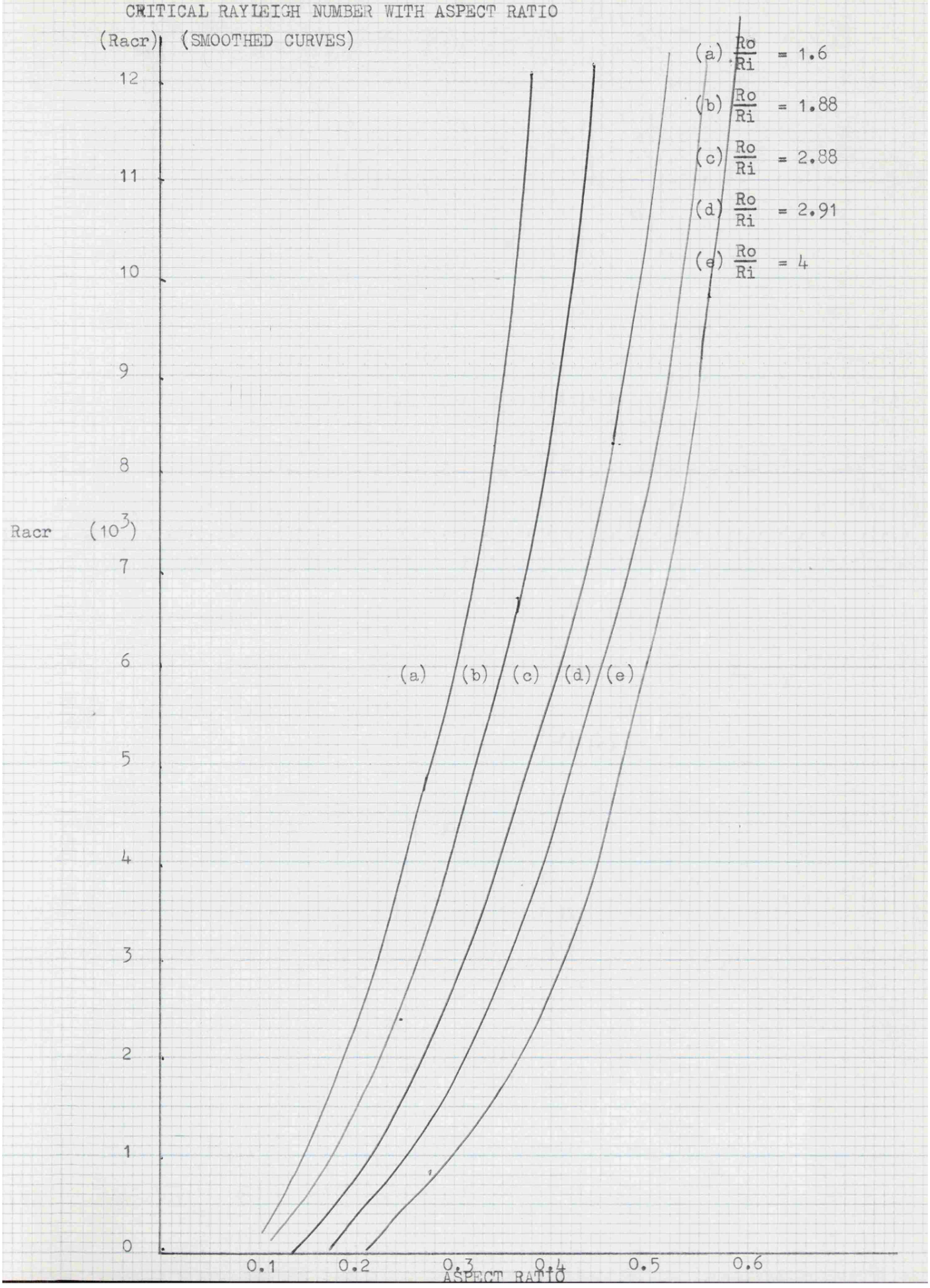

TABLE 22

The results for marginal stability for mercury at the structured states

$\frac{Ro}{Ri}$ = 1.60	Aspect ratio	Racr	σ_i	$\frac{\sigma_i}{\sigma_{th}}$
	0.400	2950	25.75	0.613
1.88	0.400	4780	29.57	(0.64)
2.28	0.200	1096	27.58	1.99
	0.422	7033	55.2	(0.92)
2.91	0.2000	1250	30.18	1.26
	0.381	8230	52.24	(0.87)
4	0.200	1530	22.00	0.79
	0.400	8536	53.38	(0.82)

The theoretical values are obtained from Table (4a). The values in brackets are obtained by extrapolation. The value of $\sigma_i = d^2 \omega (\nu \chi)^{-1/2}$ where ω is the angular frequency and the other symbols are understood.

Discussion

It is well known: Schlüter, Lortz and Busse (1961), [93] Davis (1968), [94] Stork and Müller (1972) that in a rectangular box the convective structure just above onset of convection consists of straight rolls parallel to shorter side of a rectangular frame. In the work of [95] Dubois and Berge' (1978) for low supercritical Rayleigh numbers the rolls were set up preferentially with a critical wavelength of order 2d the wavelength constant in their cell configuration up to e = 10 where $e = \frac{Ra - Racr}{Racr}$

The experimental value of Racr is of the order 1600. They noted, however, that structures with the wavelength not equal to the critical wavelength can be obtained and maintained within the same temperature range. Another important feature is that the structure was essentially two dimensional. Allowing for end flow the following preferential flow patterns or structured states for the series of experiments, conducted in the thesis, would be:

h = 0.4 two convective loops

h = 0.2 four convective loops

		Aspect ratio		Wavelength
$\frac{Ro}{Ri}$	=	Predicted	Experimental	(mm)
1.6		0.400	0.400	12
1.88		0.400	0.400	15
2.28		0.400	0.422	19
		0.200	0.200	9
2.91		0.400	0.381	20
		0.200	0.200	10.5
4		0.400	0.400	24
		0.200	0.200	12

These results are also in agreement with the work of [96] Davis (1967, 1968). He drew the following conclusions:

(i) different boundary conditions yield drastically different critical Rayleigh numbers

(ii) the preferred mode of cell pattern is always some number of finite rolls two non-zero velocity components dependent on three spatial variables with axis parallel to the shorter length with the natural exclusion of square boxes

(iii) when the depth is the smallest dimension the finite rolls of near square cross section are predicted

These two last observations are in agreement with the experimental observations.

Hurle et al (1974), states that, the basic flow pattern is a simple convective loop within the liquid metal, rising at the hot thermode and descending at the cold thermode. This is a conclusion which should be viewed with caution. Bolt (1975) suggested the existence of a set of rolls having a roll length of the order of 10 mm; this is a reasonable conclusion. The table below illustrates the typical pattern of Bolt's results:

Length of Bath (mm)	Depth of fluid (mm)	Number of probable wavelengths
99.2	6	8 or 7
99.2	7	8 or 9
99.2	8	6 or 5

Furthermore, he concluded there was no dependance of frequency with width of boat. This conclusion was to be expected as the rolls have symmetry about an axis parallel to the shorter side of the boat. In the annular configuration when baffles were introduced in a radial direction a similar feature occurred that these baffles did not alter the frequency

or amplitude.

The preferential mode of convective rolls in the annular configuration would be similar to the box geometry; however, the rolls will be constrained into an arc of a circle due to the walls of the container and they will have doughnut or torous shape. This shape does not have the stability of the box geometry. The side walls of the box tend to stabilize this form of disturbance. Oscillations in the annular geometry are generally not sinusodial having harmonics superimposed on the fundamental frequency; this could be explained as due to the absence of side walls to stabilize the disturbance. Figure (14) is a possible manifestation of the Ahlers (1974)[63] phenomena.

The Lorentz (1963)[97] model is obtained by working with three Fourier components in the truncated Boussinesq equations:

(i) one mode of velocity potential

(ii) one temperature mode with fundamental cellular wave numbers

(iii) a second temperature mode, (a second harmonic in z that has no x or y periodicity and that contributes to the mean heat flow)

The following constraints apply:

(i) for free boundaries

Hence for cell length 15 mm and depth of 6 mm

optimum wavelength = 16.97 mm

(ii) for rigid boundaries

= 9.92 mm

(iii) experimental value

optimum wavelength = 12.09 mm

The cell length, experimentally, lies between these two values of optimum wavelengths so we can conclude there is reasonable agreement between the Lorentz model and the experimental results.

The existence of a critical temperature gradient is confirmed by a typical set of results see figure (9). However, Bolt (1975) did not observe any critical temperature gradients. This is due to the fact that the Rayleigh number varies approximately inversely with the boat length (see figure (7) Hurle (1974)). Botl (1975) was working at the 'tail end' of the curve.

Examination of the amplitude variation with aspect ratio at respective fixed temperature gradients see figures (5, 6, 7 and 8) reveal a decrease in the sharpness and coupled with a general decrease in the magnitude of the curves for increasing cell length. It appears possible for the structured state to adjust the length of the convective rolls, within a relatively large cell length and produce optimum wavelengths. Hence, this affords a partial explanation why it is difficult to detect changes in the structured state in boats of large length. These conclusions in the main are also true for the frequency variation with increasing temperature gradient. The variation which Hurle (1974) and Bolt (1975) reported are to be found at the greater cell length in 99.3 mm. Another feature of Bolt's (1975) work is illustrated below.

Rayleigh Number	Temperature Gradient deg C mm^{-1}	Aspect Ratio
222	0.1	0.051
444	0.2	0.051

The general consensus of opinion is that there is no change from conduction mode to convection mode until the Rayleigh number is of the order of 1000. Yet in the above table oscillations are occuring at a minimum Rayleigh number of the order of 200.

Work was also carried out using gallium as the working fluid using the following dimensions $\frac{Ro}{Ri}$ = 1.6 with aspect ratios 0.333,

0.400 and 0.461. The fluid was heated, in each instance, to a temperature difference, across the bath of 40 deg C. However, oscillations of a small frequency were obtained with correspondingly small amplitudes. It was difficult to determine whether the critical temperature had really been exceeded. The respective Rayleigh numbers are:

(i) $Ra_{Hg} = \frac{3.54 \times 10^9 \Delta T d^4}{L}$

(ii) $Ra_{Ga} = \frac{3.20 \times 10^8 \Delta T d^4}{L}$

where d and L are meansured in m, ΔT is measured in deg C. Hence, to produce the same Rayleigh number approximately ten times the temperature difference is required. This explains the negative nature of our result. In Skafel's (1972) work see his table 2, the peak to peak amplitudes were:

(i) maximum amplitude = 7.8×10^{-2} deg C

(ii) minimum amplitude = 1.6×10^{-2} deg C

Variations of this order would be very difficult to detect in our apparatus and similar temperature measuring devices employed generally. Furthermore, there appeared no specific requirement of an integer number of waves around the annulus in the structured state.

From the work of Dubois and Berge' (1978) the maximum magnitude of the wave profile in the structured state has the following values at e = 5.76 and z = 0.22d

The horizontal components

(i) fundamental = $(337 \pm 10) \times 10^{-6} ms^{-1}$

(ii) first harmonic = $(13.7 \pm 1) \times 10^{-6} ms^{-1}$

(iii) second harmonic = $(19 \pm 1) \times 10^{-6} ms^{-1}$

The vertical component

(i) fundamental = $(340 \pm 10) \times 10^{-6} ms^{-1}$

(ii) first harmonic = $(1.7 \pm 2) \times 10^{-6} ms^{-1}$

(iii) second harmonic = $(58 \pm 5) \times 10^{-6} ms^{-1}$

There is a conservation of mass in a square roll because the fundamentals of both components are nearly equal. For low values of e, the theoretical expression which gives the maximum amplitude of the fundamental in the vertical component is given by $V_z = \frac{0.96 a^2 \chi \epsilon}{d}$ where a is the dimensionless wave number given by

$$a = \frac{2\pi d}{\lambda_c} \quad \text{when } \lambda_c = \lambda \; ; \; a_c = a = 3.117$$

Note at a fixed value of, e, the velocity amplitude is dependent only on the thermal diffusivity of the convective fluid.

Now Dubois and Berge' (1978) worked with siliconeoil and comparing the values they obtained experimentally with gallium and mercury we have:

	$\chi \; m^2 s^{-1}$	$\nu \; m^2 s^{-1}$
silicon oil	1.15×10^{-7}	1.05×10^{-4}
mercury	4.46×10^{-6}	1.19×10^{-7}
gallium	1.39×10^{-5}	2.78×10^{-7}

For silicon $V_{z \; max} = 340 \times 10^{-6} ms^{-1}$

For mercury $V_{z \; max} = 1.32 \times 10^{-2} ms^{-1}$

For gallium $V_{z \; max} = 1.7 \times 10^{-2} ms^{-1}$

This is employing the method of proportions.

Turning now to the Reynolds number; let the effective length be, say, 10 mm then respective Reynolds numbers will be

$Re_{mercury} = 1109$

$Re_{gallium} = 611$

$Re_{siliconeoil} = 0.029$

This is indicative that the oscillations are induced when relatively high velocities are present in the structured state.

A baffle system has been constructed for the suppresion of temperature oscillations and used in conjunction with a crucible for barium strontrum niobate crystal growth. The baffle and the crucible were constructed from platinum and the support wire constructed from platinum-rhodium alloy. The baffle was mounted horizontally and reduced the effective height of the liquid. With the baffle absent temperature oscillations had an amplitude of 1 deg C peak to peak. Then with the baffle in the optimum position, which was found to be one quarter the depth of the crucible from the upper surface, the oscillations were reduced to less than 0.1 deg C peak to peak. However, it has been pointed out by Whiffin and Brice [98] (1971) and [99] Brice et al (1971) that not all the factors involved in the above configuration are fully understood.

However, it should be noted that a low Prandtl number is only a necessary condition for thermal oscillations and not a sufficient one. Liquid inert gases, such as Helium, have a low Prandtl number yet do not exhibit the form of oscillations described in this thesis.

FIGURE NUMBER 12

$\frac{Ro}{Ri}$ = 1.6 aspect ratio = 0.267

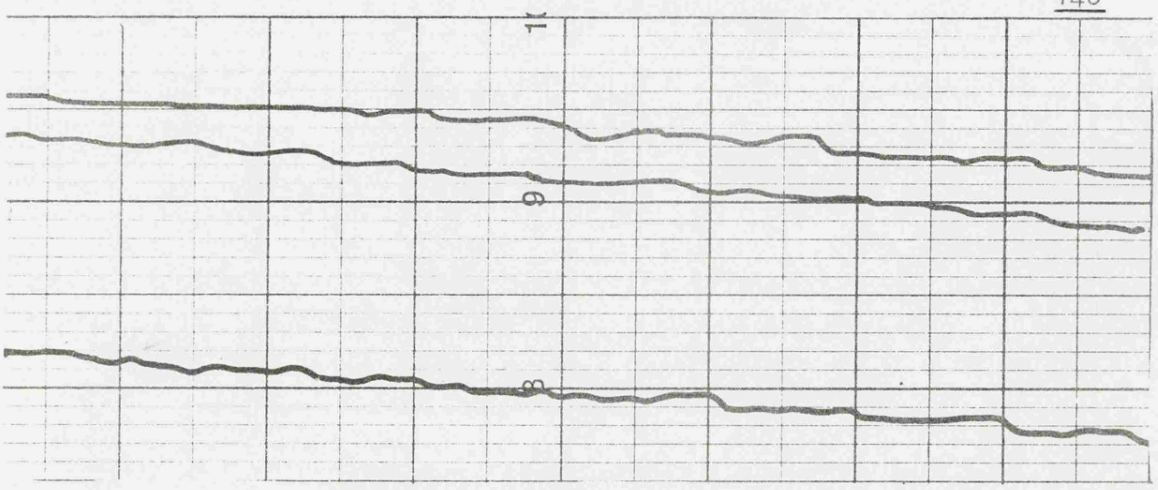

aspect ratio = 0.333

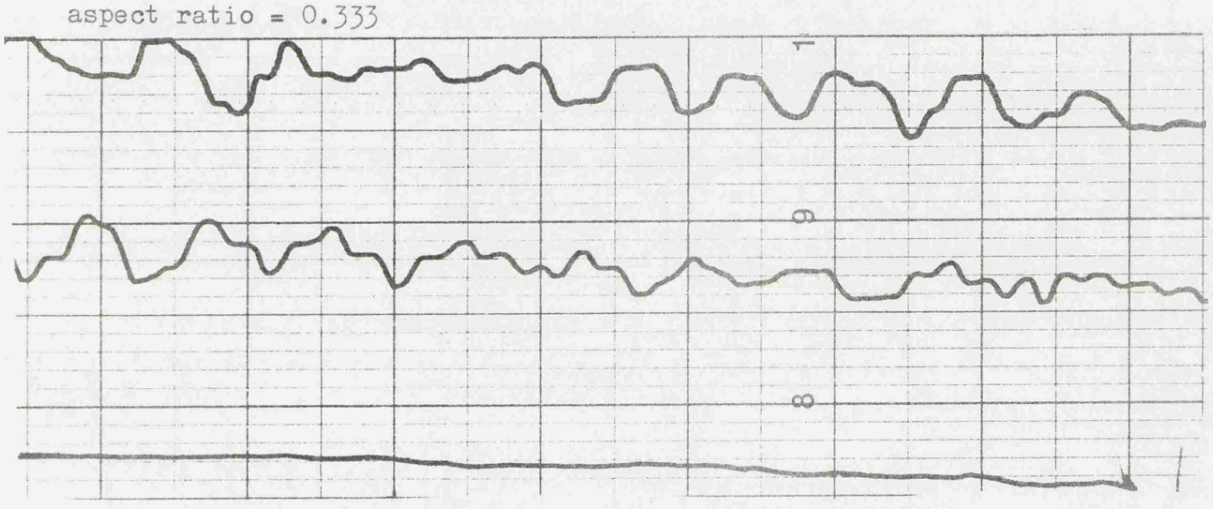

aspect ratio = 0.4000 (structured state)

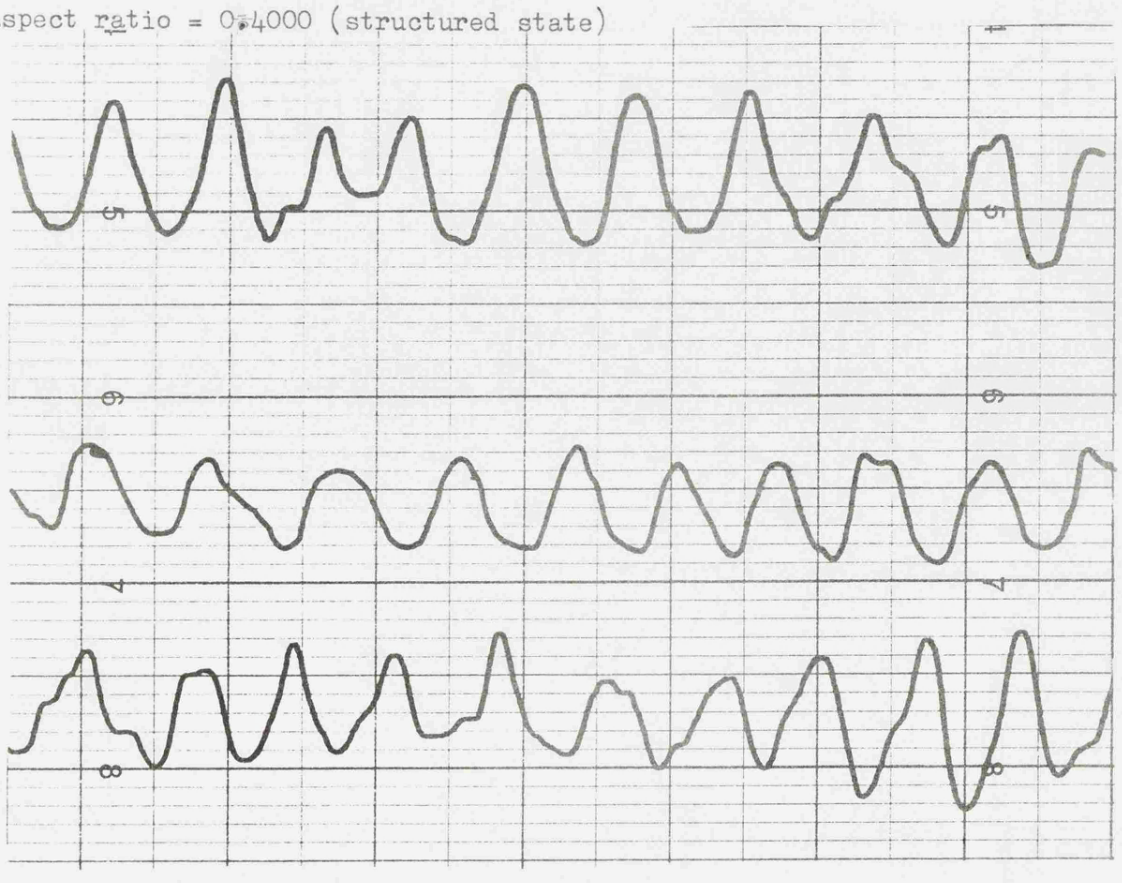

aspect ratio = 0.467

Fig 13.

aspect ratio = 0.533

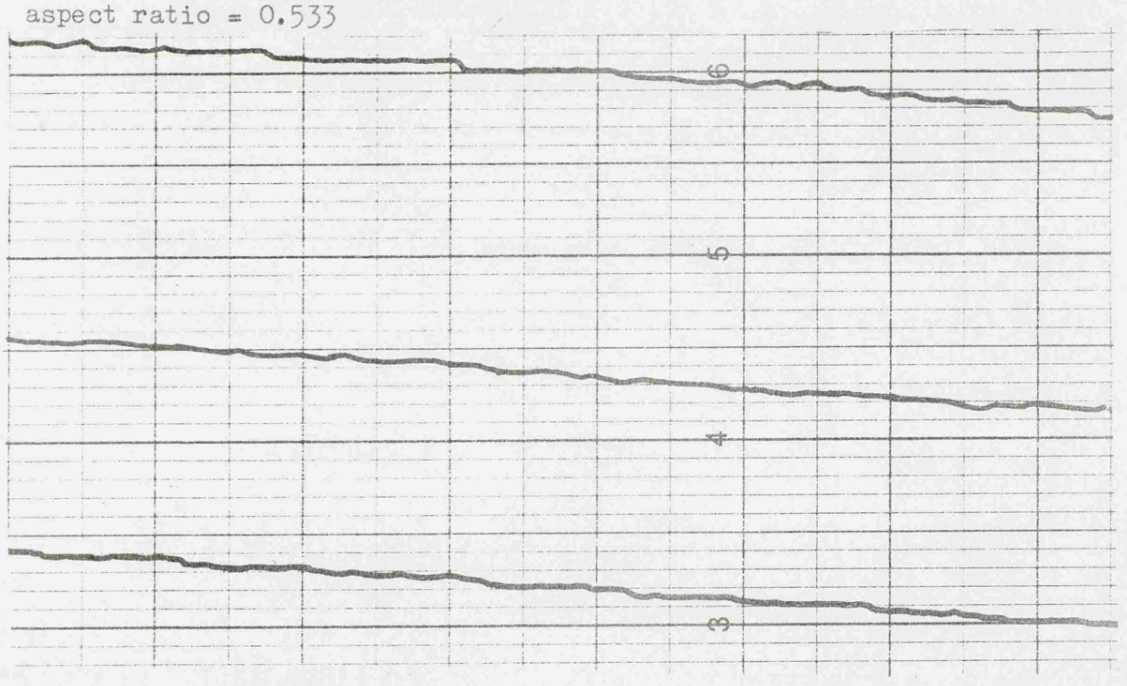

aspect ratio = 0.600

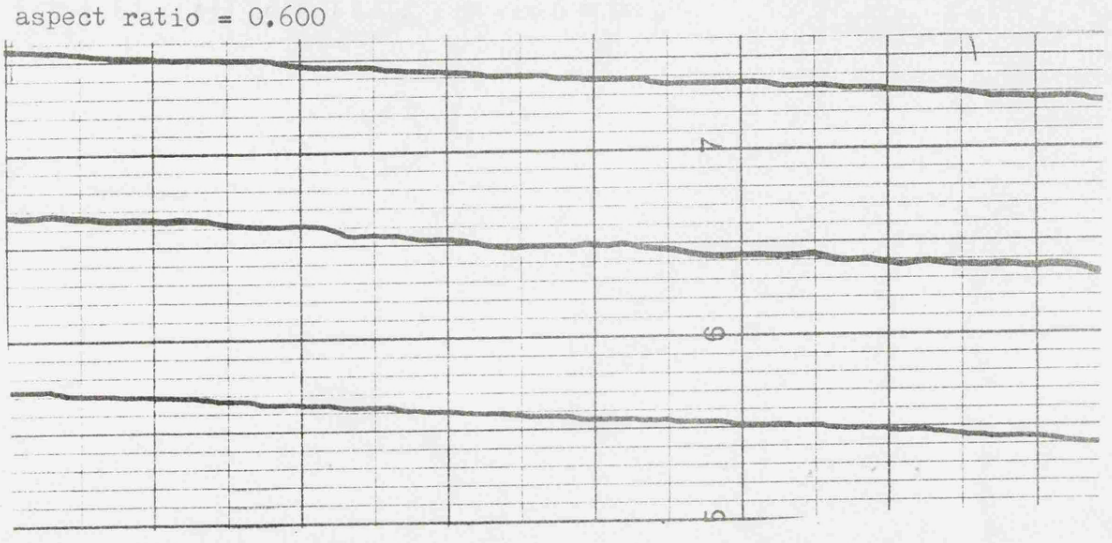

FIGURE 14 The Ahlers Phenomena

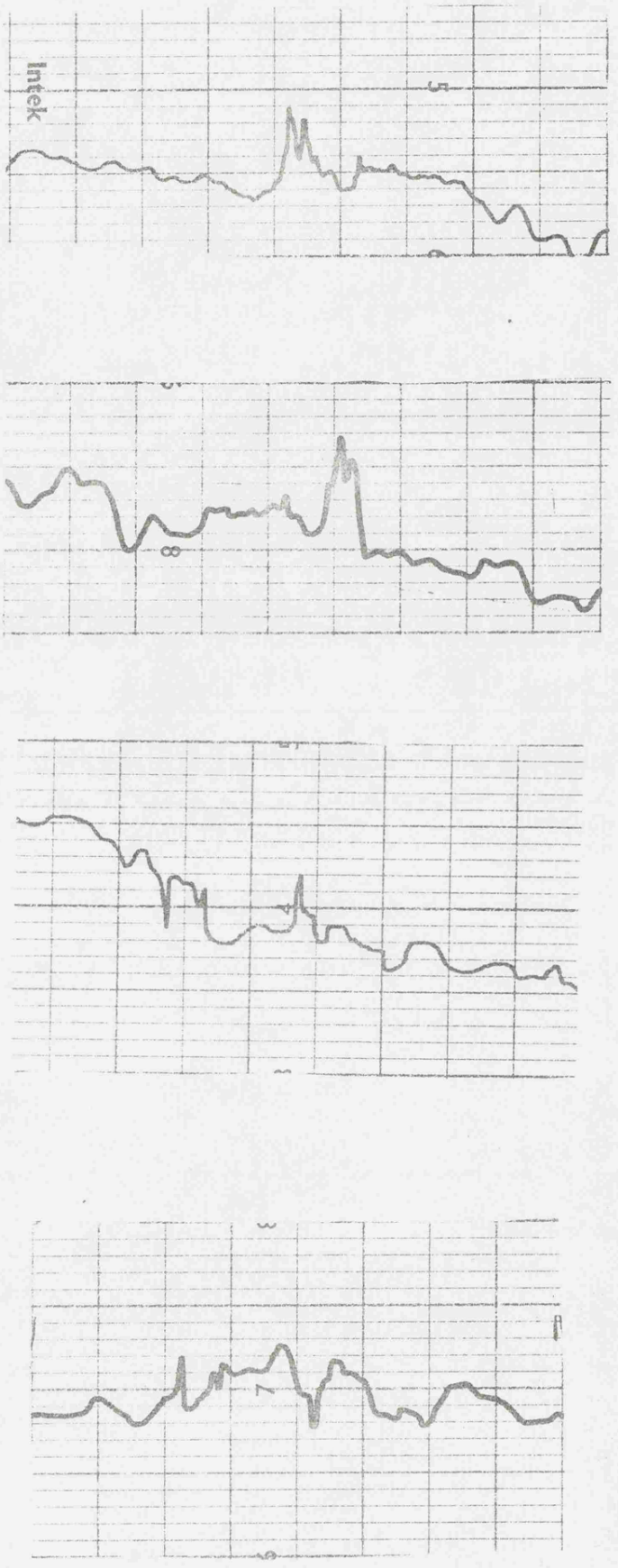

Section (iii)

Conclusions and recommendation for future work

The experimental work has thrown considerable light on the essential physics of the convective flow pattern of a fluid of low Prandtl number when heated from below or from its side. It has also brought the understanding of the flow properties of liquid metals within the encompassment of general hydrodynamical theory. The structure is essentially two dimensional when temperature oscillations occur. Allowing for end flow the following preferential flow patterns or structured states for the series of experiments conducted in the thesis will be;

(a) aspect ratio = 0.4

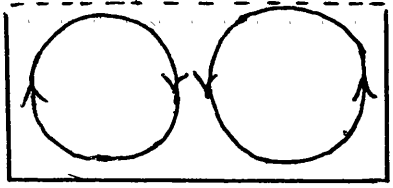

(b) aspect ratio = 0.2

Turning now to the theoretical side of the work. We have been compelled to adopt comparatively severe approximations in order to solve our basic Navier-Stokes equations with any reasonable facility. These approximations were as follows: original lack of knowledge of basic flow patterns, approximations employed in calculating stability characteristics, the neglect of end effects, weighted mean values of non-dimensional shear and temperature gradient, solution of a fourth order differential equation whereas the derived differential equation is of eighth order. The predictions of the theoretical frequency of oscillations when compared with the experimentally observed values are remarkable. Nevertheless, agreement between experimental results and theoretical predictions appear to be sufficiently close to justify the particular point of view what we have adopted.

The Prandtl number has a significant effect on whether oscillations occur or not under our experimental conditions. When the flow, for a high Prandtl number fluid, is in the transition region between conduction and convection the magnitude of the velocity is usually such that it is not large enough to provide a suitably large vertical shear strain, which is a prerequisite for the oscillations to be initiated and sustained. While this feature rules out the instability for internal convection, it does not, preclude the possibility of flow conditions such as for example, an external source input of mass flow which could possibly increase the vertical shear strain. Likewise, for high Prandtl number fluids the stabilizing effect of the vertical temperature gradient can become too large for oscillations to occur.

Certainly, the structured state condition was found to exist in low Prandtl number fluids, when the aspect ratio has particular values. Applying this observation to the problem of thermal oscillations occuring in the melt when growing crystals it should be possible to reduce their amplitude considerably. This idea is very clearly illustrated by figures (12 and 13). This will also produce a corresponding reduction in the severity of banding in the crystal growth when the structured state conditions are avoided, by suitable choice of the dimensions of the melt container. Alternatively, to introduce baffles into the fluid which could inhibit the formation of square rolls,

It is also possible that situations could arise in meteorological or oceanographic studies where suitable temperature gradients and suitable shear strains existed to support a temporal oscillatory instability analogous to the kind described in this study. The following topics are suggestions for future work:

(a) suitable modifications to the apparatus to produce larger temperature gradients for the investigation of thermal oscillations

in liquid gallium,

(b) investigation of the oscillations of mercury in a rectangular boat employing in particular aspect ratios of 0.2 and 0.4, and cell lengths of 5 mm to 20 mm. These experiments have not yet been carried out,

(c) measurement of the velocity of fluids and appropriate flow patterns. It is our conjecture that high relative velocities are a prerequisite for thermal oscillations. Measurements could possibly be accomplished by employing the Doppler effect with ultrasonic waves.

APPENDIX I

APPENDIX I

Index

Program number

(1) Determination of Bessel-Neumann Zeros

(2) Calculation of non-dimensional shear and temperature gradient

(3) Calculation of non-dimensional velocity and shear for various models

(4) Program to calculate shear, temperature, Prandtl number, wavelength and frequency

(5) Calculation of Rayleigh number, frequency, wavelength and Prandtl number for Rigid-conducting boundaries in a cyclic sweep of depth and radial distance

(6) Calculation of computed characteristics for Rigid-Rigid, Free-Free and Rigid-Free boundaries

COMPUTER PROGRAM NO 1

```
EM CALCULATION OF BESSEL NEUMANN ZEROS
10 LET R0=4
12 LET P1=3•14159
15 READ R1
20 IF R1<0 THEN 999
25 PRINT R1
30 FOR S=1 TO 20
40 LET R=R0
50 LET D=S*P1/(R-1)
60 LETM=4
70 LET P=(M-1)/(8*R)
80 LET Q=4*(M-1)*(M-25)*(R↑3-1)/(3*(8*R)↑3*(R-1))
90 LET R2=32*(M-1)*(M↑2-114*M+1073)*(R↑5-1)
100 LET R3=5*(8*R)↑5*(R-1)
110 LET R4=R2/R3
120 LET X1=D+P/D+(Q-P↑2)/D↑3
130 LET X2=(R-4*P*Q+2*P↑3)/D↑5
140 LET X=X1+X2
150 LET K=X/R1
160 LET K=K
165 LET PRINT S,K
170 NEXT S
180 PRINT
200 GO TO 15
210 DATA 1,1•375,1•75,2•125,2•5,-1
999 END
```

COMPUTER PROGRAM NO 2

```
5  REM CALCULATE SHEAR VALUES R-R,F-F,R-F
10  FOR D=•007 TO •01 STEP •1
15  PRINT "DEPTH"D
20  FOR R=•001 TO •05 STEP •005
25  PRINT "RADIAL DISTANCE"R
30  LET E=D/(2*R)
40  LET P1=3•14159
60  LET S1=(EXP(E)-EXP(-E))/2
70  LET C1=(EXP(E)+EXP(-E))/2
80  LET S2=(EXP(2*E)-EXP(-2*E))/2
90  LET C2=(EXP(2*E)+EXP(-2*E))/2
100  LET A1=4*S1*R-2*D*C1
110  LET A2=8*R*S1↑2-2*D*S2
120  LET P2=1+P1↑2/E↑2
130  LET U1=2*R↑2*A1*S1/(D↑2*A2*P2)
140  LET T1=(2*P1)↑(-2)*U1
150  LET G1=(2*P1)↑(-2)
160  LET G2=(2*P1)↑(-2)*G1
170  LET R1=G1/U1
180  LET R2=G2/T1
185  PRINT "R-R"
187  PRINT U1,T1,R1,R2
190  LET B1=1-S1/(C1*E)+4*E*S1/(4*E↑2+4*P1↑2)
200  LET U2=R↑2*B1/D↑2
210  LET T2=(2*P1)↑(-2)*U2
220  LET G3=(2*P1)↑(-2)*(1+P1↑2/3)
230  LET G4=(2*P1)↑(-2)*G3
240  LET R3=G3/U2
250  LET R4=G4/T2
260  PRINT "F-F"
270  PRINT U2,T2,R3,R4
280  LET F1=D↑2*S1/R-4*R*S1+2*D*C1
290  LET F2=4*S1*C1-2*D*C2/R
300  LET F3=-D↑2*S1/R+4*R*S1-2*D*C1
310  LET U3=2*R↑2*F1*S1/(D↑3*F2)+2*R↑2*F3*S1/(D↑3*P2*F2)+R↑2/D↑2
320  LET T3=(2*P1)↑(-2)*(P1↑2/12+1)
330  LET T3=(2*P1)↑(-2)*U3
340  LET G5=(2*P1)↑(-2)*(P1↑2/12+1)
350  LET G6=(2*P1)↑(-2)*G5
360  LET R5=G5/U3
370  LET R6=G6/T3
380  PRINT "R-F"
390  PRINT U3,T3,R5,R6
400  PRINT
410  NEXT R
415  PRINT
420  NEXT D
999  END
```

COMPUTER PROGRAM NO 3

```
5  REM CALCULATE SHEAR ,VELOCITY
10  REM DEPTH SETTING
15  FOR D=•007 TO •01 STEP •001
20  PRINT "DEPTH"D
30  FOR R=•015 TO •035 STEP •05
40  PRINT "RADIAL DISTANCE"R
50  LET E=D/(2*R)
60  LET H=D/•03
65  PRINT H,E
70  LET S1=(EXP(E)-EXP(-E))/2
80  LET C1=(EXP(E)+EXP(-E))/2
90  LET S2=(EXP(2*E)-EXP(-2*E))/2
100  LET C2=(EXP(2*E)+EXP(-2*E))/2
110  PRINT "RIGID-RIGID"
120  FOR Z=-•5 TO •5 STEP •125
130  LET S3=(EXP(2*E*Z)-EXP(-2*E*Z))/2
140  LET C3=(EXP(2*E*Z)+EXP(-2*E*Z))/2
150  LET A1=2*E*C1-2*S1
160  LET A2=4*S1↑2-2*E*S2
170  LET T1=(A1*S3/A2+Z)/(2*E)↑2
180  LET T2=(A1*C3/A2+1/(2*E))*1/(2*E)
190  LET G1=Z/24-Z↑3/6
200  LET G2=1/24-Z↑2/2
210  PRINT Z
220  PRINT T1,T2,G1,G2
230  NEXT Z
240  PRINT "FREE-FREE"
250  FOR Z=-•5 TO •5 STEP •125
260  LET S3=(EXP(2*E*Z)-EXP(-2*E*Z))/2
270  LET C3=(EXP(2*E*Z)+EXP(-2*E*Z))/2
280  LET T1=(Z-S3/(2*E*C1))*1/(2*E)↑2
290  LET T2=(1-C3/C1)*1/(2*E)↑2
300  LET G1=Z/8-Z↑3/6
310  LET G2=1/8-Z↑2/2
315  PRINT Z
320  PRINT T1,T2,G1,G2
325  NEXT Z
330  PRINT "RIGID-FREE"
340  FOR Z=-•5 TO •5 STEP •125
350  LET A1=2*E↑2*EXP(-E)+2*S1-2*E*EXP(E)
360  LET A2=2*E↑2*EXP(E)-2*S1+2*E*EXP(-E)
370  LET A3=2*S1*C1-2*E*C2
380  LET U1=-A1*EXP(2*E*Z)/(16*E↑3*A3)-A2*EXP(-2*E*Z)/(16*E↑3*A3)
390  LET U2=A1*EXP(-E)/(16*E↑3*A3)+A2*EXP(E)/(16*E↑3*A3)
400  LET U3=1/(8*E↑2)+Z/(2*E)↑2
410  LET T1=U1+U2+U3
420  LET T2=-A1*EXP(2*E*Z)/(A3*8*E↑2)+A2*EXP(-2*E*Z)/(A3*8*E↑2)
430  LET T5=1/(4*E↑2)+T2
440  LET G1=-Z↑3/6+Z↑2/16+Z/16-1/192
450  LET G2=-Z↑2/2+Z/8+1/16
455  PRINT Z
460  PRINT T1,T5,G1,G2
470  NEXT Z
480  NEXT R
490  NEXT D
500  END
```

COMPUTER PROGRAM NO 4 CONTINUED

```
382  GOTO 480
383  PRINT "RIGID CONDUCTING "
384  PRINT "POLAR MODEL"
385  LET Q=0
386  LET A1=4*R*S1-2*D*C1
390  LET A2=8*R*S1↑2-2*D*S2
400  LET A3=1+P1↑2/E↑2
410  LET A4=2*R↑2/D↑2
420  LET U=A1*A4*S1/(A3*A2)
430  LET T=U/(4*P1↑2)
435  GOTO 480
440  PRINT "COIL MODEL"
445  LET Q=1
450  LET U=(2*P1)↑(-2)
460  LET T=(2*P1)↑(-4)
480  LET L1=3*U-P1↑2*T
490  LET L2=SQR(L1↑2+8*T*(P1↑4*T-P1↑2*U))
500  LET L=(L1-L2)/(4*T)
510  LET K=L+P1↑2
515  IF Q=1 THEN 550
520  LET P3=T*K
521  LET P4=P3*L
522  LET P5=P3-U
525  LET P6=(-P4+SQR(P4↑2-4*P3*P5))/(2*P3)
530  LET P=P6↑2
540  GOTO 560
550  LET P=(U-T*K)/(K*T)
560  LET R3=SQR(2*K↑4/(L*(U-T*K)))
570  LET F3=SQR(L*R3↑2*U/K↑2)
580  LET W=2*P1/SQR(L)
590  PRINT D,H,R
600  PRINT U,T,P
610  RINT R3,F3,W
620  PRINT
630  LET N=N+1
640  IF N=1 THEN 240
650  IF N=2 THEN 280
666  IF N=3 THEN 370
670  IF N=4 THEN 383
680  IF N=5 THEN 440
999  END
```

COMPUTER PROGRAM NO 5

```
5  REM CALCULATE SHEAR FREQ,RAYLEIGH NO R=C
7  LET R0=.04
10  READ R1
15  IF R1<0 THEN 999
20  FOR D=.007 TO .01 STEP .001
30  FOR R=R1+.001 TO (R0+R1)/2 STEP .01
40  LET E=D/(2*R)
50  LET P1=3.14159
60  LET S1=(EXP(E)-EXP(-E))/2
70  LET C1=(EXP(E)+EXP(-E))/2
80  LET S2=(EXP(2*E)-EXP(-2*E))/2
90  LET A2=8*R*S1↑2-2*D*S2
100  LET A1=4*R*S1-2*C1*D
110  LET A3=1+P1↑2/E↑2
120  LET A4=R↑2/D↑2
130  LET U=A4*A1*S1/(A3*A2)
135  LET U=2*U
140  LET T=U/(2*P1)↑2
150  LET L1=3*U-P1↑2*T
160  LET L2=SQR(L1↑2+8*T*(P1↑4*T-P1↑2*U))
170  LET L=(L1-L2)/(4*T)
180  LET K=L+P1↑2
190  LET R3=SQR(2*K↑4/(L*(U-T*K)))
200  LET F3=SQR(L*R3↑2*U/K↑2)
210  LET P3=T*K
220  LET P4=P3*L
230  LET P5=P3-U
240  LET P6=(-P4+SQR(P4↑2-4*P3*P5))/(2*P3)
250  LET W=2*P1/SQR(L)
260  LET P=P6↑2
270  PRINT R0,R1
275  LET H=D/(R0-R1)
280  PRINT D,H,R
290  PRINT R3,F3,W
300  PRINT L,P
310  NEXT R
320  NEXT D
325  PRINT
330  GOTO 10
349  DATA .01,.01375,.02125,.025,-1
999  END
```

COMPUTER PROGRAM NO 4

```
  5  REM PRANDTL NO*,RAYLEIGH NO*,FREQUENCY
 10  LET R=.025
 20  LET D=.01
 30  LET E=D/(2*R)
 40  LET H=D/.03
 42  LET N=0
 45  LET P1=3.1459
 50  LET S1=(EXP(E)-EXP(-E))/2
 60  LET C1=(EXP(E)+EXP(-E))/2
 70  LET S2=(EXP(2*E)-EXP(-2*E))/2
 80  LET C2=(EXP(2*E)+EXP(-2*E))/2
 90  PRINT "RIGID -FREE,CONDUCTING"
 95  LET Q=0
100   PRINT "POLAR MODEL"
110   LET A2=4*S1*C1-2*D*C2/R
120   LET A4=D↑2*S1/R-4*R*S1+2*D*C1
190   LET U1=2*R↑2*S1*A4/(A2*D↑3)
200   LET U2=R↑2/D↑2
210   LET U3=2*R↑2*S1*(-A4)/((1+P1↑2/E↑2)*D↑3*A2)
220   LET U=U1+U2+U3
225   LET T=U/(P1↑2*4)
230   GOTO 480
240   PRINT "GILL MODEL "
245   LET Q=1
250   LET U=1/(4*P1↑2)*(P1↑2/12+1)
265   LET T=U/(P1↑2*4)
270   GOTO 480
280   PRINT "FREE CONDUCTING"
285   LET Q=0
290   PRINT "POLAR MODEL"
300   LET A2=-S1/(C1*E)
310   LET A1=4*E*S1/(4*E↑2+4*P1↑2)
320   LET A3=1
330   LET A4=R↑2/D↑2
340   LET U=A4*(A1+A2+A3)
350   LET T=U/(4*P1↑2)
360   GOTO 480
370   PRINT "GILL MODEL"
375   LET Q=1
380   LET U=(2*P1)↑(-2)*(1+P1↑2/3)
381   LET T=(2*P1)↑(-4)*(1+P1↑2/3)
```

```
5  REM COMP CHARACTERISTICS
10  LET P1=3•14159
20  LET D=•01
30  LET R0=•04
40  LET R1=•01
50  LET R=(R0+R1)/2
60  LET N=0
70  LET E=D/(2*R)
80  LET S1=(EXP(E)-EXP(-E))/2
90  LET C1=(EXP(E)+EXP(-E))/2
100  LET S2=(EXP(2*E)-EXP(-2*E))/2
110  LET C2=(EXP(2*E)+EXP(-2*E))/2
120  IF N>0 THEN 210
130  REM CALCULATE F-F
135  PRINT "F-F"
140  LET A1=2*E*S1/(4*E↑2+4*P1↑2)
150  LET A2=-S1/(C1*E)
170  LET A3=1
180  LET A4=R↑2/D↑2
190  LET U=A4*(A1+A2+A3)
195  LET U7=U*(P1*2)↑2/(1+P1↑2/3)
200  GOTO 270
210  REM CALCULATE R-R
220  PRINT "R-R"
222  LET A2=8*R*S1↑2-2*D*S2
230  LET A1=4*R*S1-2*C1*D
240  LET A3=1+P1↑2/E↑2
250  LET A4=R↑2/D↑2
260  LET U=A4*A1*S1/(A3*A2)
264  LET U=2*U
265  LET U7=U*(2*P1)↑2
270  FOR T1=-3 TO 3
275  IF T1=0 THEN 315
280  LET T=T1/(2*P1)↑4
290  LET L=3*U-P1↑2*T
300  LET L2=SQR(L↑2+8*T*(P1↑4*T-P1↑2*U))
310  LET L=(L-L2)/(4*T)
312  GOTO 320
315  LET L=P1↑2/3
320  LET K=L+P1↑2
330  LET R3=SQR(2*K↑4/(L*(U-T*K)))
340  LET F3=SQR(L*R3↑2*U/K↑2)
360  PRINT T1,T,U,U7
370  LET W=2*P1/SQR(L)
380  PRINT R3,F3,W
390  NEXT T1
400  LET N=N+1
410  PRINT
420  IF N=1 THEN 210
430  PRINT "R-C"
440  LET A2=4*S1*C1-2*D*C2/R
450  LET A4=D↑2*S1/R-4*R*S1+2*D*C1
460  LET U1=2*R↑2*S1*A4/(A2*D↑3)
470  LET U2=R↑2/D↑2
480  LET U3=2*R↑2*S1*(-A4)/((1+P1↑2/E↑2)*D↑3*A2)
490  LET U=U1+U2+U3
495  LET U7=U*(2*P1)↑2/(P1↑2/12+1)
500  IF N=2 THEN 270
999  END
```

APPENDIX II

Orthogonal curvilinear coordinates

Orthogonal curvilinear coordinates

Let the coordinates be represented by (U_1, U_2, U_3). These are defined by specifying the cartesian coordinates (x, y, z) as functions of U_1, U_2, U_3 as follows:

$$x = x(U_1, U_2, U_3) \qquad 1$$

$$y = y(U_1, U_2, U_3) \qquad 2$$

$$z = z(U_1, U_2, U_3) \qquad 3$$

When the curves are orthogonal to one another: U_1 = constant, U_2 = constant, U_3 = constant, the line element is given by

$$ds^2 = h_1^2 dU_1^2 + h_2^2 dU_2^2 + h_3^2 dU_3^2 \qquad 4$$

Then the following relationships hold:

$$\nabla U = \frac{1}{h_1}\frac{\partial U}{\partial u_1} + \frac{1}{h_2}\frac{\partial U}{\partial u_2} + \frac{1}{h_3}\frac{\partial U}{\partial u_3} \qquad 5$$

$$\nabla \cdot \underline{U} = \frac{1}{h_1 h_2 h_3}\left\{\frac{\partial}{\partial u_1}(h_2 h_3 U_1) + \frac{\partial}{\partial u_2}(h_1 h_3 U_2) + \frac{\partial}{\partial u_3}(h_1 h_2 U_3)\right\} \qquad 6$$

$$\nabla^2 U = \frac{1}{h_1 h_2 h_3}\left\{\frac{\partial}{\partial u_1}\left(\frac{h_2 h_3}{h_1}\frac{\partial U}{\partial u_1}\right) + \frac{\partial}{\partial u_2}\left(\frac{h_1 h_3}{h_2}\frac{\partial U}{\partial u_2}\right) + \frac{\partial}{\partial u_3}\left(\frac{h_1 h_2}{h_3}\frac{\partial U}{\partial u_3}\right)\right\} \qquad 7$$

$$\nabla \times \underline{U} = \frac{1}{h_1 h_2 h_3}\begin{vmatrix} h_1 i_1 & h_2 i_2 & h_3 i_3 \\ \frac{\partial}{\partial u_1} & \frac{\partial}{\partial u_2} & \frac{\partial}{\partial u_3} \\ h_1 U_1 & h_2 U_2 & h_3 U_3 \end{vmatrix} \qquad 8$$

For cylindrical coordinates

$$(r, \phi, z) \qquad ds^2 = dr^2 + r^2 d\phi^2 + dz^2 \tag{9}$$

$$h_1 = 1, \quad h_2 = r, \quad h_3 = 1 \tag{10}$$

$$\nabla u \equiv \frac{\partial u}{\partial r}, \frac{1}{r}\frac{\partial u}{\partial \phi}, \frac{\partial u}{\partial z} \tag{11}$$

$$\nabla \cdot \underline{u} = \frac{1}{r}\frac{\partial}{\partial r}(r u_r) + \frac{1}{r}\frac{\partial u_\phi}{\partial \phi} + \frac{\partial u_z}{\partial z} \tag{12}$$

$$\nabla_r \times \underline{u} = \frac{1}{r}\frac{\partial u_z}{\partial \phi} - \frac{\partial u_\phi}{\partial z} \tag{13a}$$

$$\nabla_\phi \times \underline{u} = \frac{\partial u_r}{\partial z} - \frac{\partial u_r}{\partial r} \tag{13b}$$

$$\nabla_z \times \underline{u} = \frac{1}{r}\frac{\partial (r u_\phi)}{\partial r} - \frac{1}{r}\frac{\partial u_r}{\partial \phi} \tag{13c}$$

$$\nabla^2 u = \frac{1}{r}\left\{\frac{\partial}{\partial r}\left(r\frac{\partial u}{\partial r}\right) + \frac{\partial}{\partial \phi}\left(\frac{1}{r}\frac{\partial u}{\partial \phi}\right) + \frac{\partial}{\partial z}\left(r\frac{\partial u}{\partial z}\right)\right\} \tag{14}$$

$$(\underline{u}\nabla)\underline{u} \begin{cases} \underline{u}\cdot\nabla u_r - \dfrac{u_\phi^2}{r} \\ \underline{u}\cdot\nabla u_\phi + \dfrac{u_r u_\phi}{r} \\ \underline{u}\cdot\nabla u_z \end{cases} \tag{15}$$

$$\nabla^2 \underline{u} = \begin{cases} \nabla^2 u_r - \frac{u_r}{r^2} - 2\frac{\partial u_\phi}{\partial \phi} \\ \nabla^2 u_\phi - \frac{u_\phi}{r^2} + \frac{2}{r^2}\frac{\partial u_r}{\partial \phi} \\ \nabla^2 u_z \end{cases}$$

16

APPENDIX III

Non-dimensional shear and temperature calculations

The non-dimensional shear is given by

$$S = -\frac{d^2 u_z}{\chi R_a} \qquad 1.0$$

The non-dimensional temperature gradient is related to the non-dimensional shear through the differential equations:

$$\frac{d^2}{dz_*^2}(T_z) = \frac{d^2}{R_a T_r}\left(\Theta_{zzz}\right) \qquad 2.0$$

or

$$\frac{d^2}{dz_*^2}(T_z) = -S \qquad 3.0$$

The non-dimensional shear and non-dimensional temperature gradient for rigid conducting boundaries. The equation for the shear is given by

$$u_z = \frac{A}{r}\exp\left(\frac{z}{r}\right) - \frac{B}{r}\exp\left(\frac{-z}{r}\right) - \frac{\alpha g T_r r^2}{\nu} \qquad 4.0$$

Now the shear integral is

$$\bar{u}_{z*} = \frac{\int_{-1/2}^{1/2} u_{z*}(z_*)\, W(z_*)\, dz_*}{\int_{-1/2}^{1/2} W(z_*)\, dz_*} \qquad 5.0$$

where $W(z) = \cos^2 \pi z_*$ 6.0

Consider the denominator above:

$$I_S = \int_{-1/2}^{1/2} S \cos^2 \pi z_*\, dz_* \qquad 7.0$$

Or in double angle representation

$$I_s = \frac{1}{2}\int_{-1/2}^{1/2} S\,(1+\cos 2\pi z_x)\,dz_x \qquad 8.0$$

From continuity considerations $$\int_{-1/2}^{1/2} S\,dz_x = 0 \qquad 9.0$$

Hence the other individual contributions will be:

$$-\frac{d^2 A}{2\chi R_a \nu}\int_{-1/2}^{1/2} \exp(2Ez_x)\cos 2\pi z_x\,dz_x = \frac{d^2 A \sinh E}{2E\tau R_a \chi\left(1+\frac{\pi^2}{E^2}\right)} \qquad 10.0$$

and $$\frac{d^2 B}{2\chi R_a \nu}\int_{-1/2}^{1/2} \exp(-2Ez_x)\cos 2\pi z_x\,dz_x = -\frac{d^2 B \sinh E}{2E\tau R_a \chi\left(1+\frac{\pi^2}{E^2}\right)} \qquad 11.0$$

where $$A = \frac{\alpha g T_0 t^2 d}{\nu}\left\{\frac{2\tau \sinh E - d\cosh E}{B\tau \sinh^2 E - 2d\sinh 2E}\right\} \qquad 12.0$$

and $$B = \frac{\alpha g T_0 t^2 d}{\nu}\left\{\frac{-2\tau \sinh E + d\cosh E}{B\tau \sinh^2 E - 2d\sinh 2E}\right\} \qquad 13.0$$

The final integral will be:

$$\frac{\alpha g T_0 t^2}{2\nu}\int_{-1/2}^{1/2} \cos 2\pi z_x\,dz_x = 0 \qquad 14.0$$

with $$\int_{-1/2}^{1/2} \cos^2 \pi z_x\,dz_x = \frac{1}{2} \qquad 15.0$$

Hence the non-dimensional shear will be:

$$\bar{u}_z = \frac{r^2}{d^2}\left\{\frac{4r\sinh E - 2d\cosh E}{8r\sinh^2 E - 2d\sinh 2E}\right\}\frac{\sinh E}{\left(1+\frac{\bar{n}^2}{E^2}\right)} \qquad 16.0$$

The non-dimensional temperature gradient:

$$\int_{-1/2}^{1/2} T_z \cos^2 \bar{n} z_* \, dz_* = \frac{1}{2}\int_{-1/2}^{1/2} T_z \cos 2\bar{n} z_* \, dz_* \qquad 17.0$$

since $$\int_{-1/2}^{1/2} T_z \, dz_* = 0 \qquad 18.0$$

Then (17.0)

$$\int_{-1/2}^{1/2} T_z \cos^2 \bar{n} z_* dz_* = \frac{1}{2}\left[T_z \frac{1}{2\bar{n}}\sin 2\bar{n} z_* + \frac{dT_z}{dz_*}\frac{1}{(2\bar{n})^2}\cos 2\bar{n} z_* - \frac{1}{(2\bar{n})^2}\left\{\cos 2\bar{n} z_* \frac{d^2 T_z}{dz_*^2} dz_*\right]_{-1/2}^{1/2} \qquad 19.0$$

Now $\sin 2\bar{n} z_*$ and $\frac{dT_z}{dz_*}$ vanish at $z_* = \pm\frac{1}{2}$

then $$\int_{-1/2}^{1/2} T_z \cos^2 \bar{n} z_* dz_* = \frac{1}{2}\frac{1}{(2\bar{n})^2}\int_{-1/2}^{1/2} S\cos 2\bar{n} z_* \, dz_* \qquad 20.0$$

Then $$\bar{T}_z = \frac{r^2}{(2\bar{n}d)^2}\left\{\frac{4r\sinh E - 2d\cosh E}{8r\sinh^2 E - 2d\sinh 2E}\right\}\cdot\frac{\sinh E}{\left(1+\frac{\bar{n}^2}{E^2}\right)} \qquad 21.0$$

The other values follow using a similar procedure as above.

The two figures illustrate the variation of the non-dimensional shear for free conducting and rigid conducting boundaries. For the free

FIGURE 15

GRAPH OF NON-DIMENSIONAL SHEAR FOR FREE CONDUCTING BOUNDARIES

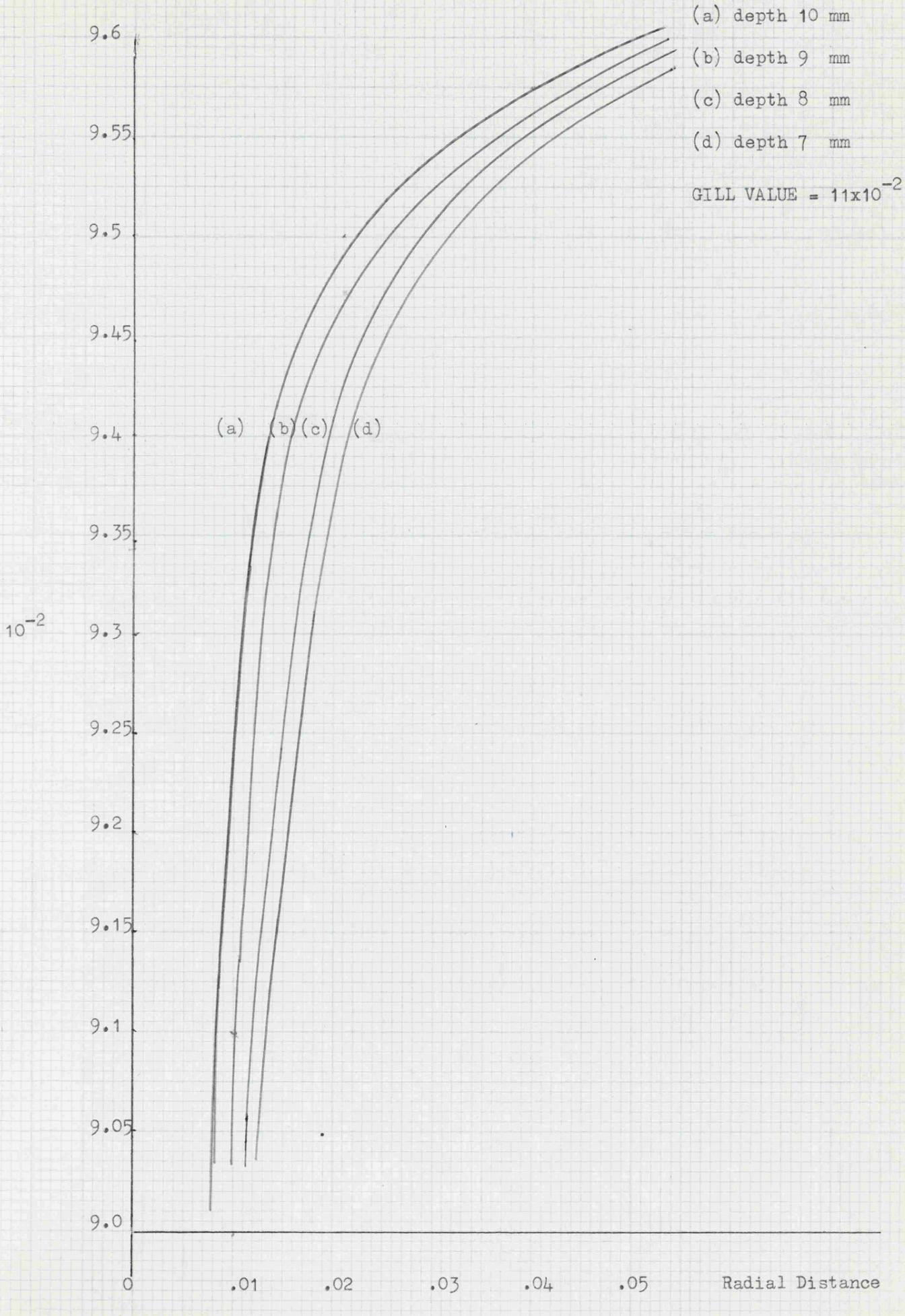

FIGURE 16

GRAPH OF NON-DIMENSIONAL SHEAR FOR RIGID CONDUCTING BOUNDARIES

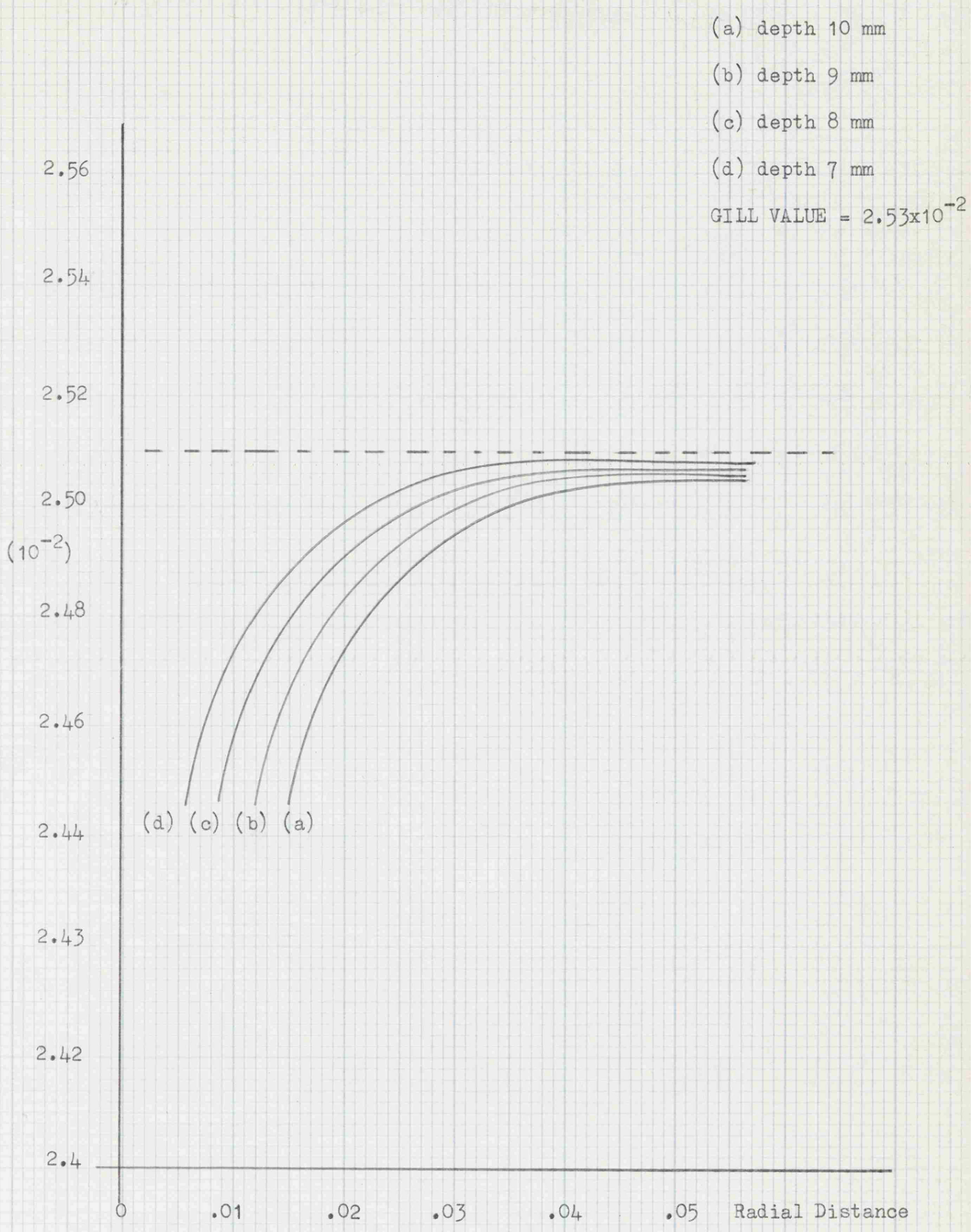

conducting boundaries the family of curves are approaching the Gill value for large r but as the depth of the working fluid is increased so initially does the value of the non-dimensional shear. This pattern of increasing shear with increasing depth also occurs with the rigid conducting boundaries.

REFERENCES

1. SPARROW E.M., GOLDSTEIN R.J., and JONSSON (1964)
Thermal instability in a horizontal fluid layer
J. FLUID MECH 18 No 4, 513 - 528

2. HURLE D.T., JAKEMAN E. and PIKE E.R. (1967)
On the solution of the Benard problem with boundaries of finite conductivity
PROC. ROY. SOC. A296 No 1447, 469 - 475

3. SUTTON O.G. (1950)
On the stability of a fluid heated from below
PROC. ROY. SOC A204 No 1078, 297 - 309

4. SEGEL L.A. and STUART J.T. (1962)
On the question of the preferred mode in cellular thermal convection
J. FLUID MECH 13 No 2, 289 - 306

5. CHANDRASEKHAR S. (1961)
Hydrodynamic and Hydromagnetic stability
Clarendon Press, Oxford

6. STUART, J.T. (1963)
Hydrodynamic stability Laminar Boundary Layer (ed. by ROSENHEAD)
Oxford Univ. Press

7. LIN C.C. (1955)
The Theory of Hydrodynamic stability
CAMBRIDGE UNIV. PRESS

8. PELLEW A, and SOUTHWELL (1940)
On maintained convective motion in a fluid heated from below
PROC. ROY. SOC A176 No 966, 312 - 343

9. RAYLEIGH (1916)
On convection currents in a horizontal layer when the higher temperature is on the underside
SCI PAPERS CAMBRIDGE UNIV. PRESS 6 432 - 443

10. LOW A.R. (1929)
On the criterion for stability for a layer of viscous fluid heated from below
PROC. ROY. SOC A125 180 - 195

11. REID W.H. and HARRIS D.L. (1958)
Some further results on the Benard problem
PHYS FLUIDS 1 No 2 102 - 110

12. CATTON I. (1966)
Natural convection in horizontal liquid layers
PHYS. FLUIDS 9 No 12, 2521 - 2522

13. BÉNARD H. (1900)
REVE GENERAL DES SCIENCES PURE ET APPLIQUÉES
11 1261 and 1309

14. CHRISTOPHERSON D.G. (1940)
Note on the vibration of membranes
QUART J. MATH. 11 No 1 63 - 65

15. STUART J.T. (1964)
On the cellular patterns in thermal convection
J. FLUID MECH 18 No 7 523 - 531

16. THOMPSON H.A. and SOGIN H.H. (1966)
Experiments on the onset of thermal convection in horizontal layers of gases
J. FLUID MECH 24 No 3 451 - 479

17. NIELD D.A. (1967)
The thermohaline Rayleigh - Jefferies problem
J. FLUID MECH 32 No 2 393 - 398

18. MALKUS W.V.R. (1954)
Discrete transitions in turbulent convection
PROC. ROY. SOC. A225 No 1161 185 - 195

19. DEARDORFF J.M. and WILLIS G.E. (1967)
The free convection temperature profile
QUART, J. ROY. METEOROL. SOC. 93 No 396 166 - 175

20. REYNOLD O. (1874)
On the dynamical theory of incompressible viscous liquids and the determination of the criterion
PHIL. TRANS. ROY. SOC. LONDON 186 123 - 161

21. SOROKIN V.S. (1953)
Variational theory in the theory of convection
PRIKL. MAT. MEKH 17 No 1 39 - 48

SOROKIN V.S. (1954)
Stationary motions of a fluid heated from below
PRIKL. MAT. MEKH. 18 No 2 197 - 204

22. JOSEPH D.D. (1965)
On the stability of the Boussinesq equations
ARCH. RAT. MECH. ANAL. 20 No 1 59 - 71

JOSEPH D.D. (1966)
Non linear stability of the Boussinesq equations by method of energy
ARCH. RAT. MECH. ANAL. 22 No 3 163 - 184

23. JOSEPH D.D. and SHIR (1966)
Subcritical convective instability Part I
J. FLUID MECH. 26 No 1 753 - 768

24. JOSEPH D.D. and CARMI S. (1966)
Subcritical convective instability Part II
J. FLUID MECH 26 No 2 769 - 777

25. JOSEPH D.D., GOLDSTEIN R.J. and GRAHAM D.J. (1968)
Subcritical instability and exchange of stability in a horizontal fluid layer
PHYS. FLUIDS. 11 No 4 903 - 904

26. LANDAU L.D. (1944)
Turbulence
DOKLADY AN USSR 44 No 8 339 - 342

27. ECKHAUS W. (1965)
Studies in non-linear stability theory
SPRINGER - VERLAG BERLIN - NEW YORK

28. PONOMARENKO Y.U.B. (1965)
On the "hard self excitation" of the stationary motions in fluid dynamics
PRIKL. MAT. I. MEKL 29 No 2 309 - 321

29. YUDOVICK V.I. (1966)
On the origin of convection
PRIKL. MAT. MEKH 30 No 6 1000 - 1005

YUDOVICK V.I. (1967)
Free convection and branching
PRIKL. MAT. MECKH 31 No 1 101 - 111
On the stability of convective flows
PRIKL. MAT. MEKH 31 No 2 272 - 281

30. GOR'KOV L.P. (1957)
Stationary convection in a plane layer of fluid near conditions of critical heat transfer
Zh. EKSP. TEOR. FIZ. 33 No 2 (8) 402 - 411

31. MALKUS W.V.R. and VERONIS G. (1958)
Finite amplitude cellular convection
J. FLUID MECH. 4 No 3 225 - 260

32. KUO H.L. (1961)
Solutions of the non-linear equations of cellular convection and heat transport
J. FLUID MECH 10 No 4 611-634

33. BISSHOPP F.E. (1962)
Non-linear effects of thermal convection
J. MATH and MECH. 11 No 5 647 - 663

34. STUART J.T. (1958)
On the non-linear mechanics of hydrodynamic stability
J. FLUID MECH 4 No 1 1-21

35. SCHLÜTER A. LORTZ D. and BUSSE F. (1965)
On the stability of steady finite amplitude convection
J. FLUID. MECH. 23 No 1 129 - 144

36. SEGEL L.A. (1966)
Non-linear hydrodynamic stability theory and its application to thermal convection and curved flows

37. HERRING J.R. (1963)
Investigation of problems in thermal convection
J. ATMOSPH. SCI. 20 No 4 325 - 338

HERRING J.R. (1964)
Investigation of problems in thermal convection for rigid boundaries
J. ATMOSPH. SCI. 21 No 3 277 - 290

38. DEARDOFF J.W. (1964)
A numerical study of two dimensional parallel plate convection
J. ATMOSPH. SCI. 21 No 5 419 - 438

39. FROMM J.E. (1965)
Numerical solutions of the non-linear equations for a heated fluid layer
PHYS. FLUIDS 8 No 10 1757 - 1769

40. VERONIS G. (1966)
Large amplitude Benard convection
J. FLUID MECH. 26 No 1 49 - 68

41. BUSSE F.H. (1967)
On the stability of two dimensional convection in a layer heated from below
J. MATH. and PHYS. 46 No 2 140 - 150

42. ROBERTS P.H. (1965)
On non-linear Benard convection in non-equilibrium thermodynamics, variational techniques and stability
The University of Chicago Press Chicago, 125 - 162

43. SCHMECK P. and VERONIS G. (1967)
Comparison of some recent experimental and numerical results in Benard convection
PHYS. FLUIDS 10 No 5 927 - 930

44. VERONIS G. (1966)
Large amplitude Benard convection
J. FLUID MECH. 26 No 1 49 - 68

45. GILLE J. (1967)
Interferometric measurement of temperature reversal in a layer of convecting air
J. FLUID MECH. 30 No 2 371 - 384

46. SEGEL L.A. (1962)
The non-linear interaction of two disturbances in the thermal convection problem
J. FLUID MECH. 14 No 1 97 - 114

47. STUART J.T. (1960)
The basic behaviour of plane Poiseuille flow
J. FLUID MECH. 9 No 3 353 - 370

48. WATSON J. (1960)
The development of solution for plane Poiseuille and for plane flow
J. FLUID MECH. 9 No 3 371 - 383

49. PONOMARENKO Y.U.B. (1968)
Process of the establishment of hexagonal convection cells
PRIKL, MAT. I. MEKH 32 No 2 244 - 255

50. PALM E. (1960)
On the tendency towards hexagonal cells in steady convection
J. FLUID MECH. 19 No 3 353 - 365

51. TIPPELSKIRCH H. (1966)
Über Konvektionszellen, Insbesondere in Flüssigem Schwefel
BEITR. PHYS. ATMOSPH. 29 No 1 37 - 54

52. PALM E. and ØIANN H. (1964)
Contribution to the theory of cellular thermal motion in Benard convection
J. FLUID MECH 30 No 4 651 - 661

53. SEGEL, L.A. (1964)
Variational principle for Rayleigh-Taylor instability
PHYS. FLUIDS 7 No 8 1114 - 1116

54. BUSSE F.H. (1967)
The stability of finite amplitude cellular convection and its relationship to an extremum principle
J. FLUID MECH. 30 No 4 625 - 649

55. PALM E, ELLINGSEN T. and GJEVIK B. (1967)
On the occurrence of cellular motion in Benard convection
J. FLUID MECH 30 No 2 289 - 306

56. DAVIS S.H. and SEGEL L.A. (1968)
Effects of surface curvature and property variation of cellular convection
PHYS. FLUIDS 11 No 3 470 - 476

57. PONOMARENKO Y.U.B. (1968)
Process of the establishment of hexagonal convection cells
PRIKL. MAT. I. MEKH. 32 No 2 244 - 255

58. BUSSE F.H. (1972)
The oscillatory instability of convection rolls in a low Prandtl number fluid
J. FLUID MECH. 52 Part 1 97 - 112

59. DEARDOFF J.W. and WILLIS (1965)
Two dimensional thermal convection of air between horizontal plates studied numerically and experimentally
J. FLUID MECH 23 337

60. ROSSBY H.T. (1969)
A study of the response of a thin uniformaly heated rotating layer of fluid
J. FLUID MECH 36 309

61. KRISHNAMURTI R. (1970)
The transitions occurring in a horizontal fluid layer before the flow becomes turbulent for liquids of Prandtl numbers 1 to 10^4
J. FLUID MECH 42 295 309

62. BUSSE F. and WHITEHEAD J.A. (1974)
Measurements of heat flux and temperature gradient in a solution stably stratified and heated from below
J. FLUID MECH 64 347

63. AHLERS G. (1974)
Low temperature studies of the Rayleigh-Benard instability and turbulence
PHYS. REV. LETT 33 1185

64. ROSSBY H.T. (1969)
A study of the response of a thin uniformly heated rotating layer of fluid
J. FLUID MECH 36 309

65. HOWARD L. (1963)
Heat transport by turbulent convection studied numerically
J. FLUID MECH 17 405

66. WELANDER P. (1967)
The oscillatory instability of a differentially heated fluid loop
J. FLUID MECH 29 17

WILLIS G.E. and DEARDORFF J.W. (1970)
The oscillatory motions of Rayleigh convection
J. FLUID MECH A4 661

67. CLEVER R.M. and BUSSE F.H. (1974)
Transition to time - dependent convection
J. FLUID MECH 65 625

68. SALTZMAN B. (1962)
J. ATMOS. SCI. 19 329

69. BATCHELOR G.K. (1954)
Heat transfer by free convection across a closed cavity between vertical boundaries at different temperatures
Q. APPLIED MATH 12 209

70. ELDER J.M. (1965)
Laminar free convection in a vertical slot
J. FLUID MECH. 23 77

71. GILL A.E. (1966)
The boundary layer regime for convection in a rectangular cavity
J. FLUID MECH 26 515

72. GILL A.E. and DAVEY (1969)
Instabilities of buoyancy-driven system
J. FLUID MECH 35

73. NEWEL M.E. and SCHMIDT F.W. (1970)
Heat transfer by laminar natural convection within rectangular enclosures
TRANS. A.S.M.E. SERIES C, J. HEAT TRANSFER 92 159

74. UEDA H. (1961)
J. PHYS. SOC. JAPAN, 16 1 61

75. COLE G.S. and WINEGARD W.C. (1964-5)
Thermal convection during horizontal solidification of pure metals and alloys
J. INST. OF METALS 93 153

76. UTECH H.P. and FLEMINGS M.C. (1966)
Elimination of solute banding in Indium Antimonide crystals by growth in a magnetic field
J. APPLIED PHYS. 37 2021

77. HURLE D.T.J. (1966)
Temperature oscillations in molten metals and their relationship to growth striae in melt grown crystals
PHIL. MAG. 13 (8) 305

78. BRADSHAW R.I. (1966)
Temperature oscillations in mercury M.Sc. Thesis Bristol College of Science and Technology

79. PAMPLIN B.R. (1967)
Waves of Temperature
NEW SCIENTIST 33 536 - 552

80. JOHNSON C.P. (1967)
Thermohydrodynamic oscillations in liquid gallium and their relationship to the perfection of melt-grown single crystals
M.Sc. Thesis, Brighton College of Technology

81. GILL A.E. (1974)
A theory of thermal oscillations in liquid metals
J. FLUID MECH (1974) 64 No 3 577 - 588

82. SKAFEL M.G (1972)
Ph.D. Thesis, University of Cambridge

83. HURLE D.T.J., JAKEMAN E. and JOHNSON C.P. (1974)
Convective temperature oscillations in molten gallium
J. FLUID MECH. 64 No 3 565-576

84. BOLT, G. (1975)
Temperature oscillations in mercury
M.Sc. Thesis University of Bath

85a. ELDER J.W. (1965)

85. THOMAS R.W. (1970)
Finite difference computation of heat transfer by natural convection
Ph.D. Thesis, University of New South Wales

86. HADLEY (1735)
Concerning the cause of general trade winds
PHIL. TRANS. ROY. SOC. LONDON 29 58 - 62

87. HART, J.E. (1972)
Stability of their non-rotating Hadley circulations
J. ATMOS. SCI. 29 687

88. GILL A.E.
Private Communication

89. RIEMANN
Partielle Differential Gleichungen

90. RAYLEIGH J.W.S. (1894)
The theory of sound volume I
The Macmillian Company London

91. McMAHON J. (1895)
On the roots of the Bessel and certain related functions
Annals of Math. Jan. (1895)

92. CALDWELL D.R. (1974)
The onset of thermohaline convection
J. FLUID MECH 64 2 347

93. DAVIS, S.H. (1968)
FLUID MECH 32 619

94. STORK H. and MILLER D. (1972)
J. FLUID MECH 54 599

95. DUBOIS M. and BERGÉ P. (1978)
Experimental study of the velocity field in Rayleigh-Bénard convection
J. FLUID MECH 85 641

96. DAVIS S.H. (1967)
J. FLUID MECH 30 465

97. LORENZ N. Edward (1963)
Deterministic non-periodic flow
J. ATMOS. SCI. 20 130

98. WHIFFIN P.A.C. and J.C. BRICE (1971)
J. Crystal Growth 10 91

99. BRICE, J.C. of Hill, P.A.C. WHIFFIN and J.A. WILKINSON (1971)
J. Crystal Growth 10 133